EVALUATION OF THE STORAGE OF DIFFUSE SOURCES OF SALINITY IN THE UPPER COLORADO RIVER BASIN

by

Jonathan B. Laronne

September 1977

Colorado Water Resources Research Institute
Completion Report No. 79

EVALUATION OF THE STORAGE OF DIFFUSE SOURCES OF SALINITY IN THE UPPER COLORADO RIVER BASIN

Completion Report

OWRT Project No. B-121-COLO

by

Jonathan B. Laronne

(Dr. Stanley A. Schumm-Principal Investigator)

Department of Earth Resources
Colorado State University

submitted to

Office of Water Research and Technology
U. S. Department of Interior
Washington, D. C. 20240

September, 1977

The work upon which this report is based was supported (in part) by funds provided by the United States Department of the Interior, Office of Water Research and Technology, as authorized by the Water Resources Research Act of 1964, and pursuant to Grant Agreement No.(s). 14-3-0001-5061.

Colorado Water Resources Research Institute
Colorado State University
Fort Collins, Colorado 80523

Norman A. Evans, Director

ABSTRACT

EVALUATION OF THE STORAGE OF DIFFUSE SOURCES OF SALINITY IN THE UPPER COLORADO RIVER BASIN

Specific electrical conductance (EC) was found to correlate highly (r^2 = 0.99) with the total dissolved solids (TDS) concentration of aqueous solutions derived from mixtures of distilled water and sediment samples collected in the Mancos Shale lowlands of the Upper Colorado River Basin. The effects of suspended sediment presence, turbulence and particle size on the EC of partially equilibrated mixtures appeared negligible. The mixing time necessary to approach equilibrium decreased with an increase of salt content (of the dissolving sediment) and with a decrease of sediment concentration, and the time span required for equilibrium ranged from a few minutes to several days.

The chemical quality of the aqueous mixtures is of the Ca^{2+}-Mg^{2+}-Na^{1+}-SO_4^{2-}-HCO_3^{1-} type. Sodium and magnesium hydrated sulfates appear to dissolve faster than gypsum or calcite. Moreover, it was determined that the relative abundance of Na^{1+}, Mg^{2+} and SO_4^{2-} decreases with a decrease in the sediment:water ratio. An increase in sediment:water ratio was followed by an increase in TDS concentration due to the addition of soluble minerals. A decrease in sediment:water ratio produced an opposite trend. However, the TDS decrease was smaller than warranted by dilution for 95 percent of the samples. This dilution effect, in which the mass of dissolved matter increases as much as 500 percent, may be partly explained by gypsum and calcite dissolution but in undersaturated

solutions it calls for the existence of slightly soluble coatings on mineral particles.

There is a large inherent variability in the soluble mineral content of sampled sediments. Soluble mineral content (calculated from the EC of 1:99 sediment:water mixtures) of Mancos Shale from hillslopes (2 percent, calculated as a weight per weight ratio) is significantly larger than that of terrace alluvium (0.62-0.29 percent) and bed materials (0.93-0.81 percent) of North Miller and West Salt Creeks, respectively. The most saline deposits (10 percent) are efflorescent bed crusts. Terrace and bed materials in narrow valleys where shallow alluvium overlies shale are highly saline (1.6 percent) and show an increase in soluble mineral content with depth. Terrace crusts are well leached; some bed material crusts accumulate salts while others do not.

Results from the experiments on the amount of dissolution and dissolution rates upon dilution indicate that the true salt load from diffuse sources of salinity may be much larger than presently assumed. Chemical analyses of samples from a single low magnitude flow event in West Salt Creek show that stormflow salinity is considerably influenced by the soluble mineral content of bed and lower bank materials. Results also confirm that major areas of diffuse sources of salinity in the Upper Colorado River Basin are also major sediment contributors. Hence, gullying will significantly increase the sediment and salt load of channels in saline alluvium and in Mancos Shale bedrock.

Jonathan Benjamin Laronne
Department of Earth Resources
Colorado State University
Fort Collins, Colorado 80523
Summer, 1977

ACKNOWLEDGEMENTS

The investigators extend their grateful appreciation to A. D. Elkin, U. S. Soil Conservation Service in Denver, for his suggestions and the data he supplied on Indian Wash; to G. C. Lusby from the U. S. Geological Survey, Water Resources Division in Denver, for unpublished data on Badger Wash; to J. C. Mundorff of the U. S. Geological Survey, Water Resources Division, Salt Lake City, for his suggestions; to R. J. Snipes, District Chief of the U. S. Geological Survey, Water Resources Division in Grand Junction, for the preliminary data he supplied on West Salt Creek; and to K. Weston and B. McClenegan from the U. S. Bureau of Reclamation in Grand Junction, for the unpublished data they supplied on tributaries in the Grand Valley. Discussions with K. Tanji and the x-ray diffraction data supplied by him and Dr. L. Whittig, both from the University of California at Davis were extremely helpful.

J. McKean and D. Whitson assisted in the laboratory. The Soils Testing Laboratory at Colorado State University, under the supervision of Dr. P. N. Sultanpour, performed the soil chemical analyses. P. Young drafted the figures, and L. Damron typed the manuscript.

This study was funded in part by a grant from the U. S. Office of Water Resources and Technology (OWRT), project Number B-121-COLO; matching funds were provided by Colorado State University.

TABLE OF CONTENTS

LIST OF TABLES

LIST OF APPENDIX TABLES

LIST OF FIGURES

CHAPTER 1

INTRODUCTION

1.1 Statement of Problem

Colorado River water serves millions of people is such diverse ways as industrial and municipal needs, recreation, irrigation and the production of electrical energy. The variety of demands on this water places great emphasis not only on the quantity of water but also on water quality. The situation is complicated internationally by Mexico's use of Colorado River water.

The most serious water quality problem in the Colorado River Basin is salinity and the progressive increase of salinity. The average annual salinity of the Colorado River at Imperial Dam, California, as well as in all the major tributaries of the Upper and Lower Colorado River Basin lowlands has almost doubled during this century (Iorns, Hembree and Oakland, 1965). Although irrigation return flow contributes significantly to this salinity increase, salts from diffuse and point sources of natural origin are the largest contributors (Maletic, 1973). Sources of salinity may be divided into point and non-point, or diffuse types. Point sources include saline seeps and springs as well as industrial and urban effluents. Diffuse sources originate from the entire drainage basin.

Geologic sources of salt have been identified regionally but, except for the recent investigation by Ponce (1975), the storage and release mechanisms of salts and the variation of salt content within

high salt producing areas have not been studied. Such a study of natural salt storage and release processes should improve the possibility for control of salt production from these diffuse sources of salt.

1.2 Objectives

The objectives of this study may be divided into two groups. The first group involved the determination of amounts of salt, i.e., soluble mineral content, stored in alluvium (bed materials of alluvial channels and terrace deposits including gully walls) and in associated Mancos Shale (both weathered and unweathered) bedrock. These determinations are required in order to evaluate the salinity potential of such deposits. The diffuse source areas studied are heavy contributors of dissolved solids. An additional objective was to determine the relation between sediment yield and salt yield by studying the physical and chemical dissolution processes of these geologic materials upon contact with water.

The second set of objectives was oriented toward the identification of the relationship between salt release and the erosion of valley alluvium. The hypothesis to be tested was that salt is stored in alluvium and released after alluvium is eroded. This goal may be achieved by comparing morphological differences between basins of high and those of low salt release and by comparing aggrading and degrading channel reaches in channels of high salt release.

It was apparent in the early stages of this study that there are very few natural basins contributing significant salt yields to the Upper Colorado River Basin that are appreciably unaffected by irrigation

and, at the same time, for which water quality data is available. Comparison of potentially low and high salt yielding areas was therefore limited to reaches within one of the studied basins. Moreover, interpretation of aerial photographs and topographic maps as well as a low-level flight over large areas of the Upper Colorado River Basin substantiated the field observation that most channels are incised or gullied. Because no typical aggrading reach (one with a high width/depth ratio and/or with thick fresh deposits) was located, no comparison was undertaken between aggrading and degrading reaches.

1.3 Salinity in Arid Regions and in the Upper Colorado River Basin

Natural water in the atmosphere, hydrosphere and lithosphere contains varying amounts of dissolved constituents. The concentration of dissolved solids in precipitation is very low (Carroll, 1962) although it may increase locally such as in coastal areas (Fanning and Lyels, 1964). Channelized and overland flow, soil water and ground water dissolve gases, liquids and solids with which they come in physical contact. The total dissolved solids (TDS) concentration of these natural aqueous solutions becomes very high if the material in contact with the solution is highly soluble or when evaporation of the water concentrates the solutions.

Arid and semiarid regions are by definition regions of low annual precipitation and high potential evaporation. The natural waters of these regions become more concentrated with dissolved solids, or 'salt loaded', as evaporation occurs. Therefore, saline accumulations appear on the surface and in the soils of these regions. The saline deposits

are composed of highly soluble minerals, the most soluble of which are the nitrates, chlorides and sulfates. The arid and semiarid environment is, therefore, conducive to the formation of saline deposits such as saline playa deposits (Hardie, 1968; Lotspeich *et al.*, 1969), and it is characterized by saline soils and by runoff and groundwater of low chemical quality.

Large parts of the Southwest and, specifically, the lowlands of the Colorado River Basin, sizeable areas in the Rio Grande Basin and in the San Juaquin Valley, California, as well as major areas in Wyoming, Montana and Idaho are characterized by saline soils. Saline and sodic (i.e., sodium rich) soils are common in the Middle East, in the Asian subcontinent, in Australia and in western South America. The saline bedrock and consequently the saline surficial materials of these regions are the diffuse sources of salinity of the rivers that drain them.

Most of the water in the Upper Colorado River Basin, defined as the drainage area (276800 km^2 or 109500 mi^2) drained by the Colorado River above Lees Ferry, Arizona, originates from spring snow melt in the high country of the Rocky Mountains. The upper parts of the drainage basin are vegetated mountain ranges exposing outcrops of Precambrian crystalline rocks. These rocks and their derived soils produce relatively insoluble weathering products, and they are characterized by low sediment production. However, the lower areas of the Upper Colorado River Basin are underlain by Paleozoic to Recent sedimentary rocks. Various marine shales are interlayered in the thick sedimentary sequence of the Colorado Plateau and the saline Mancos Shale formation of Upper Cretaceous age occurs over rather large areas.

Shales, although relatively impermeable, are erodible materials. Marine shales contain soluble minerals which were precipitated from marine water. Therefore, it is expected that Mancos Shale areas will yield high sediment and salt loads to the Colorado River. The percent of the total flow and the percent of the total salt and suspended sediment load discharged from the Upper Colorado River Basin measured at selected gaging stations are shown in Figures 1.1 and 1.2. The percentages were calculated from the total runoff, salt load and suspended sediment yield at Lees Ferry, Arizona. The Price and Dirty Devil Rivers are characterized by low water yields (0.66 and 0.58 percent, respectively) and by very high sediment yields (3.73 and 4.81 percent, respectively). It is particularly noticeable that these basins also contribute high yields of solutes (2.79 and 2.28 percent). Mundorff (1972) and Ponce (1975) clearly demonstrated the relation of high salinity to presence of Mancos Shale in the Price River Basin. Similar patterns of high sediment and salt loading occur in the central reach of the Gunnison Valley in the Delta-Montrose area of Colorado, throughout the Grand Valley and in the San Juan River drainage basin between Shiprock, New Mexico, and Bluff, Utah. All these basins, valleys and reaches are extensively underlain by Mancos Shale. Therefore, several of them were chosen as field areas for intensive sampling of surficial Mancos Shale and associated alluvial deposits in order to determine their potential as diffuse sources of salinity.

The major diffused sources of salinity yield a mixed cation (calcium, magnesium and sodium) sulfate-bicarbonate type runoff, as opposed to the low sodium and low sulfate runoff from most other areas (Price and Waddell, 1973). The natural diffuse source areas yield

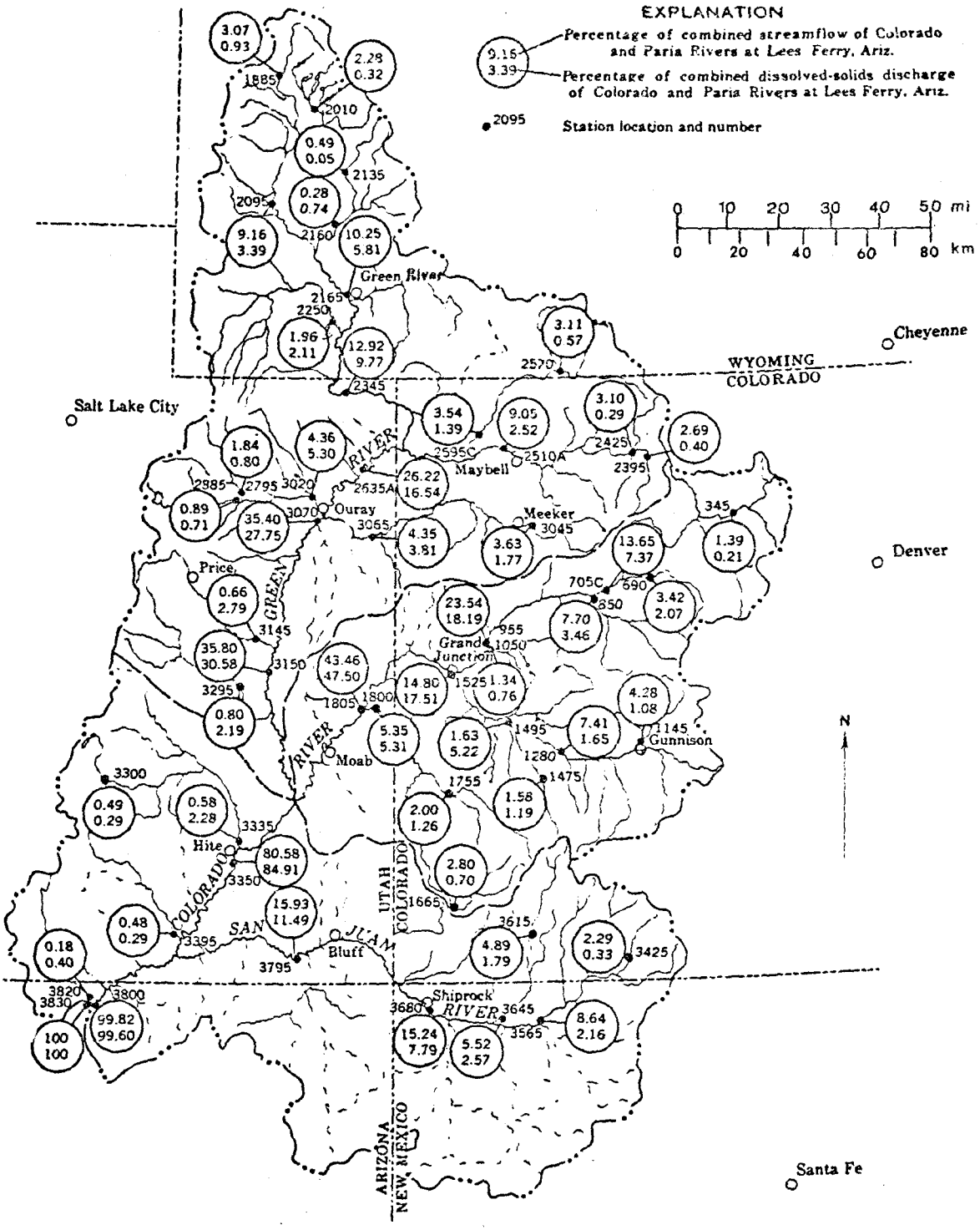

Figure 1.1. Approximate dissolved solids discharge and streamflow, expressed as percentages of the combined dissolved solids discharge and combined streamflow of the Colorado and Paria Rivers at Lees Ferry, Arizona (from Iorns, Hembree and Oakland, 1965).

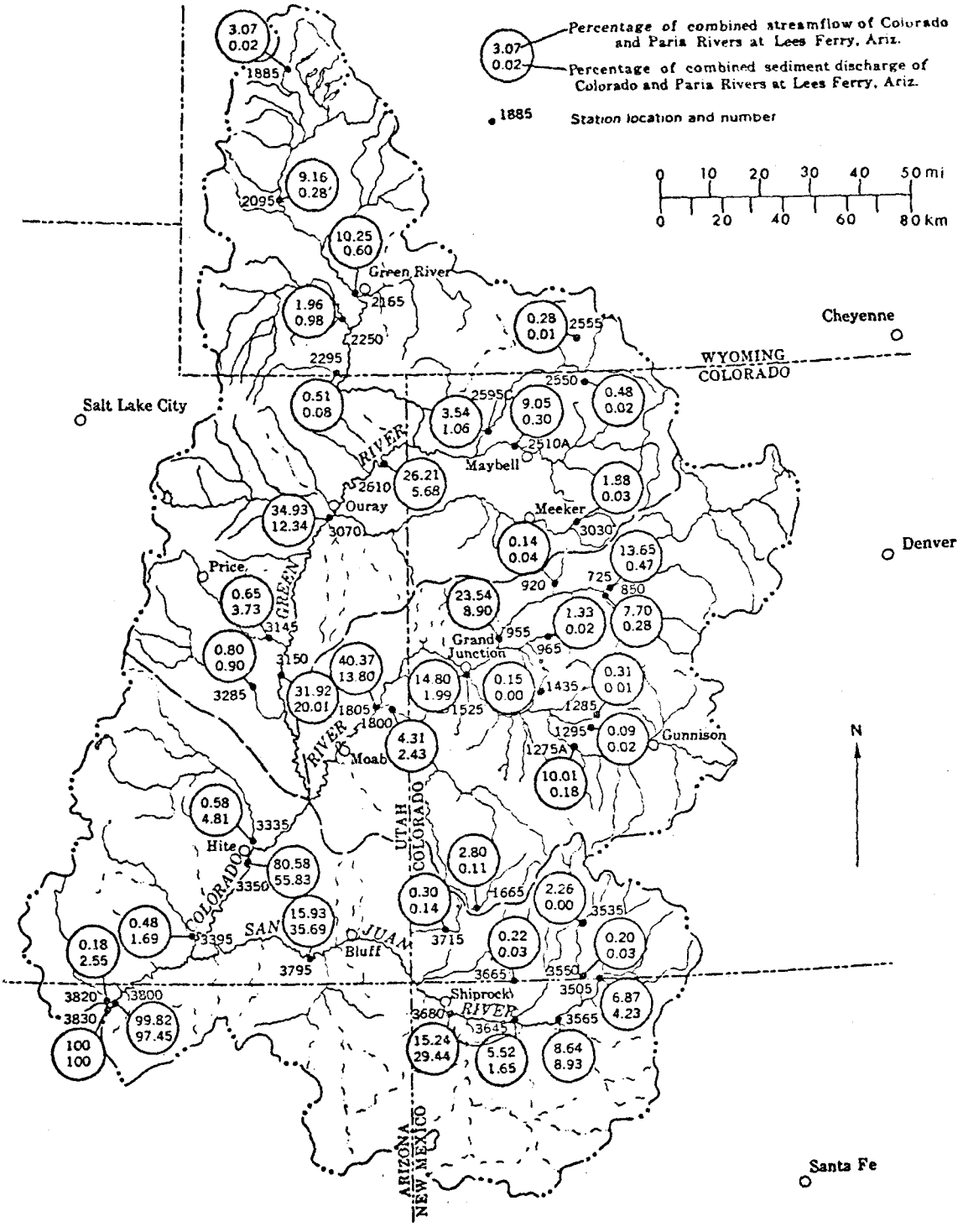

Figure 1.2. Approximate water and suspended sediment discharge expressed as percentages of the combined streamflow and combined suspended sediment discharge of the Colorado and Paria Rivers at Lees Ferry, Arizona (from Iorns, Hembree and Oakland, 1965).

approximately one-half the total salt load of the Colorado River, with the remainder contributed by point sources (one-fifth) and sources affected by man such as irrigated agriculture (about one-third) (U. S. Environmental Protection Agency, 1972). Therefore, it is essential to identify the sources of salinity and to understand the processes of salt storage, dissolution and loading from these natural sources of salinity. For the purpose of this study the research was concentrated on the high salt producing areas of the Mancos Shale.

1.4 The Mancos Shale Terrain

The Mancos Shale crops out south of the east-west trending Book Cliffs of west central Colorado and east central Utah in a broad band of rolling hills to the south and as steep hillslopes with deeply incised bedrock channels, arroyos and gullies to the north. The formation in places appears at the margins of pediments which are gravel-capped. The Mancos Shale also outcrops extensively in the central Dirty Devil and San Rafael Basins, in the central Gunnison Valley and in the Four Corners area near the town of Mancos and in the Chaco River Basin; there are additional outcrops throughout major tributary basins of the central to lower San Juan, Green and Colorado Rivers.

Mancos Shale and stratigraphically associated formations dip 10° to the north in the Grand Valley, south of which the Uncompahgre Uplift exposes Paleozoic to Precambrian rocks (Figure 1.3). Similarly, in the Price Basin area the Mancos Shale encircles the center of the basin dipping 10° away from the San Rafael Swell.

Mancos Shale is a shallow marine formation of Upper Cretaceous age. The lower shales of the formation are of late Cenomanian to early

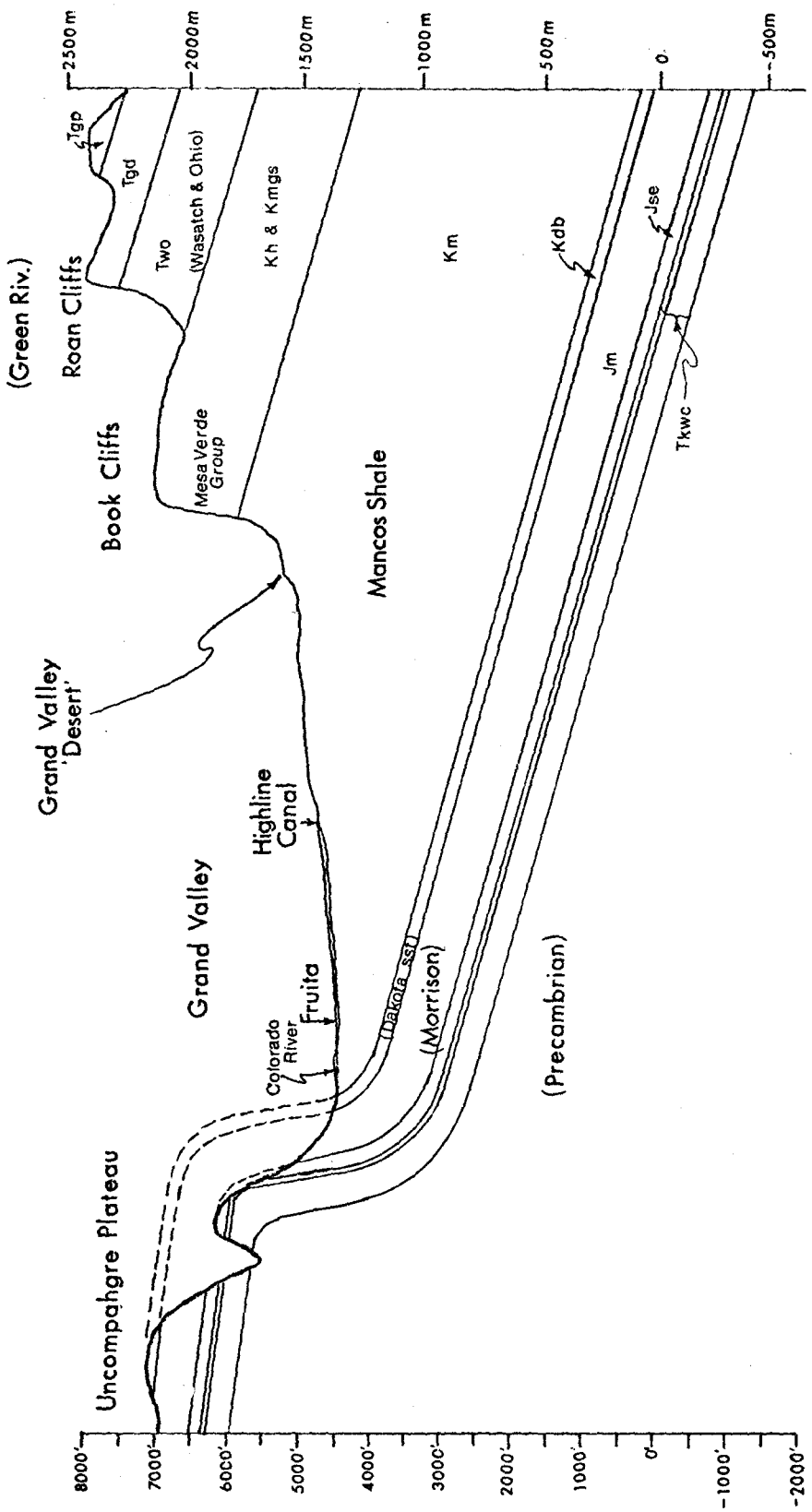

Figure 1.3. Geologic cross section of the Grand Valley (after Schneider, 1975). The vertical exaggeration is 8X. Formation names are given in parentheses.

Turonian age and the upper shales in the sequence are Campanian (Fisher, Erdmann and Reeside, 1960). It is a westward facies of parts of the Pierre Shale which crop out east of the Rocky Mountains and in the Great Plains. Its thickness ranges between 1050 m (3450 ft) and 1265 m (4150 ft) in most areas. It is a saline monotonous marine shale, drab gray where weathered and dark gray, thinly bedded and lacking pronounced fissility when fresh. The dark shale abounds in veinlets of gypsum and calcite and it is often covered with patches of "white alkali" or salt efflorescence. The weathering of the shale produces a friable semi-powdery mass that is sticky and impervious when wet.

Mancos Shale generally includes thin sandstone layers which intertongue eastwards with shales. The thickness and abundance of these increases to the northwest. Minor, gas-rich, hogback-forming sandstone beds are found at different places and horizons. In the Price River area the Mancos Shale has been divided into several members (Stokes and Cohenour, 1956). In ascending stratigraphic sequence these are the Tununk member, a gray marine siltstone and claystone, the concretionary fluviatile partly marine Ferron Sandstone, the light gray and calcareous Blue Gate Shale, the marine to deltaic light colored Emery Sandstone and the gray marine Masuk Shale.

The fluviatile Dakota Sandstone conformably underlies the Mancos Shale and usually crops out as prominent hogbacks or cuestas. The lower part of the Mesa Verde Group, which conformably overlies the Mancos Shale, are interlayered cliff-forming sandstones, coal seams and saline marine shales. Deposition of the late Cretaceous Mesa Verde Group began earlier to the northwest. The Wasatch and Green River

Formations, which unconformably overlie the Mesa Verde Group, are all terrestrial rocks.

Generally, the drainage density is high (100) due to the low infiltration rates and high erodibility of weathered Mancos Shale (Schumm, 1964). Where relief is high, intricate drainage patterns resembling badlands form. Rolling hills characterize only the lower parts of the drainage basins. The shale slopes steepen appreciably toward the Mesa Verde cliffs, and active mass wasting occurs which includes creep, mudflows and rockfalls. These processes are very active in the incised bedrock channels as North Miller Creek.

The climate in the lowlands of the Upper Colorado River Basin is of a semiarid continental type with frequent high intensity convective storms of small areal coverage. Maximum monthly precipitation occurs in July-August. Daily and seasonal temperatures vary widely with extremes of from 42°C (108°F) to -41°C (-42°F) in the Price River Basin (Mundorff, 1972). The average potential evaporation measured with a class-A pan at the Grand Junction airport was 233.0 cm (92.1 in) during the years 1954-1960, and the maximum monthly average was 46.5 cm (18.3 in) during July (Lusby, Reid and Knipe, 1971). Annual precipitation at Fruita in the Grand Valley ranged from 117.9 mm (4.64 in) to 459.2 mm (18.08 in) during 1954-1966. Mean annual precipitation is 250 mm (10 in) at Price, 200 mm (8 in) at Woodside in the lower Price Basin, and 215.9 mm (8.5 in) at Badger Wash with a gradual increase eastward (Mundorff, 1972; Branson and Owen, 1970). The mean annual precipitation at Cortez, Colorado, is 381 mm (15.0 in) (U. S. Dept. of Commerce, 1956).

Soils in parts of the study areas have been investigated and classified by the Soil Conservation Service (Swenson *et al.*, 1970), by the interagency study group at Badger Wash (Lusby, Rheid and Knipe, 1971) and by Knobel *et al.* (1955). Generally, the area is underlain by three Lithosol soil types that are represented by the Chipeta and Persayo soil series. The Billings soil series represents the Alluvial soil group. The lithosols are of the loose sandstone type, reddish loam soils of low salinity and high pH (9.3). The thin gray and brown silty shale loam soils that develop on Mancos Shale have high salinity and a lower pH (8.0). The third lithosol is a mixture of the sandy and shaly soils. It has been determined (Schumm, 1964) that fresh and somewhat weathered Mancos Shale swell considerably when wetted with 25-58 percent volume increase in free swell tests.

Vegetation on most of the Mancos Shale and associated alluvium is of the salt-desert shrub type with subtypes reflecting local differences in soil characteristics and available soil moisture. Except in local areas, the plant cover is sparse with crowns of living perennial plants covering 10-20 percent of the surface (Lusby, Reid and Knipe, 1971). Plant cover is somewhat increased in early summer and in wet years.

CHAPTER 2

PROCEDURE

2.1 Introduction

Two separate research plans were required for this study. The determination of soluble mineral content in surficial deposits requires abundant sampling of these materials at the surface and at depth. Field sites where alluvium and shale were collected are all in Mancos Shale terrain because of the high solute yields from diffuse sources in these areas. Based on two reconnaissance trips to the area, fieldwork was planned such that samples would be collected from sampling units of both alluvium (bed, bank and mass wasted materials) and bedrock (from bedrock channels and from hillslopes). Laboratory experimentation was planned to determine the effects of various parameters on the kinetics of dissolution and on the dissolution potential of the samples. Based on these results, a procedure was adopted to determine salt content.

2.2 Selection of Study Areas

2.2a Location

The study areas were selected to meet the following requirements: they are located in accessible tributary basins of the Upper Colorado River Basin that are known to be high salt contributors to the river system; no irrigation takes place in the study areas.

Soils and surficial sediments were sampled in four such basins during the field season of 1975. The samples of surficial alluvium and Mancos Shale were collected from the unnamed northern branch of Miller Creek (herein called North Miller Creek) in the Price Basin, Utah, from Leach and West Salt Creeks in the Grand Valley, Colorado, and from the unnamed 'Mesa' Creek, a tributary of McElmo Creek near Cortez, Colorado (Figure 2.1).

All of the study areas are located in the High Plateaus and Canyonland sections of the Colorado Plateau Physiographic Province (Fenneman, 1931), and they are partly or completely underlain by Mancos Shale.

2.2b Description of Study Areas

North Miller Creek, with a drainage area of about 10.5 km^2 (4.1 mi^2) above the lower sampling section denoted by number U6, was chosen because of its location in the Price River Basin, one of the single largest contributors of salt from diffuse sources in the Upper Colorado River Basin, and because man's influences are minimal. The U. S. Geological Survey monitors water discharge and specific conductance of the Price River at Woodside, Utah. Moreover, several researchers from Utah State University have also been involved in salinity studies in the Price River Basin (e.g., Ponce, 1975).

Numbers of samples from North Miller Creek and from other studied basins are comprised of a first character which identifies the general sampling area ('U' stands for the Price Basin, Utah, 'G' for the Grand Valley and 'M' for Mesa Creek). For samples from North Miller Creek, the second character identifies a channel reach, the third corresponds

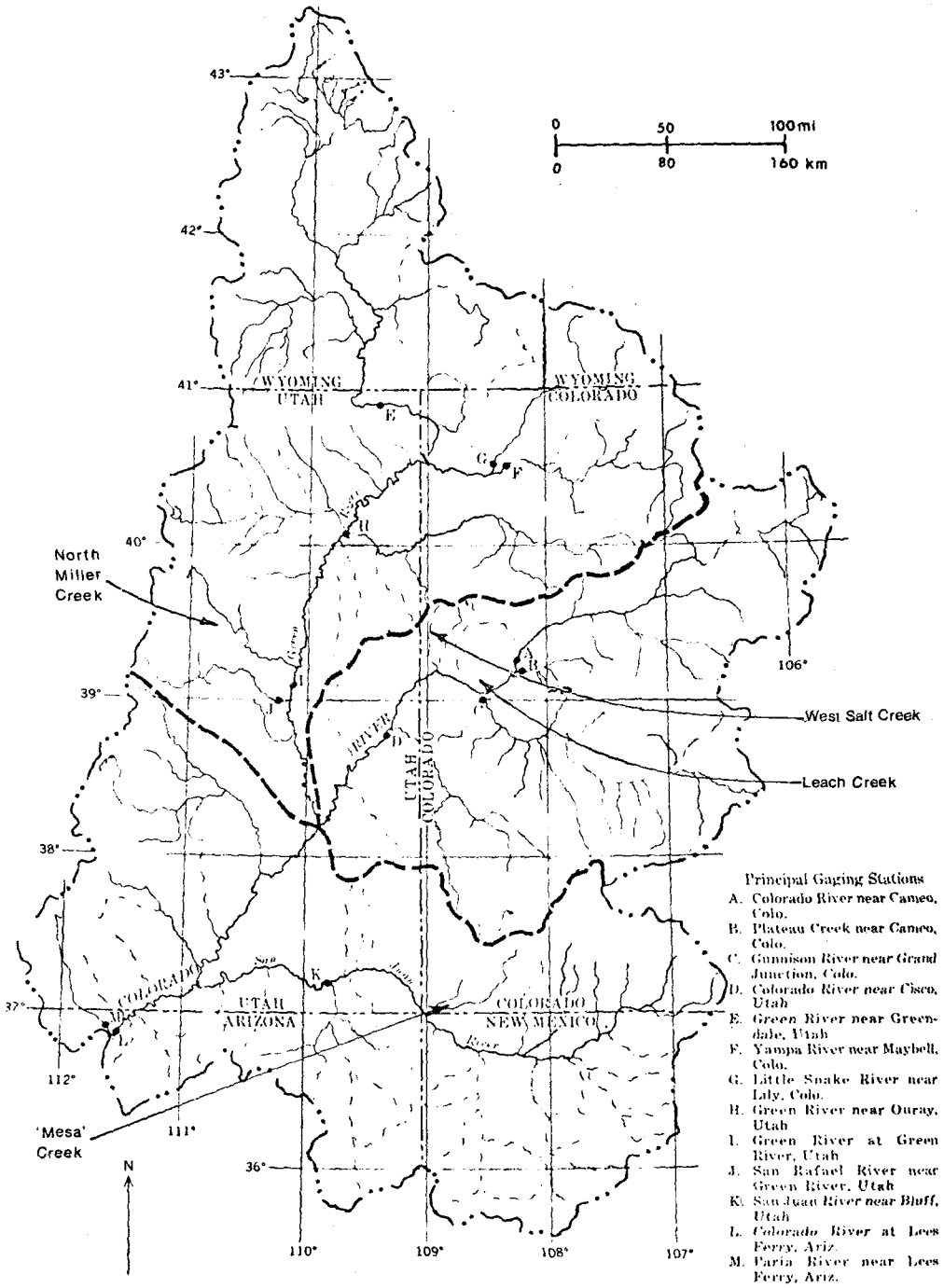

Figure 2.1. Map of the Upper Colorado River Basin showing location of study areas.

to a channel section, the fourth corresponds to a sampling unit and the last character corresponds to a given sampling depth. Because only one section was sampled intensively within each studied reach in West Salt, Leach and Mesa Creeks, samples from these areas are denoted by four characters. The course of the main channel of North Miller Creek is parallel to the Wattis coal mine road. Samples U5B1 to U5Z1B correspond to locations sequentially more upstream in the upper reach as shown in Figure 2.2. The upper reach of North Miller Creek that was chosen for detailed study is deeply cut into the Mancos Shale bedrock and it is bounded by unstable vertical walls which may reach 15 m (49 ft) in height. As the channel meanders shifted and downcut through the shaley bedrock, alluvial aprons formed on the abandoned bends (the convex or inside banks). The channel bed is presently downcutting and bedrock is exposed throughout the studied reach. Most of the alluvial deposits are terraces 2-15 m (6-49 ft) above the present elevation of the channel bed. The alluvium, which is primarily comprised of sands and gravel, together with the unstable shaley bedrock, provides a large sediment load as it mass wastes from the gully walls.

The Mancos Shale 'desert' of the northern Grand Valley has been studied for a number of years in connection with sediment yields (Lusby, Reid and Knipe, 1971) and with the salt contribution of the valley to the Colorado River (e.g., Skogerboe, 1972). Leach Creek (Figure 2.3) drains the Book Cliffs and the adjacent Mancos Shale lowland, which is partly occupied by large dissected pediments. The basin is small (22 km^2 or 8.7 mi^2) and a road follows the creek up to its headwaters in the Book Cliffs. In the lower area of the drainage basin (above the Government Highline Canal) the channel bed is only slightly

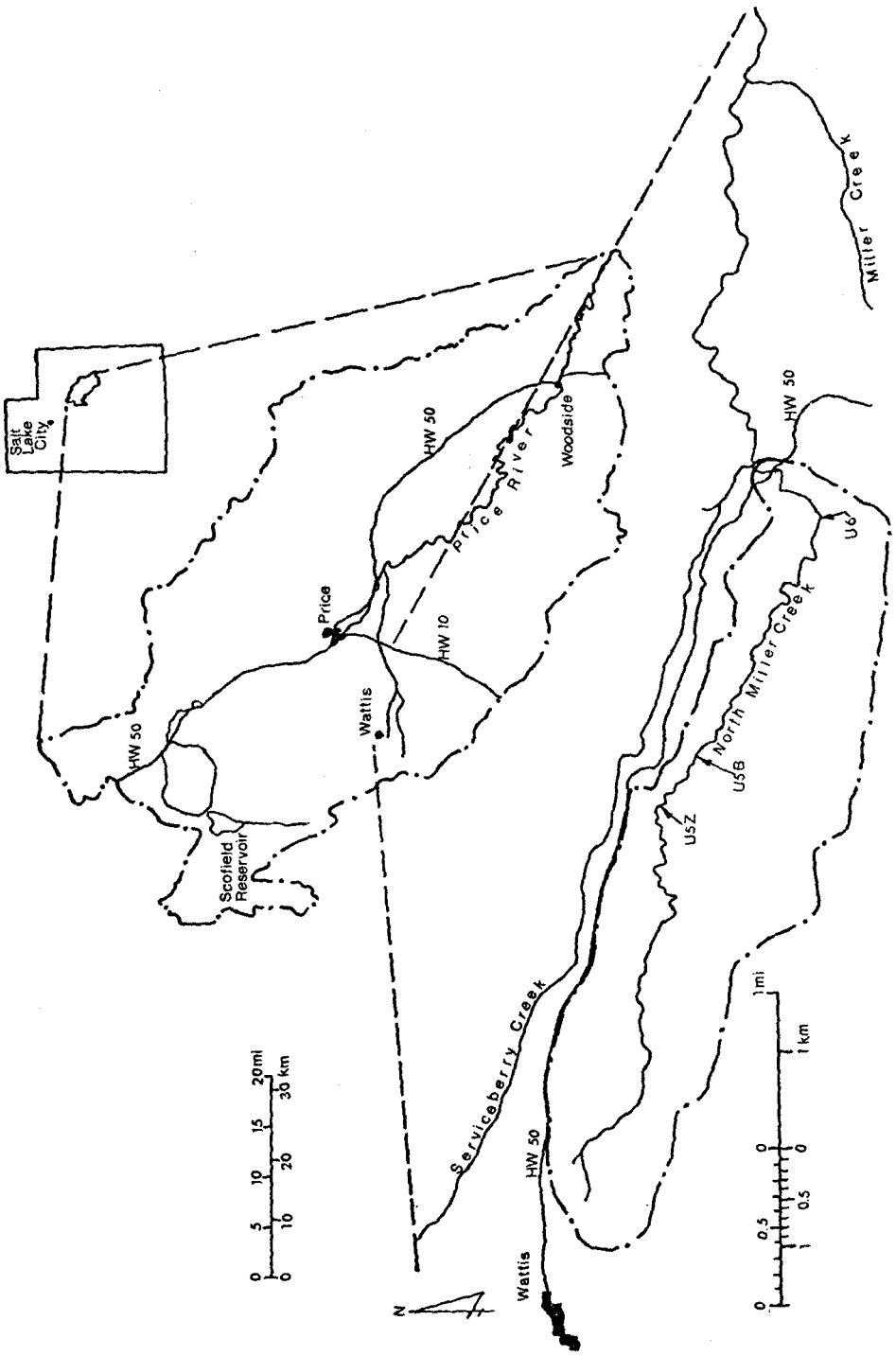

Figure 2.2. Map of the Price River Basin showing the location of the North Miller Creek study reach.

gullied and overlies 5-8 m (16-26 ft) of alluvial fill like the neighboring Indian Wash (U. S. Dept. Agr., 1964).

West Salt Creek drains an area of 435 km^2 (170 mi^2) and it is located in the westernmost extremity of the Grand Valley (Figure 2.3). The headwater channels drain the southern face of the Roan Cliffs which are underlain by the lower Green River siltstones and marls. The upper part of the basin is underlain by sandstones and shales of the Mesa Verde Group and below section G11 (Figure 2.3) the valley broadens as West Salt Creek enters the Mancos Shale. A Geological Survey station is located in the southernmost area broadly underlain by shale. Between this gaging station and the confluence with the Colorado River, West Salt Creek flows over the deep alluvial fill of the Grand Valley. West Salt Creek is unique in having a gaging station and an EC metering facility.

Sections G7 through G10 are in the main West Salt channel (Figure 2.3) where it is incised in alluvium (100-150 m or 320-480 ft thick) to a depth of 5-10 m (16-32 ft) below the upper terrace. This terrace constitutes the valley floor. At section G8, the junction of the channel with the Mitchell Pass Road, the channel abutts against a Mancos Shale slope where a small saline seep is perenially active. Salt efflorescence is very conspicuous downstream of the seep. Section G11 is located in the main channel above the confluence with South Canyon Gulch. Here the valley narrows between the steep slopes and cliffs of alternating sandstones and shales, and the channel, which is incised into the alluvium, is a source of many small saline seeps. These seeps become more numerous upstream.

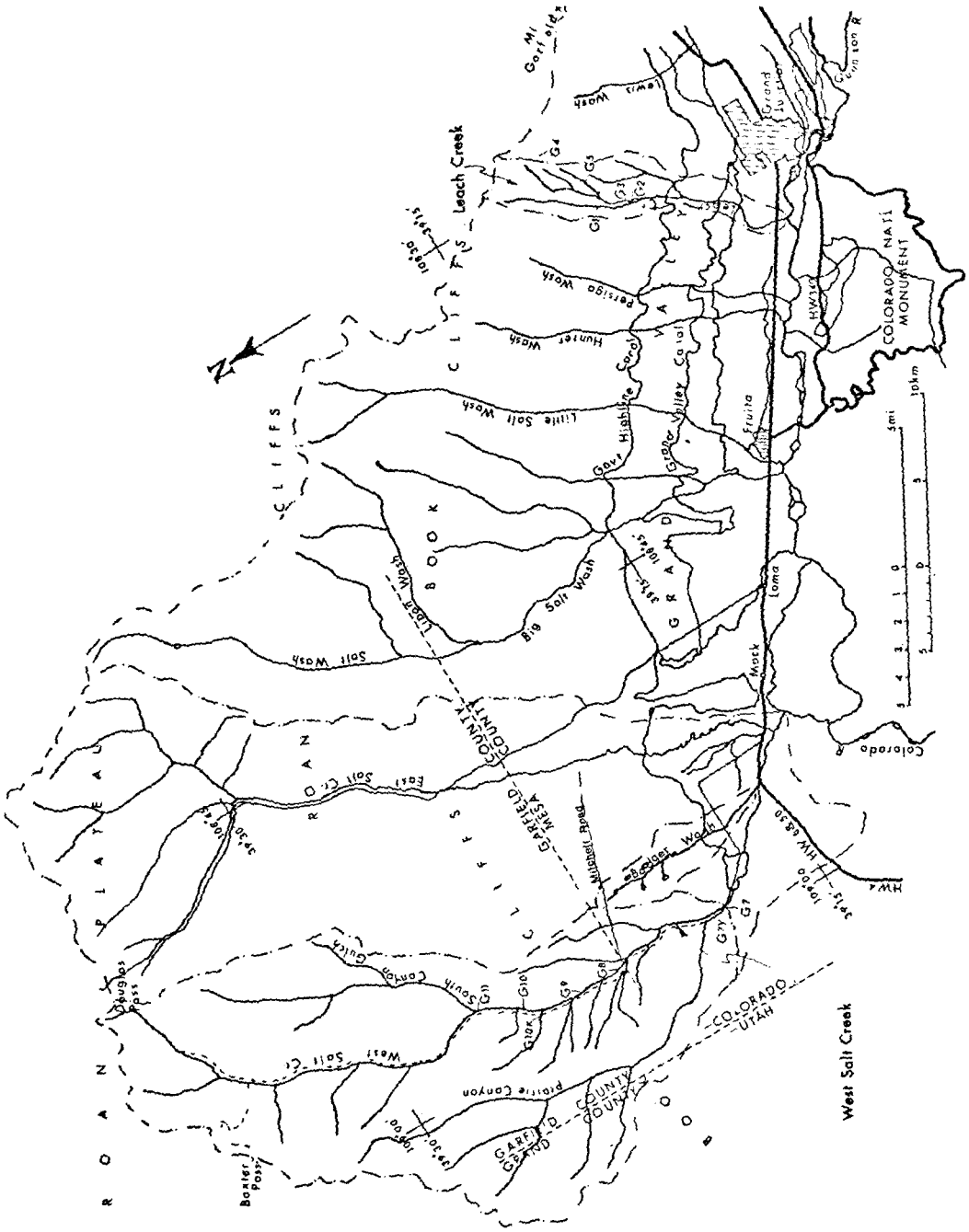

Figure 2.3. Map of the Grand Valley showing location of sampling sections in Leach and West Salt Creeks.

McElmo Creek is a highly saline tributary of the San Juan River. Grab samples (U. S. Geol. Survey, 1969-75) indicate a large range in TDS with a relatively high (1.6-2.7) sodium absorption ratio. The salinity of McElmo Creek is considered to originate from diffuse sources including irrigation in the basin. Several of the tributaries of McElmo Creek are underlain by Mancos Shale. Among these, only the unnamed 'Mesa' Creek (Figure 2.4) has a stage recording gaging station but data from this station is not available. Mesa Creek is essentially a smaller version of Leach Creek although it is not accessible in its headwaters which lie within Mesa Verde National Park. Therefore, data was collected only in three lower reaches.

M1 and M2 samples represent a reach where the channel abutts against an actively mass wasting Mancos Shale bluff. The M3 samples were taken to determine variations in salt content with depth in an alluvial reach. The M3 and M4 reaches are similar except for the coarser bed of the latter.

2.3 Methodology

2.3a Sampling Techniques and Sampling Error

Soils and surficial sediments were drilled with a 10 cm diameter bucket-type auger. Drilling direction was perpendicular to the surface. Salt efflorescence and crusts were sampled by hand. Crusts normally form in semiarid regions and crusts were present at many sampling sites except on terraces and in some sandy channels. Because crust thickness (0.1-10 cm or 0.04-4 in) may vary with the sediment size distribution, mineralogy and antecedent moisture conditions, the crusts were collected in their entirety.

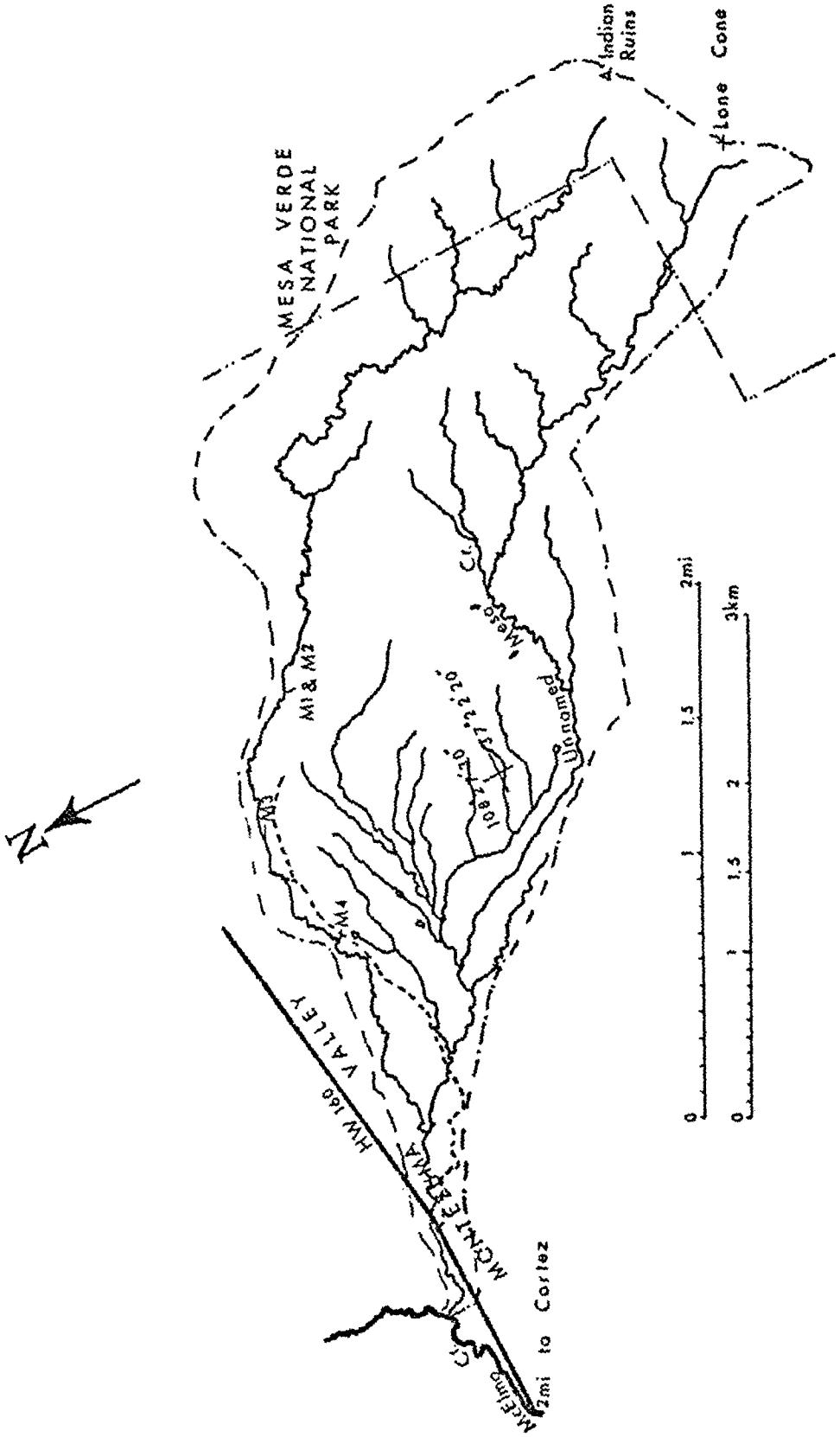

Figure 2.4. Map of the un-named 'Mesa' Creek Basin showing location of sampling sections.

Sampling holes were drilled in the bed, banks and in the terrace of each channel cross section. These morphologic units, in conjunction with hillslopes, are herein referred to as sampling units. Sections were chosen to represent a fairly long channel reach. More than one set of samples of a given sampling unit was taken whenever variability was either noted or expected.

These sampling errors may be identified. The first is related to the drilling process whereby the sampled material includes matter originating from previously-sampled parts of the same drilling hole. Another, more significant, sampling error results from the large natural variability in salt content of sampled materials. The third sampling error results during splitting of a sample in the laboratory and it is related to the variability in salt content of the given samples. Yet another error may arise when a selected cross section or sampling unit does not adequately represent a channel reach.

Drilling in dry sand and in gravelly sand often disturbed overlying materials which, in turn, fell into the sampler bucket. Table 2.1 summarizes the size distributions of samples G8I4 to G8I7 and G8H1 and G8H2. The G8H samples were drilled horizontally into the vertical bank of West Salt Creek 60 cm (24 in) below the terrace and they represent a sandy layer lacking gravel with a thickness of about 20 cm or 8 in (i.e., extending approximately 50-70 cm or 20-28 in below the terrace). The G8H samples were drilled vertically in the terrace proper. Comparison between the size distribution of samples G8I4 and G8I5 reveals their similarity (gravelly coarse sand) while samples G8H1 and G8H2 are also similar (sandy). Although samples G8I6 and G8I7 are supposed to represent the sandy layer, they both

Table 2.1. Size distribution (percent finer than) data for selected terrace (G8I) and gully wall (G8H) samples from West Salt Creek.

Sample Number	Depth (cm)	Particle Size (mm)									
		0.061	0.125	0.250	0.500	1.000	2.000	4.000	8.000	16.00	32.00
G8I4	25-35	3.37	8.18	20.46	34.27	44.71	58.54	70.34	80.54	91.61	100.01
G8I5	35-45	2.71	7.49	22.20	36.79	45.67	55.46	63.07	72.21	89.98	100.00
G8I6	45-57	5.17	16.50	53.55	79.21	85.87	90.53	93.19	96.03	98.31	100.00
G8I7	57-73	4.00	14.93	58.25	93.37	97.45	98.76	99.46	99.90	100.01	
G8H1	0-13	3.64	14.60	69.41	98.48	99.59	99.83	100.00			
G8H2	13-21	3.66	14.80	71.09	98.50	99.53	99.76	99.89	99.99		

(but to a lesser extent G8I7) contain appreciable amounts of coarse sand and gravel, the percentage of which is an indicator of in-place sampling error.

Unlike sediment size, soluble mineral content will be subject to change after deposition. Slightly soluble sediment particles remain stationary after sedimentation while salt may be dissolved and transported by percolating ground water. Soluble mineral content is expected to vary with aspect, being higher on slopes where evaporation is also higher and gives rise to accumulations of saline crusts, and it varies with surface elevations. The thalweg, being the lowest surface in any given cross section is wettest and it collects water even during low flows and consequently it will be rich in salts upon evaporation of the water.

Specific conductance of saturated paste extracts of Mancos Shale crusts from two large scale sampling grids reportedly varies as much as tenfold (Ponce, 1975). This variation in salt content decreases as the sampled area decreases, which is most likely due to the greater homogeneity in lithology, aspect and moisture content in a given locale. Ponce (1975) also shows that one salt content determination is inadequate for areal representation of salinity. The standard deviation of many of the soluble mineral contents of specific sampling units is indeed very large, as will be discussed in detail in Chapter 4.

In addition to the forementioned variability in soluble mineral content of surficial materials it appears that there is a small but significant variation within parts of a sample. Portions of a given sediment mass were randomly sampled by splitting. Samples G8G1 and

U5D1A were mixed with water at 1:999, 1:99 and 1:9 ratios. Five to six subsamples at each sediment concentration were shaken until equilibrium was approached. The determinations of specific conductance at given contact times are summarized in Tables A3.1 and A3.2 of the Appendix. Mean EC and standard deviation (σ) for each contact time are also included. The variability index, $100(\sigma/\overline{EC})$, in percent, is equal to the coefficient of variation times 100 and it is used to compare the variability of mixtures of different ionic strengths.

The variability in EC, and hence in soluble mineral content, decreases with increased sediment concentration for the equilibrated alluvial (G8G1) mixtures. The variability index is 34.7, 5.0 and 2.0 percent for the equilibrated 1:999, 1:99 and 1:9 mixtures. No such trend is obtained with sample U5D1A. Because more material is involved as mixture concentration increases (0.4, 4.0 and 40.0 g, respectively) it might be argued that the larger subsamples better represented the sample as a whole, thus explaining the variability trend of sample G8G1. The variability index of the G8G1 1:999 mixture is large ($\sigma \simeq \overline{EC}/3$) due to the late acceleration in dissolution rate of the third subsample. The variability is, however, reasonably small (i.e., one standard deviation is equal to less than 12.7 percent of the mean) for all other mixtures. It may therefore be inferred that the standard deviation of soluble mineral content within a given subsample is in the order of $\pm$ 10 percent for most samples. Additionally, no significant trend of variability decrease with contact time was noted.

2.3b Laboratory Procedure

Agronomists and agricultural engineers use filtered saturated-paste extracts or 1:1 sediment:water ratio extracts to determine the salt content of soil materials (U. S. Dept. Agr., 1954). These determinations are based on a shaking time of one hour or, at times, of 24 hours. The extracts are obtained in order to evaluate the amounts of dissolved solids present in soils with moisture contents ranging from a few percent to a maximum of about 50 percent. The effects of contact time and sediment:water ratios reported in this study were found to be crucial in the determination of the amount of solutes released from soils and surficial sedimentary deposits and therefore, a new procedure was adopted which is based on these effects.

Because the 'salt content' of a sediment ultimately depends on the contact time and on the amount and quality of the diluting agent as demonstrated in Chapter 3, it was decided to simulate the behavior of alluvium and Mancos Shale sediments in channel flow by using a 1:99 sediment:water mixture (i.e., equivalent to 10,000 ppm solid sediment concentration). Hence, soluble mineral (SM) content (in percent) was calculated as follows:

SM content =

$$[(TDS_{1:99}\ \text{mg/l})\ (\text{g}/10^3\text{mg})\ (\text{liter}/10^3\text{ml})\ (99\ \text{ml/g})]\ 100 =$$

$$(TDS_{1:99})\ 0.0099$$

Samples were air dried at room temperature for several days. The sediment:water mixtures were shaken in 500 ml Erlenmeyer flasks. For 1:1 weight ratios of sediment:water, 200-300 g of sample were placed

in the flask to which the same volumetrically measured weight of water was added. The flasks were closed with rubber stoppers to eliminate evaporation and then were shaken one hour on a horizontal 15-bottle capacity shaker at 110-130 cycles per minute. The mixture was allowed to stand in contact with air for several minutes prior to EC measurement. During this time 25 ml of the mixture was poured into the EC meter cup and its temperature was recorded. A 'Lectro Mho Meter' (Lab-line Instruments, Inc.) EC meter was used throughout the laboratory experiments. The solvent and diluting agent in all experiments was distilled water of $8 > EC > 1.5$ μmho cm^{-1} at 25°C and of $5.5 < pH < 6.5$.

In order to maintain a consistent degree of turbulence in the mixing flasks, the preparation of the samples consisted of splitting them (in order to ensure a representative size distribution) so that the total volume in the mixing flask was approximately constant (400 cm^3). The coarsest particles used in 1:99 mixtures of gravelly samples were eliminated by the splitter or by the operator because of the small weight (4.0 g) of sediment used. Mixture temperatures varied with room temperature, with mixing time due to heating by the shaker, and with location on the shaker plate. Mixture temperatures were mostly in the 23-27°C range with recorded minimum and maximum values of 21°C and 33°C, respectively. The EC at 25°C was ensured by a temperature calibrating dial on the EC meter.

Plots of EC *vs* time (Figures 3.1a and 3.1b) were used to determine the approximate time necessary to shake 1:4, 1:9 and 1:99 mixtures. From these plots the one-hour $EC_{1:1}$ was plotted against the time (t_{90}) necessary to reach 90 percent of the approached 24-hour equilibrium

(EC_{90}) for 1:4, 1:9 and 1:99 mixtures (Figure 2.5). For most samples which appear in Figures 3.1a and 3.1b, t_{90} increases as the sediment: water ratio increases. t_{90} increases as the potential soluble mineral content decreases. Because of the approach towards equilibrium, $(EC_{1:99})/(EC_{1:9})$ ratios remain essentially constant with time during late dissolution stages. Therefore, the longer mixing times of 1:9 as opposed to 1:99 mixtures ensure that the more concentrated mixtures are in the same dissolution stage (in terms of equilibrium approach) as are the dilute mixtures.

The chemical analyses of soil solutions and runoff samples were undertaken by the Colorado State University Soils Laboratory using standard methods (U. S. Dept. Agr., 1954). Only Ca^{2+}, Mg^{2+}, Na^{2+}, SO_4^{2-} and HCO_3^{1-} were analyzed in most solutions. For the large majority of the analyses, $100\left|(\sum C_i^{z-} - \sum C_i^{z+}) \;/\; \sum C_i^{z-}\right| < 10$ percent, where C_i denotes concentration in meq l^{-1} of the i^{th} ion, and $z+$ and $z-$ are the charges of the cations and anions, respectively. Following the recommendation of the American Public Health Association (1965, in Lane, 1975), most of the present analyses fall within the acceptable limits of

$$\sum C_i^{z+} - \sum C_i^{z-} = \pm(0.165 + 0.0155 \sum C_i^{z+}).$$

This range is reportedly ± one standard deviation of an average analytical error.

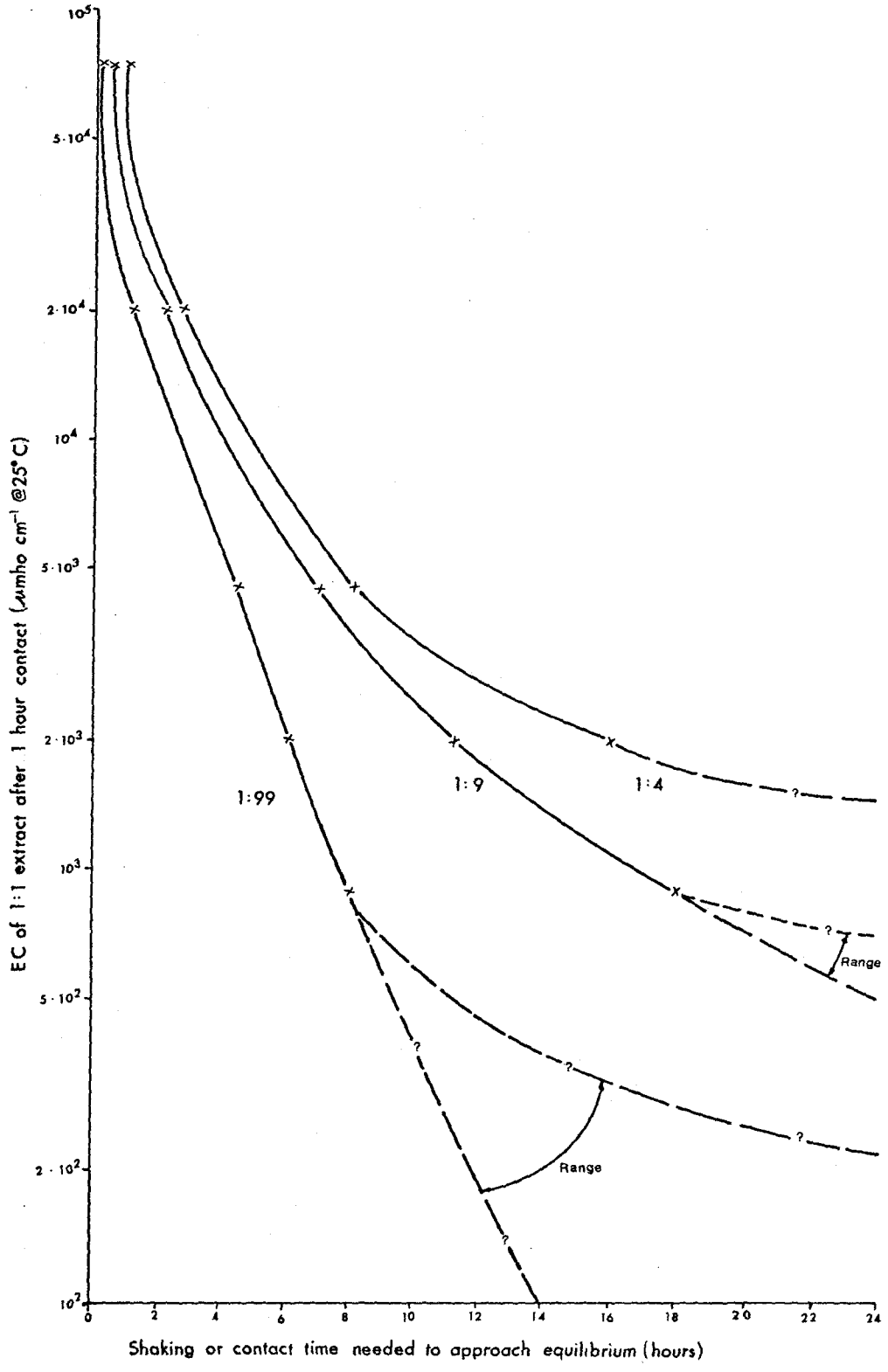

Figure 2.5. The 1:1 electrical conductance and mixing time necessary to approach equilibrium for 1:99, 1:9 and 1:4 sediment: water mixtures.

CHAPTER 3

THE POTENTIAL FOR MINERAL DISSOLUTION

In order to determine the amount and the type of salts that are stored in geologic formations, one may study the samples mineralogically or petrographically, or else dissolve them in water for chemical analysis. A review of the vast literature on dissolution of minerals reveals that both the type and the amount of dissolved matter, which is released from geologic materials in contact with water, depend on the dominant soluble minerals, temperature, pressure, turbulence, contact time, particle size and sediment:water ratios (i.e., sediment concentration). In this chapter the results and analyses pertaining to the dissolution potential of alluvium and related surficial Mancos Shale will be presented and discussed.

Minerals are soluble to some extent in any solvent. Some minerals such as halite or mirabilite ($Na_2SO_4 \cdot 10H_2O$) are highly soluble in water; but most rock-forming minerals such as calcite, feldspar and quartz are only slightly soluble. Solubility is defined as the mass of a substance contained in a solution which is in equilibrium with an excess of the substance (Weast, 1975, p. F109). The solubility of minerals is given by their concentration in the solvent. The magnitude of individual or specific ionic concentrations also depends on the presence of dissolved matter derived from other mineral sources. The concentration of ion species is given by their solubility product, which is related to the mineral that precipitates from solutions

containing these ions. The solubility product (K_{sp}) of a mineral is an intrinsic parameter that varies with temperature, pressure and the concentration of the solution.

3.1 Electrical Conductance as an Index of Dissolution

Dissolved matter includes electrically charged ions and charged ion complexes (e.g., Na^{1+} and $NaSO_4^{1-}$, respectively) as well as uncharged molecules such as CO_2 and H_2CO_3 and uncharged associated molecules, ion pairs in true solution such as $CaSO_4^{\circ}$. The capability of a solution to transmit electrical current depends on the characteristics of the solvent and on the presence of electrically charged dissolved matter. Specific electrical conductance, usually referred to as specific conductance and herein abbreviated EC, is therefore used as an index of total dissolved solids (TDS) concentration. EC is the electrical conductance of a substance between opposite sides of a cube, one centimeter in each direction. The units of EC are ohm^{-1} cm^{-1} or mho cm^{-1}.

It can be shown (Stumm and Morgan, 1970, p. 37) that the equilibrium product (K_{eq}) and, therefore, the solubility product and the EC are dependent on temperature and on pressure. In general, the effect of pressure on mineral dissolution is smaller than the effect of temperature. Gypsum and calcite are common in the geological materials sampled in this study and, therefore, it may be added that the solubility of gypsum (i.e., also the EC of such a solution) increases while that of calcite decreases with increase in temperature at atmospheric pressure.

The effect of contact time on EC is shown in Figures 3.1a and 3.1b where EC is plotted against time for seven alluvial samples at different

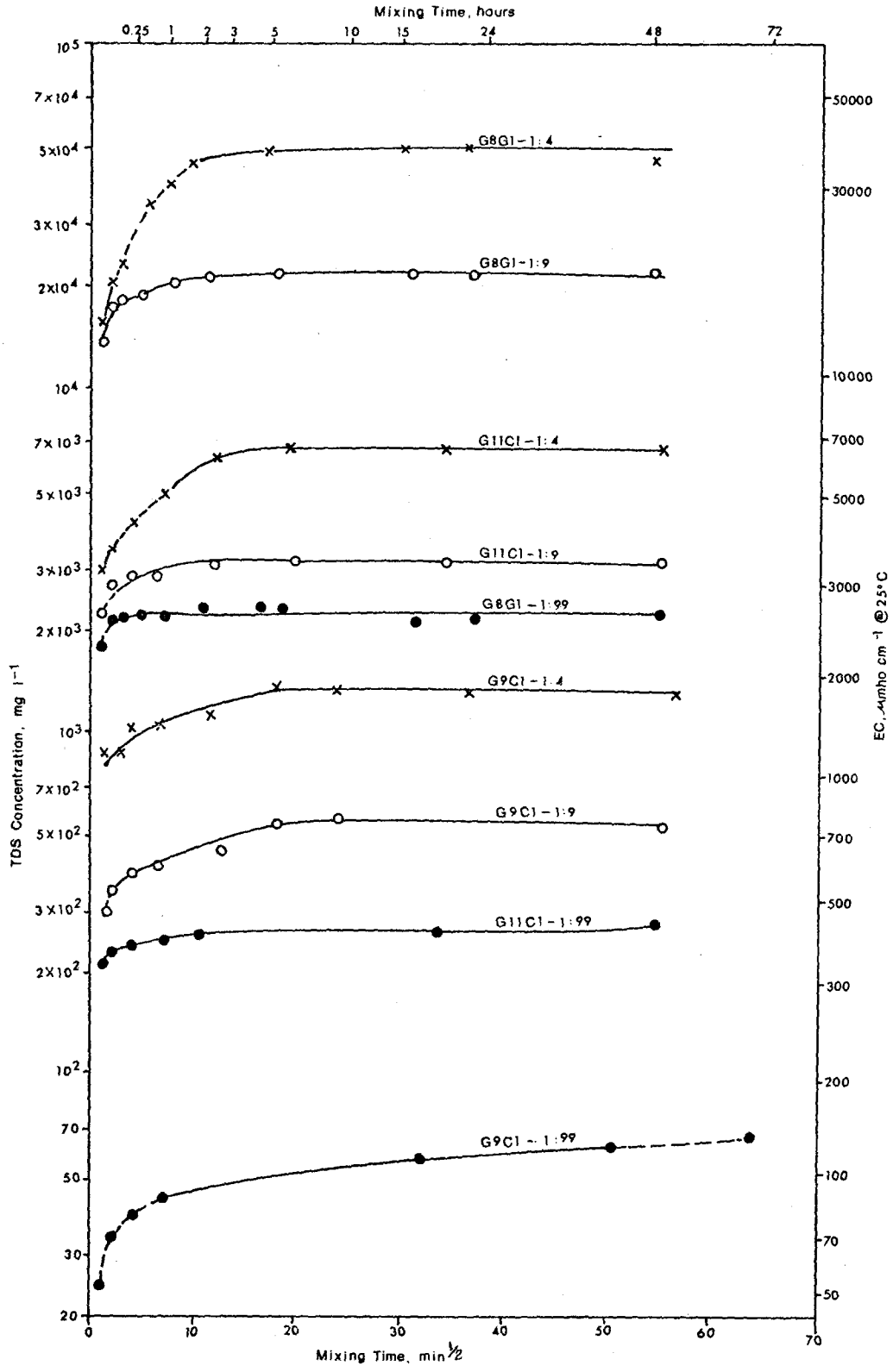

Figure 3.1a. Dissolution kinetics of selected surficial materials.

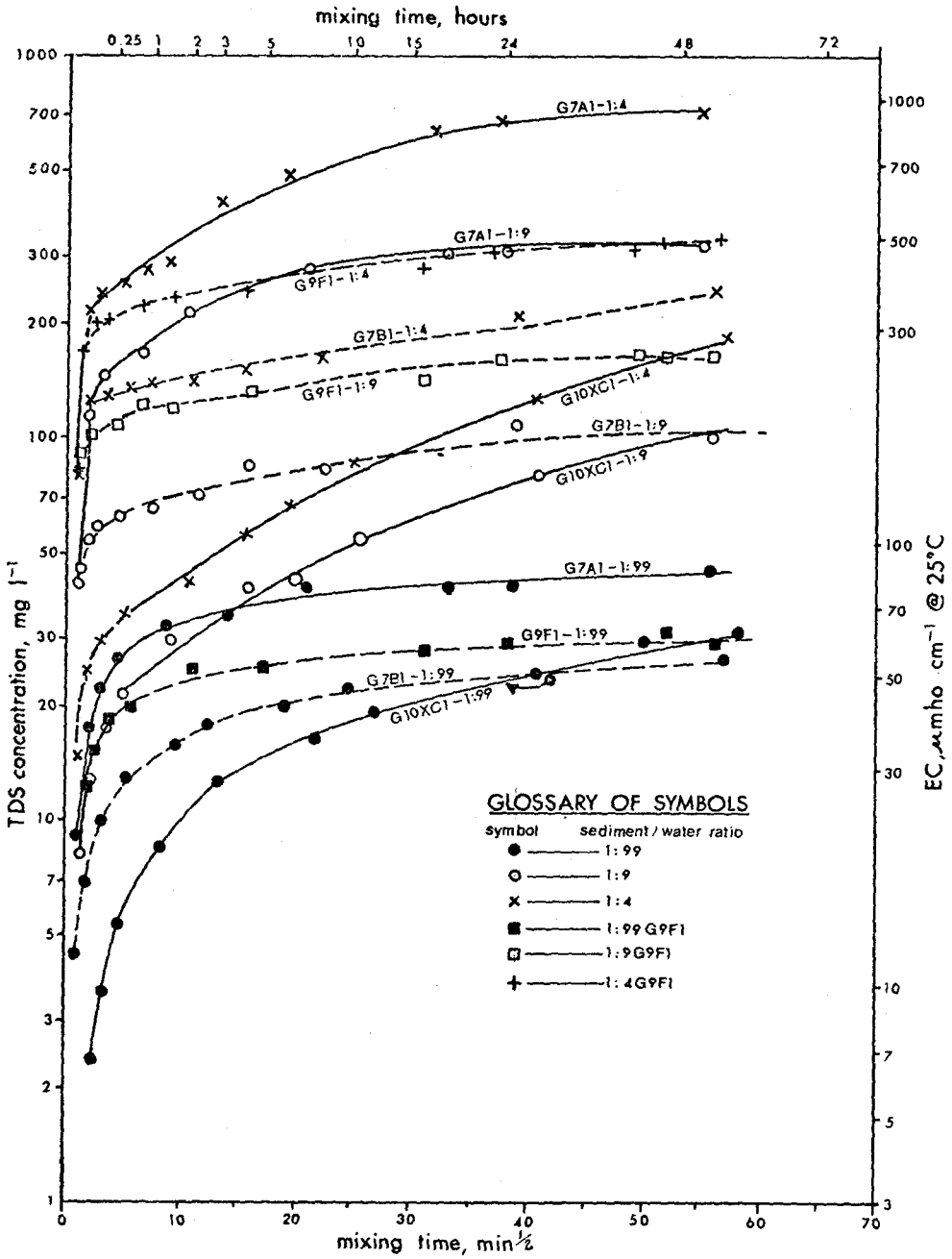

Figure 3.1b. Dissolution kinetics of selected surficial materials.

sediment:water ratios. For all the samples EC increases with contact time. The dissolution rates are similar to several diffusion functions but the reaction paths are of many varied types and the only general equation to which they fit is a high-ordered logarithmic function of the form:

$$EC = a + b \log t^n$$

where a and b are constants and $n>>1$.

Non-metalic and uncharged solid matter in contact with a solution does not enhance the transfer of electrical current through the solution. Therefore, the presence of varying amounts of such solids (e.g., quartz particles) will not affect the EC of the suspension. However, clay particles with charged surfaces as well as with non-perfect crystal lattices with charged broken edges may orient themselves (a plating phenomenon) and actually enhance the transfer of current. The degree of plating may increase with the duration of direct current (DC) transfer. Therefore, with merely several (1-5) seconds available for the measurement (with AC current) of the resistance of the mixture, plating effects should be minimal.

EC data for various types of suspension and their filtered solutions are summarized in Table 3.1. From this table it appears that the amount and presence of solid matter does not affect EC substantially.

The change of concentration with time (Berner, 1971, p. 26) may be derived from Fick's laws of diffusion and be described by

$$dC/dt = D\bar{A}(C_s - C)/1 \qquad (3.1)$$

where $\bar{A}$ is the total surface area of material being dissolved per unit volume of solvent, C is the non-equilibrated concentration in the rapidly mixed solution, C_s is the concentration at the surface of the

Table 3.1. Equilibrium EC (μmhos cm^{-1} @ 25°C) values of selected mixtures (unfiltered) and solutions (filtered or centrifuged).

Sample Number	N[a]	1Q[b]	40[c]	C[d]
G9F1 (1:99)	63	85.5	86	62
G9F1 (1:9)	277	300	290	250
G9F1 (1:4)	520	480	460	452
G9G1 (1:99)	132	161	148	135
G9G1 (1:9)	708	713	681	720
G9G1 (1:4)	1490	1440	1280	1510
G11C1 (1:99	440	443	430	448
G11C1 (1:9)	3310	3100	3100	3385
G11C1 (1:4)	6400	6000	5940	6500

[a] N = settled solution, remixed for test.

[b] 1Q = filtered through #1 Qualitative Whattman paper.

[c] 40 = filtered through #40 Ashless Whattman paper.

[d] C = centrifuged at 4500 rpm and 5 cm radius for 5 minutes.

dissolving mineral minus the equilibrium solubility, and 1 is the thickness of a layer which is formed near the dissolving surface if the solution is not quiescent. This equation (3.1) shows that the rate of dissolution increases with increase in surface area of the solvent. Hence, as particle size decreases the surface area per unit volume increases and, therefore, at least initially, finer material should dissolve faster than coarser material.

Figures 3.2a and 3.2b describe the dissolution paths of a silty shale (number U5D1A) and a gravelly sandy alluvium (number G8G1) in distilled water. Both samples were individually sieved into 1 phi in-

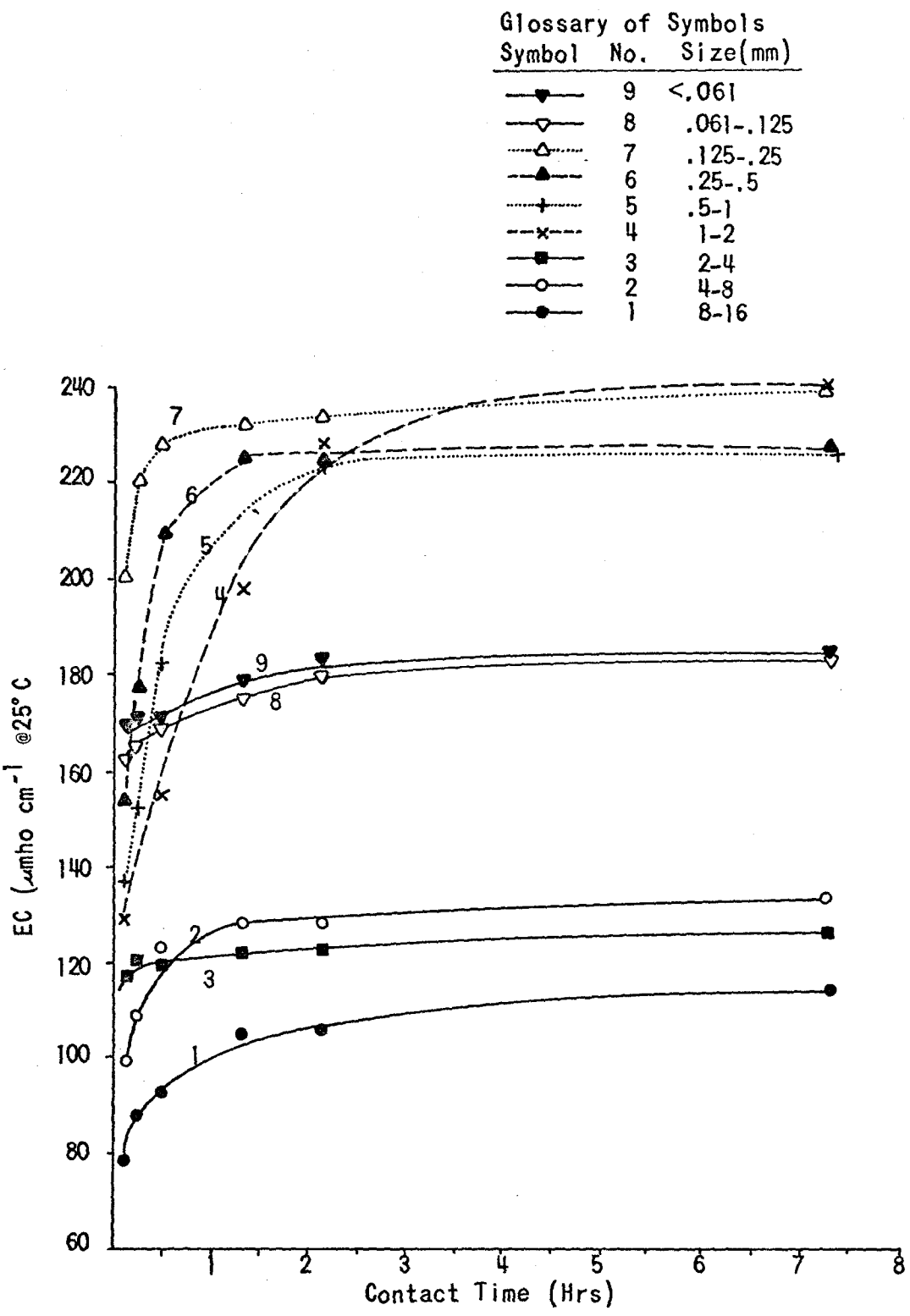

Figure 3.2a. Dissolution kinetics of a shale-rich sample (U5D1A, 1:99) by size groups.

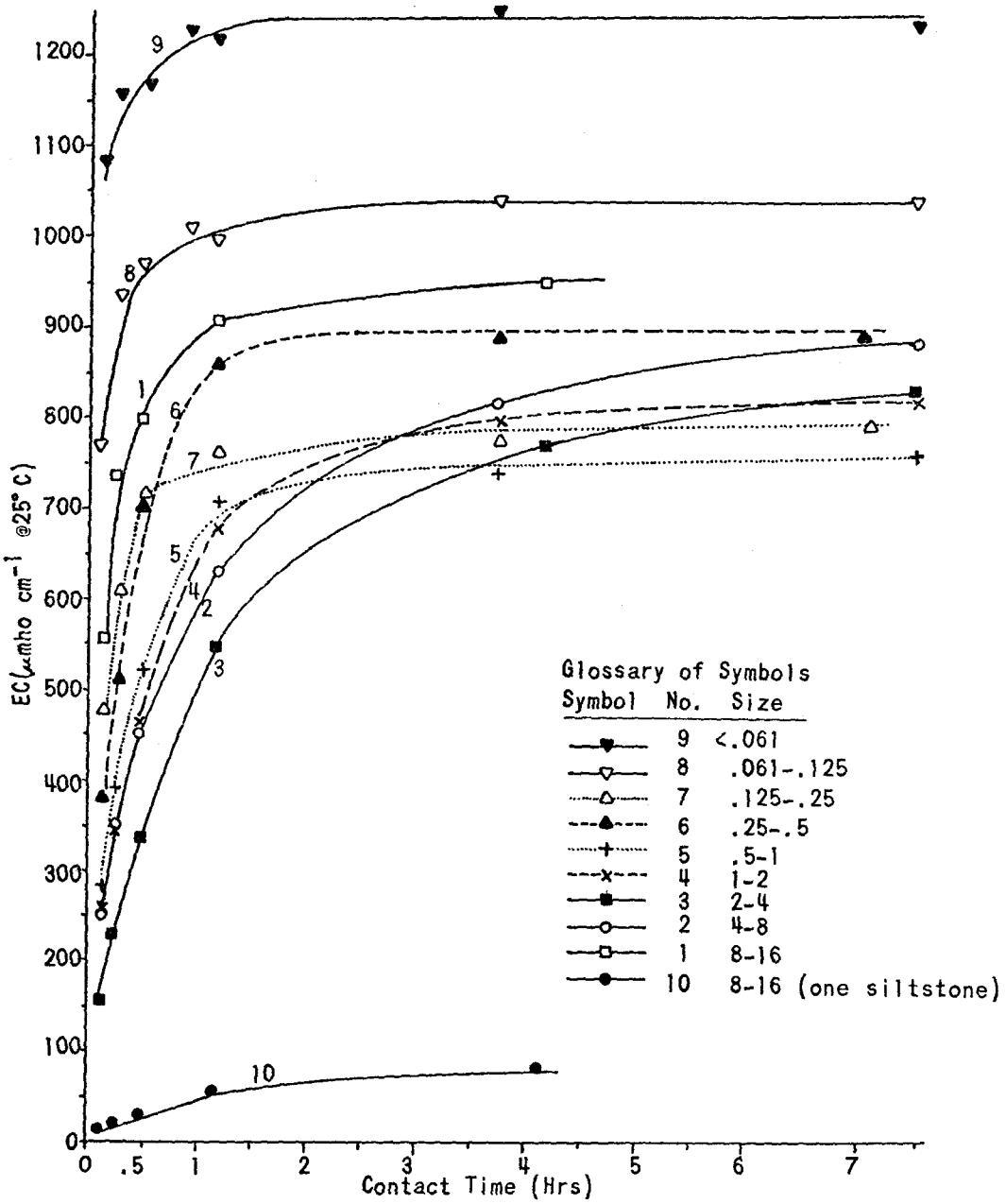

Figure 3.2b. Dissolution kinetics of an alluvial sample (G8G1, 1:99) by size groups.

terval size units. It was observed for each of the 1 phi size groups of sample U5D1A that the rate of decrease of particle size with sieving time was very high. The derived particles of this sample were essentially aggregates of shale and silty particles. These aggregates also broke down very fast (< 30 min) during shaking in the subaqueous environment. Hence, the 1 phi interval size distribution, acquired after 5 min of sieving, must be regarded as artificial. Certainly, because of the fast subaqueous breakdown of the aggregates it is only meaningful to regard the first few minutes of the dissolution experiment. The 1 phi size group curves of Figure 3.2a do not show an increase in dissolution rate with decrease of particle size. The same is true for Figure 3.2b. The discrepancy between theory and measurement is most probably a result of the use of non-pure solids comprised of mineral aggregates.

The effect of turbulence on the magnitude of the electrical conductance is directly deduced from equation 3.1, where l is the thickness of a layer surrounding a dissolving particle. Because l is by definition inversely proportional to the extent of mixing (i.e., to the magnitude of turbulence) then dC/dt increases as turbulence increases.

Table 3.2 summarizes EC *vs* time data for samples U5D1A and G8G1 for 1:9 and 1:99 sediment:water ratios. The EC measurement for a given sediment:water ratio applies to the EC of a particular shaking time of a subsample undergoing a given amount of turbulence. Turbulence must decrease as the total mixture volume increases in a given container. This is due to the increase in burial of part of the sediment (which, therefore, progressively experiences less turbulence) as its amount increases. The results of these experiments (Table 3.2) do not demonstrate the effect of turbulence. It is inferred that the heterogeneous

Table 3.2. EC (μmhos cm^{-1} @ 25°C) values of aqueous mixtures at varying levels of turbulent mixing.[a]

Sample Number	Weight (g)	EC (μmhos cm^{-1} @ 25°C) Values				
- - - - - - -	Contact Time:	10	130	218	483	690
G8G1 (1:9)	5	2190	2820	2920	3060	3100
	10	1940	2780	2860	2980	3000
	20	2210	2820	2900	3005	3040
	40	980	1840	2240	2620	2760
- - - - - - -	Contact Time:	14	54	159	894	
G8G1 (1:99)	0.5	553	739	801	316	
	1.0	563	737	773	775	
	2.0	525	722	830	857	
	4.0	253	485	652	712	
- - - - - - -	Contact Time:	14	31	78	367	
U5D1A (1:9)	5	1110	1238	1350	1320	
	10	880	1055	1205	1295	
	20	940	1050	1320	1330	
	40	361	560	735	1045	
- - - - - - -	Contact Time:	16	43	114	1894	
U5D1A (1:99)	0.5	120	13.7	150.5	184	
	1.0	?	170.5	212	226	
	2.0	?	183	194	210	
	4.0	?	246	322	341	

[a]Note: The following table summarizes the magnitude (qualitative) of turbulent mixing for 1:99 and 1:9 sediment:water ratios.

Weight of Sample (g)	Particle Movement
0.5	particles saltate and suspend
1.0	particles move fast on "bed"
2.0	particles move slowly on "bed"
4.0	coarse particles stagnant, some fines are in suspension

composition of these sediments precludes the determination of the turbulence effect.

The ionic strength of a solution must increase as more solid matter is added to it unless saturation (i.e., equilibrium) is obtained. Conversely, as the sediment:water ratio decreases so must the ionic strength of the solution decrease for ionic activities below saturation. The plots of EC *vs* mixing time shown in Figure 3.1a and Figure 3.1b indeed show that at any given mixing time the EC, and hence the ionic strength of the mixture of a given sample, increases as the sediment:water ratio increases. For example, after 24 hours of mixing the EC in μmho cm^{-1} at 25°C is 300 and 40 for sediment:water ratios of 1:9 and 1:99 of sample G7A1; the respective EC values for sample G10XC1 are 70 and 20.

The following discussion excludes highly concentrated solutions (e.g., G8B1 and G11C1 in Figure 3.1a) that approach saturation with respect to any of the major dissolving minerals. The data of Table A1 of the Appendix confirm the general statement that the mixtures of many surficial alluvial and shale samples of EC larger than about 2 mho cm^{-1} approach saturation with respect to gypsum, the least soluble among the major dissolving minerals (see, for example, the calculations in Table A4 of the Appendix). This solubility is approached whenever $(Ca^{2+})\ (SO_4^{2-}) \simeq 2.5 \cdot 10^{-5}\ M^2\ 1^{-2}$.

Using the regression equation of Figure 3.3 to solve for the TDS (mg l^{-1}) values of the 1:9 and the 1:99 mixtures of samples G7A1 and G7XC1, we arrive at $11\ (TDS_{1:99})/(TDS_{1:9}) = 11\ (21.0)/(201.0) = 1.15$ and $11(TDS_{1:99})/(TDS_{1:9}) = 11(9.65)/39.3 = 2.70$, respectively. The multiplier is used to account for the eleven-fold dilution. The above

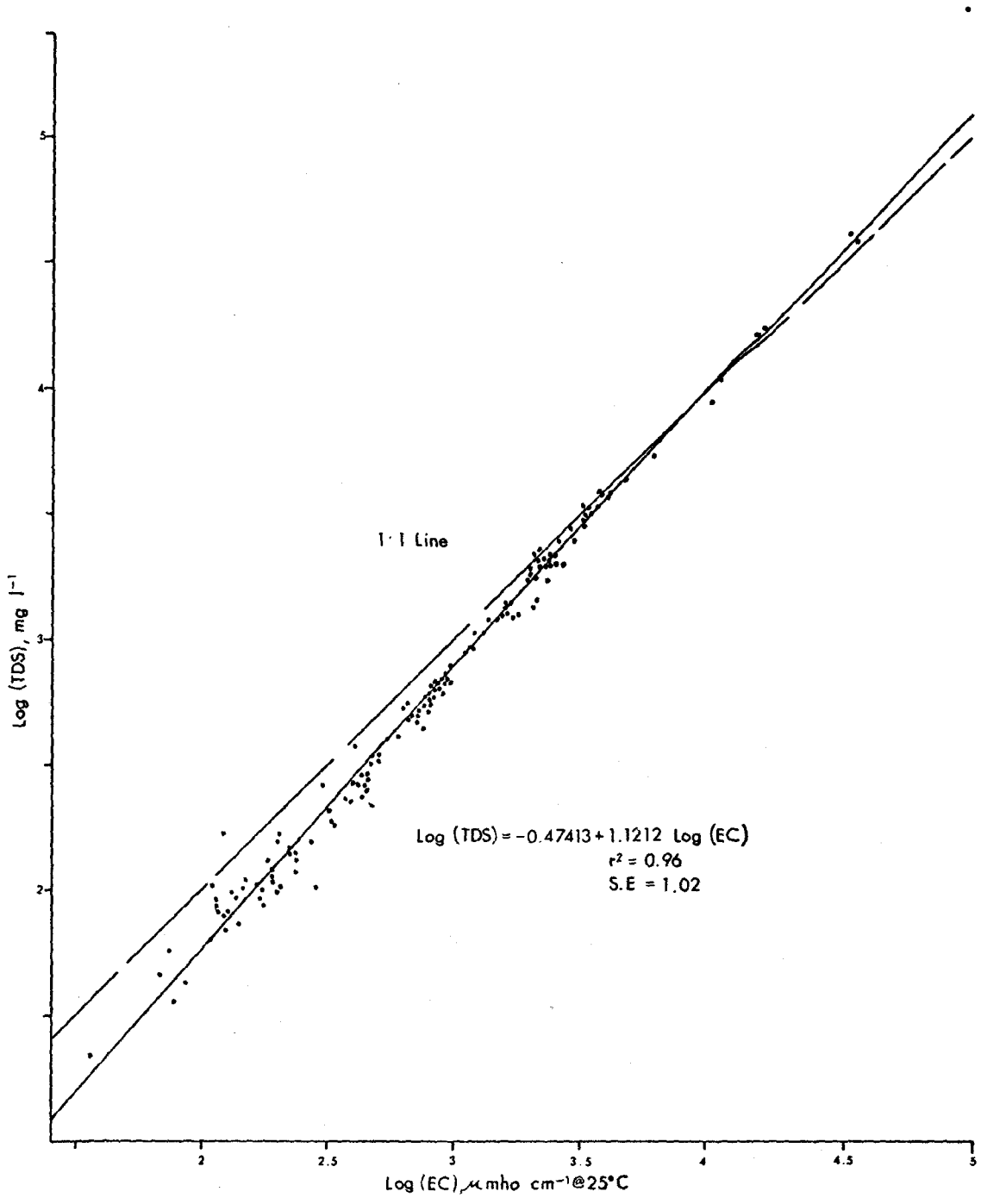

Figure 3.3. Total dissolved solids (TDS, in mg l^{-1}) concentration dependence on electrical conductance (EC).

calculated ratios are larger than unity. This might imply incorrectly that saturation with respect to a major dissolving mineral is attained at 1:9 mixtures. These larger-than-unity ratios therefore prove that there is a dissolution limiting phenomenon which is more effective at larger sediment:water ratios. A discussion of such a phenomenon follows in section 3.3.

3.2 Specific Ion Data

The concentration of specific ions extracted from or in contact with geologic materials depends on temperature and pressure, as discussed previously, and on the nature of the dissolved matter and that of the solvent. An example of a solvent effect is the increased solubility of most minerals when contacting an acidic solution. The 'common ion' and 'salt ion' phenomena are solute effects.

The rate at which mineral dissolution takes place is governed by kinetic principles as outlined in section 3.1. When a sediment:water mixture is filtered before approaching equilibrium it will contain less soluble matter than it ultimately would have contained. Equilibrium is useful as a concept denoting the kinetic equivalence of forward (V_f) and backward (V_b) rates of reaction such as dissolution and precipitation during solid-solution contact and also to denote that the solid is completely dissolved ($V_f = V_b = 0$). However, true equilibrium for dissolution, hydrolysis and redox reactions in nature is rarely achieved (Morgan, 1967). For instance, partial equilibrium is attained when all the gypsum and calcite have dissolved from a soil contributing mostly Ca^{2+}, SO_4^{2-} and HCO_3^{1-} to a solution with which it is in contact. This is not a total equilibrium because other minerals such as silicates and oxides have not as yet approached equilibrium with the

aqueous environment. None of the dissolution processes investigated in this study are considered to have attained true equilibrium.

Sample G8G1, a sandy-pebbly thin crust of the alluvial bank of West Salt Creek was diluted at 1:1, 1:9 and 1:99 sediment:water ratios. Electrical conductance readings were taken after 1/3, 1, 3, 9 and 25 hours of contact time. These mixtures were filtered and were subsequently analyzed for the major ion species. These included Ca^{2+}, Na^{1+}, Mg^{2+}, SO_4^{2-}, HCO_3^{1-} and Cl^{1-} (Table 3.3). Note that various dilute solutions contained less than 0.1 meq l^{-1} of HCO_3^{1-}.

The data reported in Table 3.3 show that the relative abundance of several specific ions changes with contact time. Ca^{2+} tends to increase while Na^{1+} and Mg^{2+} decrease in relative abundance with increase of contact time of the 1:9 and 1:99 mixtures. The major ionic species point to a fast dissolving soluble mineral phase of $CaSO_4 \cdot 2H_2O$, hydrated Na_2SO_4 and hydrated $MgSO_4$. The dissolution of these minerals is apparently governed by a rate limiting process which accounts for the faster dissolution of the more soluble minerals. This process might be identical to the one which accounts for the dilution effect (see section 3.2). The changes in abundance of specific cations with contact time is not realized in the 1:1 derived solutions.

The changes of specific ion abundance with contact time account for the shift from a Na-Ca-Mg-SO_4 to a predominantly Ca-SO_4 type water with increase of the residence time of these sediments in their aqueous environment. Most of this change apparently takes place during the first hour of contact. The corresponding anionic change is too small to be considered herein. Whatever these total changes might be, those summarized in Table 3.3 incorporate the effects of inherent variability of dissolution rates among subsamples of the same material as well as random variations of soluble mineral content (see section 2.2a).

Table 3.3. Summary of specific ion concentrations (meq l^{-1}) of G8G1 aqueous mixtures at progressively increasing contact times.

Sediment:Water Ratio	EC (μmhos/cm @ 25°C)	Computed TDS (mg l^{-1})	Contact Time (hours)	meq l^{-1}					
				Ca^{2+}	Mg^{2+}	Na^{1-}	SO_4^{2-}	HCO_3^{1-}	Cl^{1-}
1:1	5700	5410	1/3	13.4(17.2)[a]	21.6(27.7)	42.9(55.1)	77.7(96.8)	0.4(0.49)	2.1(2.62)
1:1	6500	6270	1	20.7(22.5)	17.3(18.9)	53.8(58.6)	29.1(96.4)	0.5(0.54)	2.8(3.08)
1:1	6000	5870	3	24.1(27.4)	17.4(19.7)	46.6(52.9)	82.8(96.3)	0.6(0.70)	2.6(3.02)
1:1	6000	6180	9	20.3(22.4)	16.7(18.4)	53.8(52.9)	87.1(96.0)	0.8(0.88)	2.8(3.09)
1:1	6000	7110	25	24.5(22.4)	23.8(21.7)	61.3(55.9)	99.3(96.2)	0.6(0.58)	3.3(3.20)
1:9	938	645	1/3	4.4(46.3)	1.1(11.6)	4.0(42.1)	9.4	b	c
1:9	1610	1300	1	12.5(64.8)	1.9 (9.8)	4.9(25.4)	19.0	b	c
1:9	2210	1980	3	19.7(66.1)	3.6(12.1)	6.5(21.8)	29.0	b	c
1:9	2520	2590	9	25.5(73.3)	3.6(10.3)	5.7(16.4)	33.3	b	c
1:9	2710	2520	25	27.6(71.0)	3.9(10.0)	7.4(19.0)	36.5	b	c
1:99	298	148	1/3	1.4(63.6)	0.2 (9.1)	0.6(27.3)	2.0	b	c
1:99	610	394	1	5.0(83.3)	0.3 (5.0)	0.7(11.7)	5.7	b	c
1:99	430	226	3	2.7(79.4)	0.2 (5.9)	0.5(14.7)	3.3	b	c
1:99	958	706	9	9.6(88.9)	0.4 (3.7)	0.8 (7.4)	10.2	b	c
1:99	828	590	25	7.6(85.4)	0.5 (5.6)	0.8 (9.0)	8.6	b	c

[a]Numbers in parentheses are abundance ratios ($C_i^{z+}/\Sigma C_i^{z+}$ or $C_i^{z-}/\Sigma C_i^{z-}$), in percent.

[b]$[HCO_3^{1-}] < 0.1$ meq l^{1-}.

[c]Not determined.

Specific ion information on the solutions of the 1 phi size groups (Table 3.4) of samples U5D1A and G8G1 (see Figures 3.2a,b) may explain part of the inconsistency between available relative magnitudes of dissolution rates and those derived from theory. Referring back to Figure 3.2b, the 8-16 mm sample denoted by 1 has a very high initial dissolution rate; it is comprised of the largest particles but dissolves faster than all other samples coarser than 0.125 mm. This sample, comprised of two granule aggregates, contains a higher soluble mineral content than the finer particles do. If availability to dissolve (i.e., availability of soluble minerals) increases as soluble mineral content increases it explains the dissolution behavior of the two granules. However, this assumption is certainly not universal. For instance, the initial dissolution rates of the size groups denoted by 2, 3 and 4 of Figure 3.2b are small but their relative soluble mineral content is high. An inspection of the ratio $100[Na^{1+}]/\sum C_i^{z+}$ may, however, explain part of this behavior. In decreasing particle size (excluding the siltstone particle) this abundance ratio (derived from the data in Table 3.4) is 5.9, 5.1, 8.2, 9.6, 10.7, 7.3, 7.3, 5.9 and 6.7 percent. Thus, number 5 (0.5-1 mm) might initially dissolve fast due to a relatively high Na_2SO_4 hydrate content (see Chapter 3.3) even though the total soluble mineral content is the smallest of all. The generalization that availability for immediate dissolution is related to high soluble mineral contents applies to all the samples of Figure 3.2b except numbers 2, 3 and 4. A similar situation is also encountered in the shale sample of Figure 3.2a.

Table 3.4. Specific ionic concentrations (meq l^{-1}) of equilibrated solutions derived from 1:99 mixtures of separate 1 phi particle size groups.[a]

Sample Number	Size (mm)	K^{1+}	Na^{1+}	Mg^{2+}	Ca^{2+}	ΣC_i^{z+}	ΣC_i^{z-}	HCO_3^{1-}	SO_4^{2-}	Fe^{3+} (ppm)
U5D1A (1:99)	8-16	0.2	0.7	0.2	0.4	1.5	1.3	0.6	0.7	1.50
	4-8	0.1	0.8	0.2	0.4	1.5	1.2	0.6	0.6	
	2-4	0.1	0.9	0.2	0.4	1.6	1.5	0.8	0.7	0.06
	1-2	0.1	0.9	0.2	1.3	2.5	2.2	0.6	1.6	
	0.5-1	0.1	0.9	0.2	1.0	2.2	1.8	0.5	1.3	
	0.25-0.5	0.1	0.8	0.2	1.0	2.0	1.8	0.5	1.3	
	0.125-0.25	0.1	0.9	0.2	1.0	2.2	1.8	0.4	1.4	
	0.061-0.125	0.1	0.7	0.2	0.9	1.9	1.6	0.3	1.3	
	< 0.061	0.1	0.7	0.2	1.1	2.1	1.7	0.4	1.3	
G8G1 (1:99)	>16		0.4	0.3	0.6	1.3	1.4	0.5	0.9	
	8-16		0.6	0.4	9.1	10.1	9.6	0.2	9.4	
	4-8		0.5	0.3	9.1	9.9	9.4	0.3	9.1	
	2-4		0.7	0.4	7.4	8.5	8.2	0.2	8.0	
	1-2		0.7	0.5	7.3	8.5	8.2	0.2	8.0	
	0.5-1		0.8	0.5	6.2	7.5	7.1	0.2	6.9	
	0.25-0.5		0.6	0.4	8.2	9.2	9.0	0.2	8.8	
	0.125-0.25		0.5	0.2	6.2	6.9	6.8	0.2	6.6	
	0.061-0.125		0.6	0.4	9.2	10.2	10.2	0.1	10.1	
	< 0.061		0.9	0.6	12.0	13.5	13.2	0.2	13.0	

[a]It has been shown that the detected Fe^{3+} is essentially a precipitate in suspension. Those samples for which Fe^{3+} and K^{1+} concentrations are not listed contained <0.05 ppm and <0.01 meq l^{-1} of these respective ions.

Table A1 of the Appendix summarizes 1:1, 1:9, 1:99 and some 1:4 and 1:999 sediment:water ratio data of 52 different samples of surficial shale and alluvium. The measured EC, as well as the calculated TDS concentration are supplied in addition to the specific ion concentrations. In general, most of the cationic analyses are more complete than the anionic ones; the sum of the former in meq l^{-1} is larger than that of the latter.

Several of the solutions of Table A1 are saturated with respect to gypsum. The following discussion will, therefore, apply to lower concentrations of dissolved species for which $[Ca^{2+}]\ [SO_4^{2-}] < 2.5 \cdot 10^{-5}\ M^2\ l^{-2}$ unless stated otherwise. Analyses are also excluded for which the stochiometric concentration of Ca^{2+}, Mg^{2+}, Na^{1+}, SO_4^{2-} and HCO_3^{1-} is smaller than 0.1 meq l^{-1} or those for which no specific ion concentration decrease is attained upon dilution.

The specific ion concentrations tabulated in Table A1 consistently increase with increase in sediment:water ratio. This is expected for unsaturated solutions to which potentially soluble minerals are added. It is noteworthy that upon dilution, the decrease in specific ion concentration is not identical for all major ions. This variability is diagrammatically shown in Figure 3.4 where the mean 1:99/1:9 concentration ratio is shown for the five major dissolved species of solutions undersaturated with respect to gypsum. This ratio should be 9/99 = 1/11 = 0.09 for every ion due to the eleven-fold dilution. However, the decrease in ionic concentration is roughly 1/6, 1/3.5 and 1/2.5 of the expected values for HCO_3^{1-}, Ca^{2+} and for the Na^{1+}, Mg^{2+} and SO_4^{2-} group, respectively. Thus, two and one-half times Na^{1+}, Mg^{2+} or SO_4^{2-},

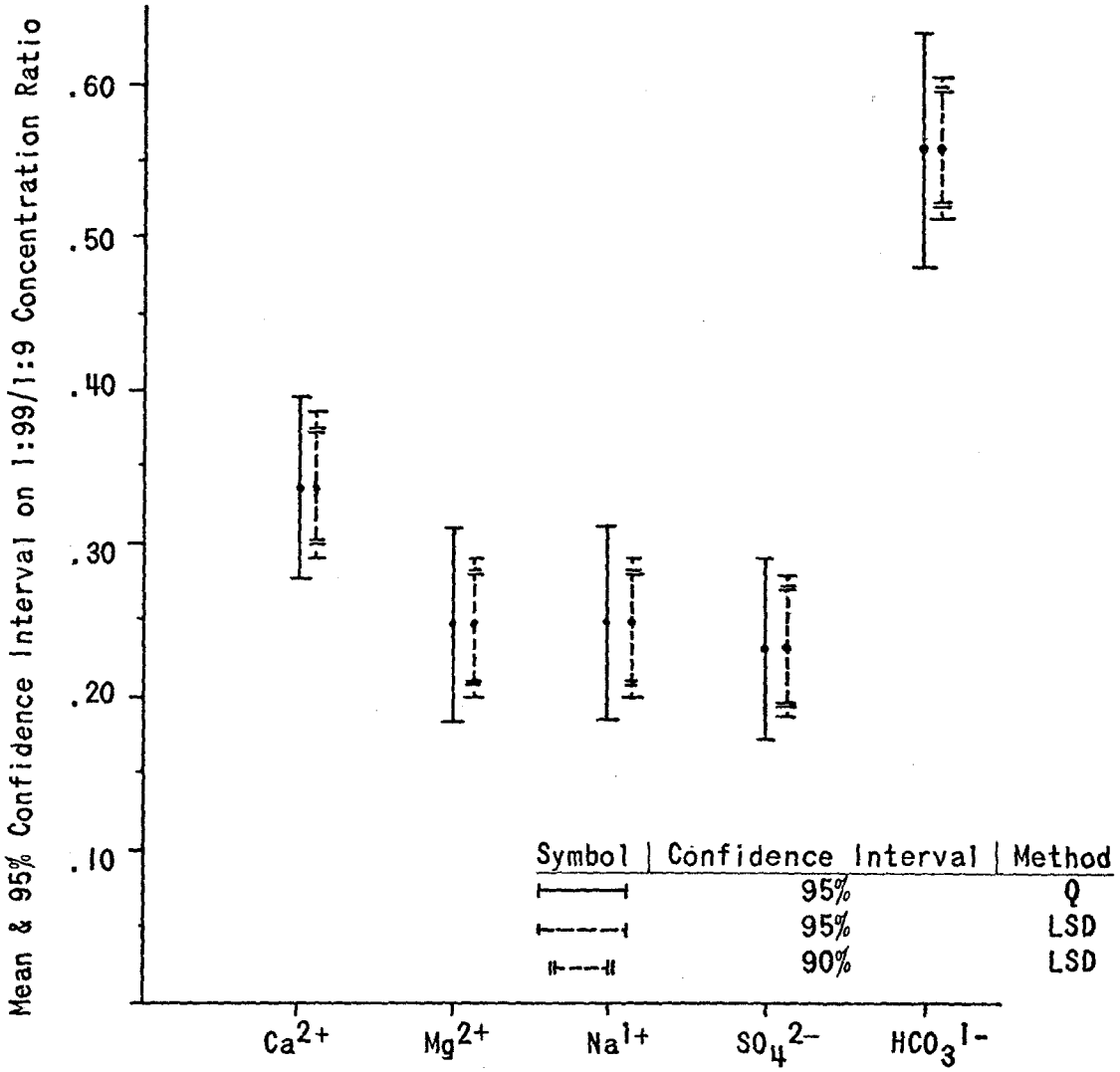

Figure 3.4. Means and various confidence intervals on means of (1:99/1:9)11 specific ion concentration ratios for all sample solutions for which $[Ca^{2+}][SO_4^{2-}] < 2.5 \cdot 10^{-5}\ M^2\ 1^{-2}$.

three and one-half times Ca^{2+} and six times higher HCO_3^{1-} concentrations are attained upon the eleven-fold dilution. These additional amounts of solutes have their source in the sediments although bicarbonate may be partly derived from the atmosphere. It may therefore be inferred that under concentrated conditions the dissolution of sodium and magnesium sulfates is less inhibited than that of gypsum, calcite and possibly dolomite.

Similarly, it was shown earlier that these more soluble sulfates dissolve faster than gypsiferous and carbonate minerals. An explanation for the faster and more complete dissolution of highly soluble sulfates is attempted in the following discussion.

3.3 Discussion

Solutions that are in partial equilibrium or that are approaching true equilibrium contain concentrations of specific ions which can be computed from equilibrium theory. Therefore, the concentration of the major dissolved solids will remain constant upon dilution of a concentrated solution as long as the dissolving minerals are present. When a solution is undersaturated with respect to the minerals contributing its major dissolved constituents it is surmised that these minerals have been completely dissolved. If, however, the concentration of the dissolved matter decreases upon dilution less than does the dilution factor then there must be an additional source for the dissolved matter, a source which had not been exhausted under conditions of higher ionic strengths.

As an example consider a solution for which $(Ca^{2+}_{free})\ (SO_4^{2-}{}_{free}) = 10^{-7}\ M^2\ l^{-2}$ and $[Ca^{2+}_{total}] = 10^{-3}\ M\ l^{-1}$. Such a solution should

contain 10^{-4} M 1^{-1} of $[Ca^{2+}_{total}]$ upon a ten-fold dilution. The ratio $10[Ca^{2+}_{total}]_{final} / [Ca^{2+}_{total}]_{initial}$ is unity for this example. Ratios smaller than unity imply accelerated precipitation upon dilution. Ratios larger than unity prove that there is an incomplete exhaustion of the source of major dissolved constituents at higher ionic strengths.

Tables A1 and A2 of the Appendix list the $11(TDS_{1:99})/(TDS_{1:9})$ ratios for all the samples. It is most noticeable that the ratio is larger than unity for 95 percent of the samples. Therefore, it is inferred that most of the studied sediment samples contain salts that continuously dissolve upon dilution, even under conditions of undersaturation with respect to gypsum.

From a comparison with Reitemeier's (1946) study it is suggested that although ion exchange processes may very well be operable in the studied mixtures, they do not explain the results. Some of the studied solutions are saturated with respect to calcite. Whenever this situation arises it is expected that calcium and bicarbonate concentrations would not decrease substantially upon dilution. Calcite dissolution and bicarbonate dissociation, as well as dissolution of gypsum and other minerals are considered in the calculations of Appendix Table A4. The calculations for sample U5E3C at different concentrations of sediment show that one of the Ca^{2+} and HCO_3^{1-} sources is carbonate minerals. This source cannot, however, account for the increased dissolution of these ions in solutions originally undersaturated with respect to calcite, nor can it account for the continued dissolution of Na^{1+}, Mg^{2+} and SO_4^{2-} upon dilution.

An explanation of the dilution effect is based on a hypothesis of particle coating. It may be postulated that the studied sediments comprise particles of all sizes which are surrounded with coatings of slightly soluble minerals. These might be siliceous or ferric oxide coatings, the latter being very common in arid environments. It may further be postulated that particle coating takes place contemporaneously with the precipitation of evaporites. During the continuous concentration of the soil solution due to evaporation, the slightly soluble minerals are the first to precipitate out of the solution. This precipitation continues indefinitely during the concentration process. Therefore, a slightly soluble mineral such as gypsum is expected to be surrounded by a more complete and thicker coating than that on more soluble minerals such as sodium and magnesium sulfates, which begin to precipitate (when the solution is initially undersaturated with them) at a later stage. Upon contact with water the most soluble minerals, least coated with the slightly soluble ferric oxides, will dissolve rapidly and more completely than, say, gypsum or calcite. Moreover, if the coating is thick enough some of the particles comprised of gypsum or calcite (and to a lesser extent, those of more soluble minerals) may not, in fact, dissolve in the soil solution. Although such a solution amy be saturated with respect to a ferric oxide, it may be undersaturated with respect to gypsum.

In conclusion, it is evident that soluble minerals continuously dissolve upon addition of water even under conditions that at first imply that these minerals are already completely dissolved. Particle coating with slightly soluble minerals provides a possible explanation for this dilution phenomenon.

CHAPTER 4

DISTRIBUTION OF SOLUBLE MINERAL CONTENT IN SURFICIAL DEPOSITS

The amount and type of minerals present in sediments is a function of storage, leaching and accumulation processes. The various sources of soluble minerals are rainfall, which may only account for small amounts due to its relative purity (Carroll, 1962), leaching from overlying layers and upward solute transport as well as *in situ* soluble matter.

4.1 Soluble Mineral Content of Surficial Mancos Shale and Alluvium

The Mancos Shale is a deposit that has been in contact with seawater. Upon erosion and mixing with aqueous solutions (overland and channelized flow) it is therefore expected that this formation will yield appreciable amounts of common (19‰ chlorinity; pH = 8.1) ions. In decreasing order of molal abundance, Na^{1+}, Mg^{2+}, SO_4^{2-}, Ca^{2+}, K^{1+}, HCO_3^{1-} and CO_3^{2-} make up practically all of the dissolved mass of seawater (Garrels and Thompson, 1962). These ions should be readily available in Mancos Shale. The alluvium is, however, derived from particulate matter originally transported by channelized flow which, upon contact with the sediment, depleted it of much of its potentially soluble minerals.

The mean soluble mineral content of Mancos Shale derived from hillslopes is 1.99 percent. The mean for terraces in North Miller

Creek, West Salt Creek and Mesa Creek is 0.62, 0.30 and 1.69 percent, respectively (Table 4.1). The surficial shale deposits contain more soluble minerals and are therefore a greater potential salinity hazard. With 95 percent confidence limits the mean soluble mineral content of the shale is significantly larger than that of North Miller Creek and West Salt Creek surficial terrace alluvium. It is noteworthy that the soluble mineral content is largest for Mesa Creek and lowest for West Salt Creek terraces. The North Miller Creek alluvium is richer in soluble minerals than the alluvium of the wide West Salt Creek valley due to the physical closeness to the source, i.e., Mancos Shale. Indeed, the alluvium in West Salt Creek consistently contains low soluble mineral contents except where it approaches Mancos bedrock outcrops, such as in section G8 and upstream, where it encroaches close to the marine shales of the Mesa Verde Group (section G11, see Table A2 of the Appendix).

In fact, the influence of distance to Mancos Shale is well demonstrated in Leach Creek. Section G2 is located in the lower basin where the channel is gullied about 1 m but meanders in a narrow valley between Mancos slopes. For this section the soluble mineral content of the terrace and bed materials is exceptionally high, 2.21 and 3.67 percent, respectively (Table A2). The soluble mineral content of Mesa Creek alluvium is also rather high and it is postulated that this results from the proximity to bedrock.

The dominant soluble mineral in Mancos Shale is gypsum but appreciable amounts of sodium and magnesium hydrated sulfates and some carbonates are present. The clorides are leached, which is characteristic of other saline shales throughout the world (Billings and

Table 4.1. Summary of mean soluble mineral content ($\bar{X}$), its standard deviation ($\hat{\sigma}$), and the number of samples (n) of sampling units in North Miller, West Salt and Mesa Creeks.[a]

	North Miller Creek											
	CT	T	CUMW	UMW	CA	A	CLMW	LMW	EB	B	CMS[b]	MS[b]
$\bar{X}$	0.186	0.620	0.760	0.690	1.037	1.118	1.067	0.974	10.098[c]	0.936	0.703	1.987
$\hat{\sigma}$	0.066	0.778	0.275	0.445	0.954	1.020	0.699	0.634	14.884[c]	0.525	0.030	0.301
n	7	22	12	7	3	9	10	13	13	21	3	9

	West Salt Creek						
	CT	T	CW	W	A	CB	B
$\bar{X}$	0.141	0.296	0.323	1.009[d]	1.335	0.509	0.665
$\hat{\sigma}$	0.043	0.196	0.292	1.606	1.562	0.544	0.813
n	7	26	4	24	13	21	60

	Mesa Creek			
	T	W	UB	B
$\bar{X}$	1.690	1.734	1.130	2.081
$\hat{\sigma}$	0.622	0.509	0.430	1.630
n	14	8	9	55

[a] C=crust; T=terrace; U=upper; L=lower; M=Mancos Shale; S=hillslope; W=gully wall, A=mass wasted material; B=bed material; E=efflorescence or salt crust.

[b] From North Miller and Mesa Creeks.

[c] Without one value the mean and standard deviation change to 6.281 and 4.090, respectively.

[d] These wall samples include two Mancos-affected G8 sites; excluding these, the $\bar{X}$, $\hat{\sigma}$ and n are 0.314, 0.284 and 17, respectively.

Williams, 1967). In the alluvium the dominant soluble minerals are calcite, dolomite (x-ray diffraction studies by L. Whittig, personal comm., 1976) and gypsum. The relative abundance of the sulfate ion is larger in the Mancos Shale samples from North Miller Creek than in the West Salt Creek alluvium; the mean $SO_4^{2-}/\sum C_i^{z-}$ concentration ratios are 3.09 and 0.46, respectively. Figure 4.1 shows the 95 percent confidence interval on the mean $Na^{1+}/\sum C_i^{z+}$ and on the $(Na^{1+} + Mg^{2+}) / \sum C_i^{z+}$ concentration ratios for Mancos Shale and for alluvial samples. The former contains significantly and appreciably higher contents of highly soluble sulfate minerals.

4.2 Distribution of Soluble Minerals

4.2a Salt Buildup in Crusts

Soil crusts form due to cementing of materials on the soil surface. The cement may be a ferric oxide, but more commonly it is calcareous. Encrustation may also take place during drying due to adherence of fine silt and clay particles to the rest of the soil mass. When soil water is highly concentrated with dissolved constituents, these will precipitate from it during evaporation after being transported to the surface by capillary action (or, possibly, due to thermal gradients and their effect on diffusion). These precipitates will cement the surface layer to form a saline crust.

Materials rich in soluble minerals should develop saline crusts under proper conditions. An example is the efflorescent crusts developed on the bed of North Miller Creek. Because this is a bedrock channel incised in the slightly permeable Mancos Shale formation, most

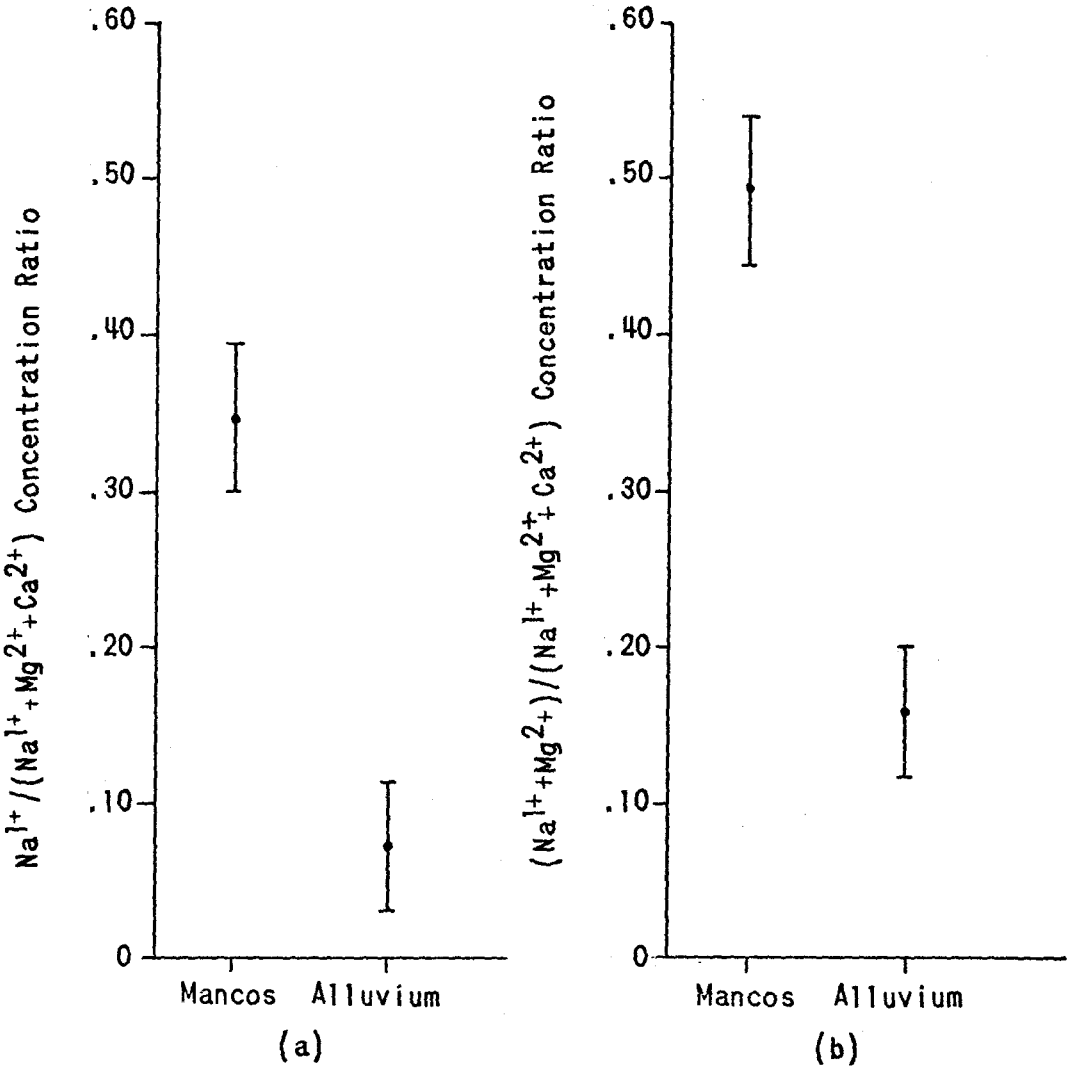

Figure 4.1. Means and 95 percent confidence intervals about the means of Na^{1+} (a) and $Na^{1+} + Mg^{2+}$ (b) abundance ratios from 1:99 solutions of Mancos Shale and alluvium.

of the overland flow reaching the channel does not percolate into the bed and bed materials dry primarily by evaporation rather than by infiltration thereby forming very saline crusts. Thus, the mean salt content of bed crusts developed in North Miller Creek is 10.10 percent compared with 0.94 percent in the bed proper (see Table 4.1).

The crusts of the lower and of the upper Mancos Shale gully walls of North Miller Creek contain 1.07 and 0.76 percent soluble minerals. The lower and upper walls beneath the crusts contain 0.63 and 0.69 percent respectively (Table 4.1). The crusts are slightly richer in soluble minerals than their source (i.e., the wall) but the difference is not statistically significant. It is believed that the apparent difference between the upper and lower walls is due to the low moisture content of the upper wall which prevents formation of saline crusts. However, the lower wall comes in contact with water frequently enough that transport of solutes to the outer surface is more pronounced than in the upper wall.

Where permeability is very high the upper part of the surficial materials will be thoroughly leached. This applies to the coarse alluvial terraces of North Miller, West Salt and Leach Creeks. The mean soluble mineral content of the crusts is significantly lower ($p<0.05$) than that of underlying materials (Table 4.1). No significant difference among the means of salt contents of the crust and that of underlying materials exists for the permeable alluvial bed materials, including fresh bank material deposited on the channel bed, where leaching and evaporation are both active. However, a mean soluble mineral content comparison between the surface layer and material immediately underlying shows the crust to be richer in soluble minerals. This

difference was found to be significant ($p < 0.05$ with a 95 percent confidence interval) for the bed of Mesa Creek (see the following section). This difference suggests that solutes are transferred to the saline crust surface primarily from the soil layer immediately underlying the crust.

The preceding analysis shows that soil crust salinity increases as the permeability decreases and as the soluble mineral content of the underlying material increases. Much of the soil buildup in saline crusts appears to originate from the material in immediate contact with them.

4.2b Variation of Soluble Mineral Content with Depth

Figures 4.2 and 4.3 show the variations in soluble mineral content with depth in bed materials as determined from 1:99 mixtures. The mean salt contents for the 6-, 15- and 50-cm depths in the bed of section M3 of Mesa Creek (Figure 4.2) are 1.13, 0.91 and 1.46 percent, respectively; these means are significantly different ($p < 0.025$). With increase in depth the mean salt content increases to an average maximum 5.6 percent at a depth of 2.8 m. The bed material in section M3 is coarse alluvium that overlies saturated and deeply weathered Mancos Shale at a depth of 2.5 m. Because the alluvial fill of this channel is shallow it is expected that a strong gradient of salt content with depth would appear in the bed material. The effect of solute concentration due to increased evaporation at the surface is also well defined in this section, where the crust is somewhat enriched in comparison with the layer immediately beneath it.

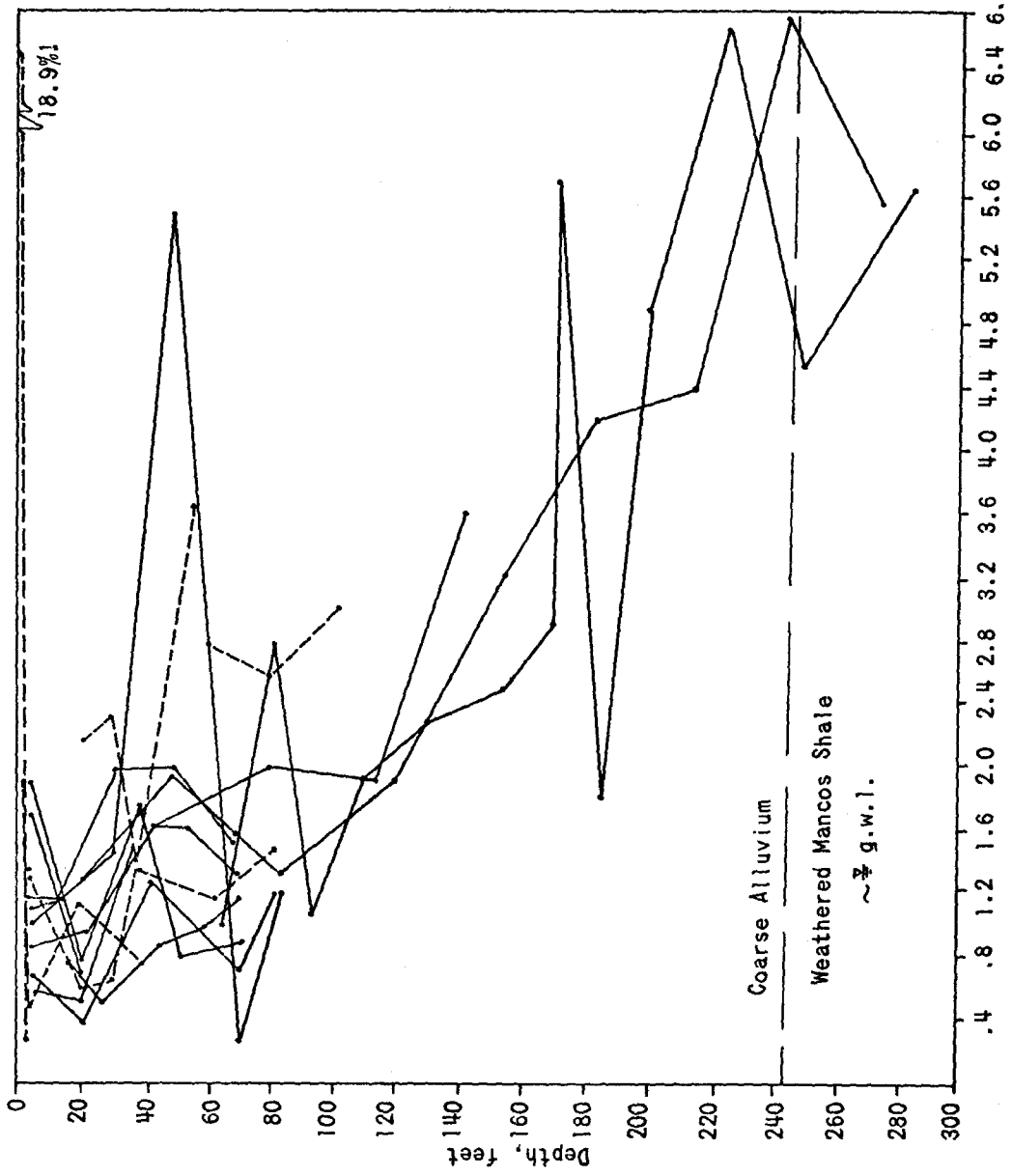

Figure 4.2. Variation of soluble mineral content with depth of Mesa Creek bed materials (solid lines) and bed materials from section G8, West Salt Creek (dashed lines).

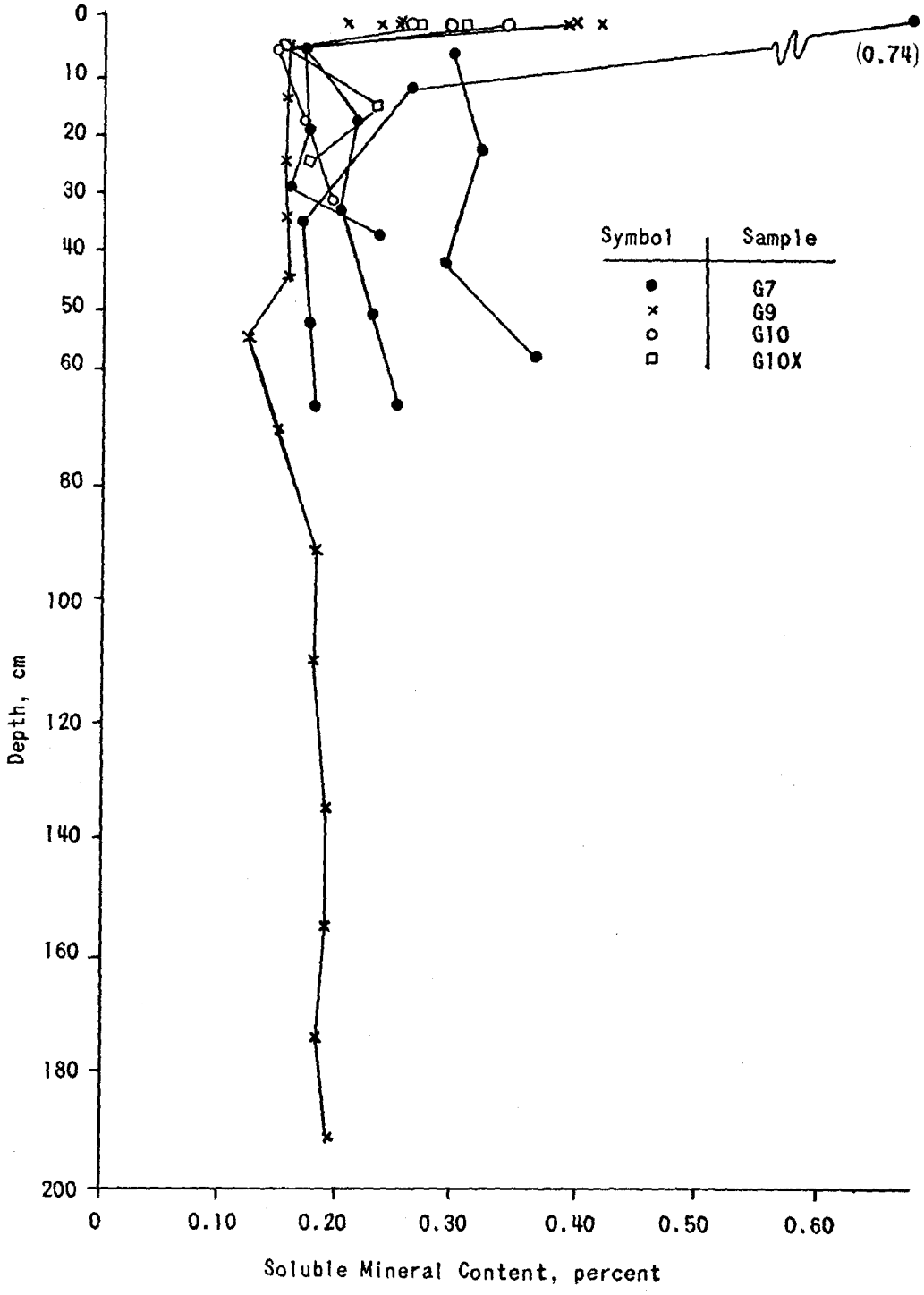

Figure 4.3. Variation of soluble mineral content with depth of West Salt Creek bed materials.

The increase in soluble mineral content with depth is not noted in the bed of West Salt Creek (Figure 4.3). Although the mean content of the crust is higher than that at any other depth the difference is not significant (i.e., F not significant in analysis of variance). An explanation for the constant soluble mineral content in these bed materials is the general sterility of West Salt Creek alluvium and its remoteness from contamination by ground water which was formerly in contact with Mancos Shale. Samples G8A, G8B and G8C were taken from the bed of West Salt Creek where the channel abutts against Mancos Shale (see Table A2). Moreover, the alluvial fill of the present channel is very shallow at this section. Therefore, the soluble mineral content of the bed at section G8 increases with depth as at the M3 section. These data are plotted in Figure 4.3.

Figures 4.4 and 4.5 show the variability in soluble mineral content with depth for the Mesa Creek terrace and gully wall and for the various gully walls of North Miller Creek. No trend is apparent in these deposits. Although there is no statistically significant change in soluble mineral content with depth in the sterile terraces of West Salt and North Miller Creeks, an increase with depth appears to take place. The significance of this trend, as shown in Figure 4.6, is obscured by the general large variability in salt content throughout the deposits.

In summary, soluble mineral content increases with depth in shallow alluvium overlying Mancos Shale. A uniform soluble mineral content with depth characterizes deep and leached bed materials and terrace deposits.

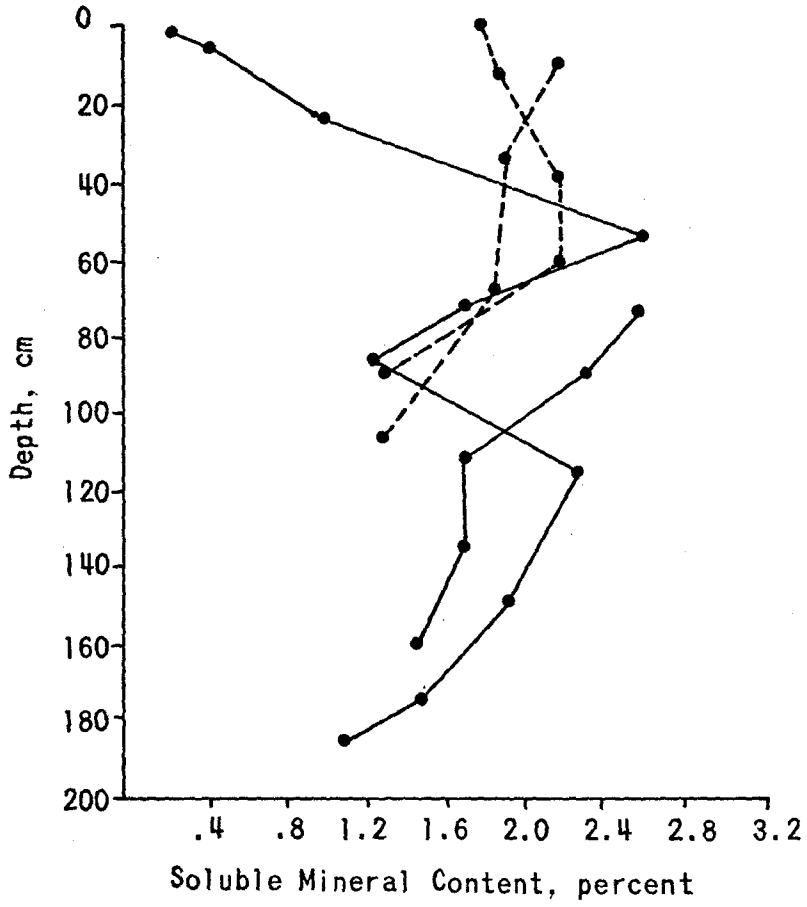

Figure 4.4. Variation of soluble mineral content with depth of terrace (solid lines) and wall samples (dashed lines) from Mesa Creek.

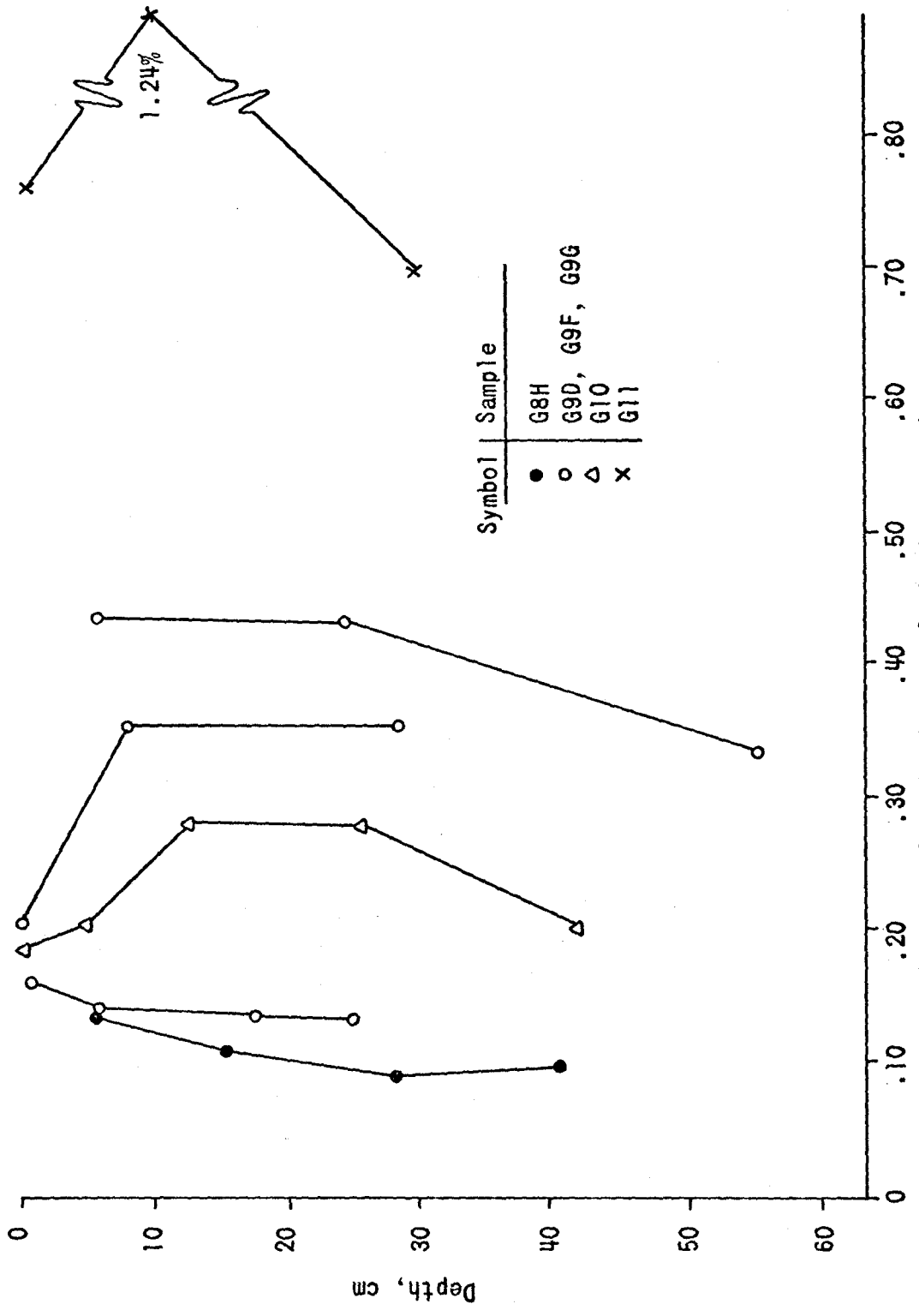

Figure 4.5. Variation of soluble mineral content with depth of alluvial gully wall samples from West Salt Creek. (Note the salinity of Section G11.)

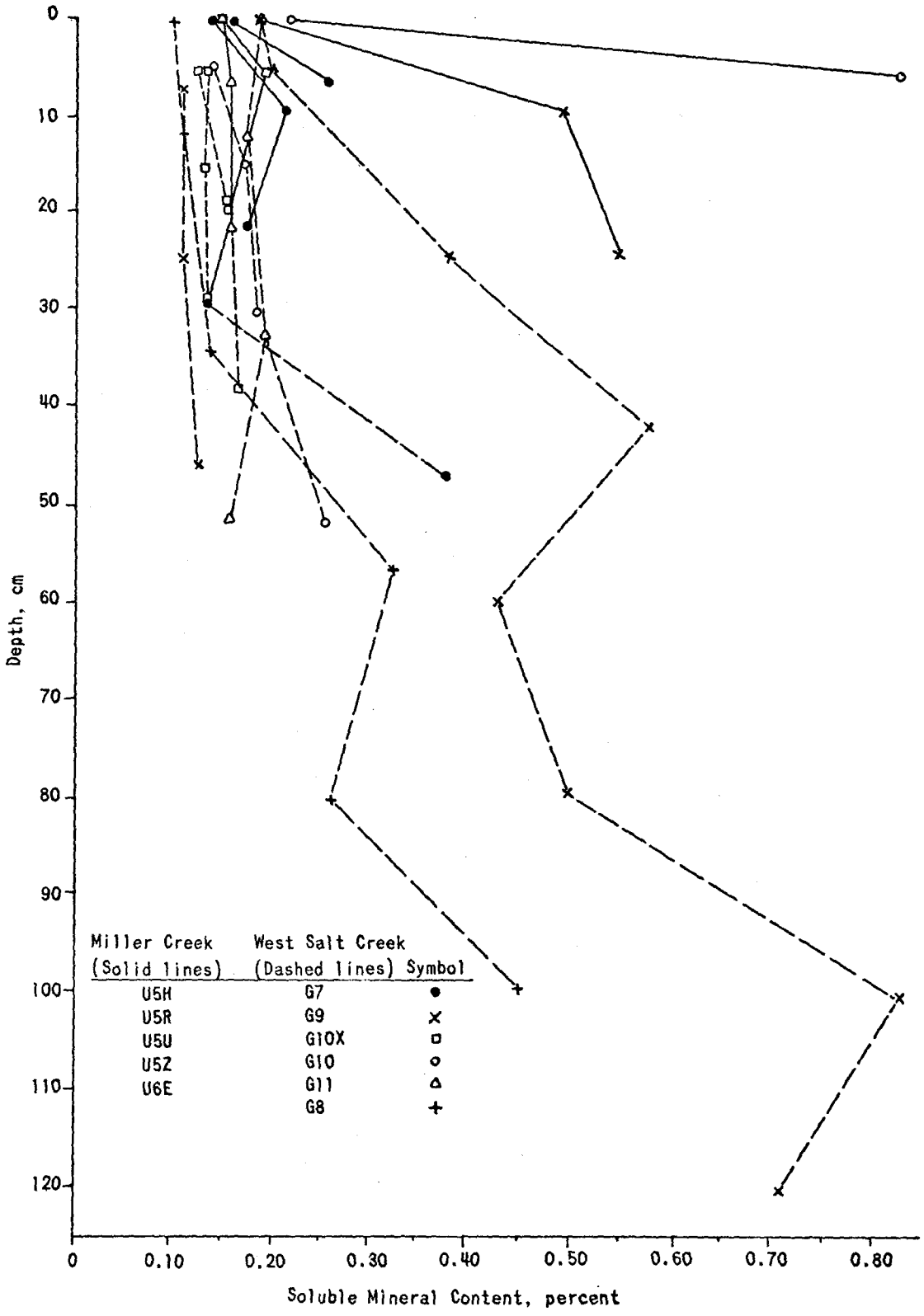

Figure 4.6. Variation of soluble mineral content with depth of terrace samples from North Miller Creek (solid lines) and from West Salt Creek (dashed lines).

4.2c The Soluble Mineral Content of Sampling Units

Differences in soluble mineral content between sampling units are marked by the generally large inherent variability of this parameter. In other words, the variance within any group defining, say, a terrace, is larger than the variance in soluble mineral content between a terrace and banks of Mancos Shale. The extent of this variability is shown in Table 4.1, in which a summary is given of the mean and the standard deviation about the mean soluble mineral content of sampling units.

An analysis of variance of the mean soluble mineral content of all sampling units (excluding Mancos Shale slopes) in West Salt Creek reveals that a difference ($p < 0.05$) between them does exist. This difference, however, is not significant at a 95 percent confidence interval about the means. In this connection it should be noted that the standard deviation of the compared property must be approximately equal in all groups (i.e., sampling units) undergoing an analysis of variance. Note, however, that the soluble mineral content of the terrace crusts has a considerably smaller standard deviation than that of other groups. Deleting the data of terrace crusts and mass wasted materials ('A' of Table 4.1, with a very large standard deviation) does not alter the situation. It is therefore inferred that the variability within an alluvial unit is almost as large or larger than it is between units. This conclusion also applies to North Miller Creek (significant F with $p < 0.05$) as well as to the alluvium of Mesa Creek. It may be added that the analysis of variance for the Mesa Creek units showed no significant difference whatsoever (i.e., F not significant) in salt content.

Notwithstanding the large inherent variability in soluble mineral content, one significant difference (at a confidence interval about the means of 95 percent) stands out clearly. This is between the soluble mineral content of alluvial materials in West Salt and North Miller Creeks and the Mancos Shale walls, bed and slopes. These slopes are significantly richer in soluble minerals than any other sampling unit excluding the efflorescent crusts. Also, the lower Mancos walls and bed material of North Miller Creek contain more soluble minerals than the overlying terraces (though only at a confidence interval slightly less than 90 percent). Figure 4.7 shows these differences in a schematic diagram.

Mancos Shale is the main source of soluble minerals. The shale contains approximately 2 percent soluble minerals in 1:99 mixtures. It is conceivable, however, that the surficial part of Mancos Shale is more leached than the deeper layers. For instance, Leythaeuser (1973) has shown that surficial Mancos Shale (50 cm depth) contains 0.9 percent organic carbon, which increases to 1.05 percent for underlying layers; the soluble organic matter component (in mg per gram organic carbon) is 16.5 at a depth of 50 cm and for underlying layers it increases to a value of 30.0.

4.3 Functional Relationship between Inorganic Water Quality and Soluble Mineral Content of Bed Materials

Texture and structure of fluvial sediments are causally related to hydraulics, channel form and channel shape (Schumm, 1960; Karcz, 1968; Reineck and Singh, 1975). This means that information on the shape, form and hydrologic regime of a channel may be acquired via the

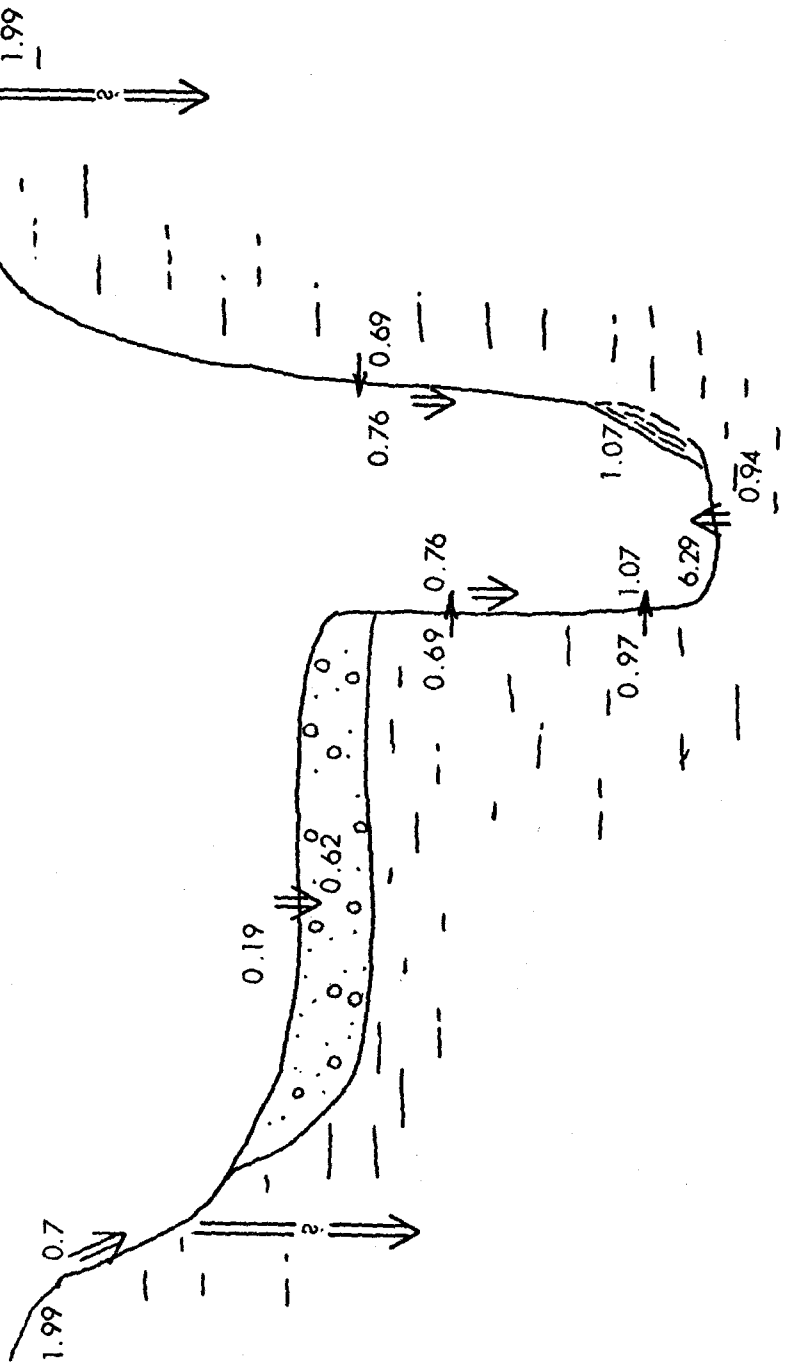

Figure 4.7. Schematic cross section in North Miller Creek showing the mean soluble mineral content (in percent) of sampling units. In this model, the arrows point to the transport direction of solutes.

alluvium which it deposits. Similarly, a hypothesis can be advanced that a cause and effect relationship exists between the salinity of runoff and the soluble mineral content of channel deposits. Specifically, it is proposed that salt content of bed materials is an indication of the water quality of storm runoff.

Various studies such as those of Davis (1961), Hembree and Rainwater (1961) and Miller (1961) have shown that water quality of low flows is strongly correlated with the lithology and geochemistry of the country rock. Feth, Robenson and Polzer (1964) also attribute much significance to the role of climate in weathering and, hence, to its effect on water quality of low flows. The chemical quality of storm runoff is, however, primarily influenced by the availability of soluble minerals on the surface and in crusts. This dependency may be more easily studied in ephemeral channels of semiarid and arid regions where the overland flow component of the hydrograph may be separated from the small low-flow contributions due to the peakedness of most flow events. Ponce (1975) has shown that there is a high correlation ($r = 0.955$) between the 1:1 EC of the crust (0-2.5 mm) and the EC of runoff produced on hillslope segments by simulated rainfall on Mancos Shale and related formations. His study also showed a generally high correlation between specific ion concentrations in 1:1 crust extracts and those in overland flow.

Grab samples of water were collected in sections G7 through G11 on July 10, 1975, during a small runoff event in West Salt Creek. The center of the storm appeared to have been located due west of the G10X site (see Figure 2.3 for this location). High intensity precipitation lasted for 40 minutes and it produced a maximum estimated discharge of

0.085 m^3 sec^{-1} (3 ft^3 sec^{-1}) at the G10X section and a maximum recorded discharge of 0.920 m^3 sec^{-1} (32.4 ft^3 sec^{-1}) at the gaging station (section G7).

The chemical quality of the collected water samples is summarized in Table A5 of the Appendix. The table also includes chemical analyses of samples collected at the gaging station (G7) and one at section G11 during low flow produced by a small storm on July 9, 1975. A list of the mean 1:99 EC of bed material crust mixtures at each site is summarized in Table 4.2 together with the EC of the water samples. A comparison between the EC of the bed material curst mixtures and that of the runoff reveals a difference between sections G7, G9, G10 and G10X and sections G8 and G11. The former group of sediments is low in soluble mineral content (0.6 percent) and includes channel reaches in the center of the alluvial valley. Both G8 and G11 sections are close to Mancos and Mesa Verde shales, respectively, and this proximity is manifested by the occurrence of saline seeps and the generally high salt content (1.8 percent) of the bed materials. As the storm runoff passed through the reaches characterized by saline bed materials its quality definitely deteriorated.

The $Na^{1+}/\Sigma C_i^{z+}$ ratios listed in Table 4.2 indicate the effect of soluble minerals in bed materials on the ionic composition of the storm runoff. As the runoff passed sections G11 and G8 it dissolved sodium and magnesium sulfates; it also mixed with the saline seeps, which contain high concentrations of Na^{1+}, Mg^{2+} and SO_4^{2-} (see the chemical composition of the seep at section G8 in Table A5 of the Appendix). In this connection it might be noted that all the water samples described in Table A5 are saturated or supersaturated with respect to calcite.

Table 4.2. Mean EC of 1:99 aqueous mixtures of bed materials and water discharge, EC and $Na^{1+}+Mg^{2+}$ abundance ratios of run-off samples at the studied sections in West Salt Creek.

Section	Sample Collection Date	Sample Collection Time	Estimated Discharge (m^3/sec)	Estimated Discharge (ft^3/sec)	pH	EC ($\mu mhos\ cm^{-1}$)	1:99 EC of Bed Material Crusts ($\mu mhos\ cm^{-1}$)	$(Na^{1+}+Mg^{2+})/C_i^{z+}$ ($meq\ l^{-1}/meq\ l^{-1}$)
G10	7-10-75	15:25	$2.83 \cdot 10^{-2}$	1.00	7.7	1400	60.0	0.531
G10	7-10-75	16:00			7.7	1200		0.503
G10X	7-10-75	16:00	$8.50 \cdot 10^{-2}$	3.00	7.9	1300	58.7	0.797
G9	7-10-75	15:00	$1.10 \cdot 10^{-3}$	0.04	7.6	2100	61.0	0.449
G9	7-10-75	16:20	$5.66 \cdot 10^{-2}$	2.00	7.7	2000		0.625
G7	7-9-75	12:00	$6.50 \cdot 10^{-3}$	0.23[a]	7.7	2800		0.588
G7	7-9-75	23:45	$2.83 \cdot 10^{-3}$	0.10[b]	7.7	3400	68.3	0.371
G7	7-10-75	16:55	$1.29 \cdot 10^{-1}$	4.54[a]	7.9	2700		0.302
G7	7-10-75	17:25	$1.22 \cdot 10^{-1}$	4.30[b]	7.9	3500		0.439
G7	7-10-75	18:20	$1.13 \cdot 10^{-1}$	4.00[b]	8.0	3200		0.365
G8	7-10-75	14:35	$1.42 \cdot 10^{-3}$	0.05	8.1	8700	170.7[c]	0.809
G8	7-10-75	16:40	$5.50 \cdot 10^{-4}$	0.02	7.9	1900		0.437
G11	7-10-75	13:00	$1.42 \cdot 10^{-3}$	0.05	8.7	12000	196.3	0.883
G11	7-10-75	13:45	$2.80 \cdot 10^{-3}$	0.10	8.1	8700		0.886
G11	7-10-75	13:35	$8.00 \cdot 10^{-4}$	0.03	8.0	12000		0.897
G11	7-11-75	12:00	$8.00 \cdot 10^{-4}$	0.03	8.7	12000		0.890

[a] Measured discharge; preliminary U. S. Geological Survey data subject to revision.

[b] Based on stage discharge relationship; preliminary U. S. Geological Survey data subject to revision.

[c] Exludes one efflorescent crust; if it is included, the mean $EC_{1:99} = 823\ \mu mhos\ cm^{-1}$.

Moreover, the samples collected in sections G7, G8 and G11 (excluding the first G7 sample) are also saturated or supersaturated with respect to gypsum. It is therefore inferred that West Salt Creek transported incompletely dissolved soluble minerals (as its sediment load) in these reaches. It must be recognized, however, that the contribution of solutes from such saline reaches cannot be separated at this stage to that part directly contributed by the flowing seep and to the saline bed materials contaminated by earlier seep flows. A distinction between point and diffuse sources of salts is therefore not warranted in this context.

In summary, it may be concluded that water quality of storm runoff in ephemeral semiarid channels is affected substantially by the salt content of bed and lower gully wall crust materials. This conclusion is based on a single low magnitude, high frequency event in one channel. Additional information is clearly needed to substantiate this phenomenon and to determine its significance for flow events of higher magnitude.

CHAPTER 5

CONCLUSIONS

5.1 Summary and Conclusions

Specific electrical conductance (EC) was found to be a reliable estimate of the total dissolved solids (TDS) concentration of aqueous solutions derived from mixtures of distilled water and alluvium and Mancos Shale samples collected in the Upper Colorado River Basin. The effect of solids (i.e., no filtration) on the EC of such mixtures appeared negligible and, therefore, fast and low cost determinations of the EC of several hundred unfiltered mixtures of samples of bed, bank, terrace and slope materials provided information on the TDS concentration of the mixtures. Dissolution continued with contact time but reached an asymptotic value which represents partial equilibrium. The initial dissolution rate of soluble compounds in surficial Mancos Shale and alluvium generally increased as particle size decreased but particle size alone or increased turbulence did not exert an influence on the equilibrated concentration of the mixtures.

An increase in sediment concentration (i.e., in the sediment:water ratio) was followed by an increase in the TDS concentration of the mixtures. The source of additional dissolved minerals is the soluble matter in the added sediment. From the change in specific ion concentrations with contact time it appears that sodium and magnesium hydrated sulfates dissolve faster than gypsum or calcite. Also, it is evident that in most of the samples, not all potentially soluble minerals

dissolved in mixtures containing high (100,000 ppm) sediment concentrations. Dissolution of the samples was more complete as sediment concentration decreased. The main added dissolved constituents were Ca^{2+} and HCO_3^{1-}.

The dilution effect mentioned above also takes place in 1:9 mixtures undersaturated with respect to both gypsum and calcite as shown in the calculations of Table A4 of the Appendix. Hence, there exists a dissolution limiting phenomenon which probably takes place due to the coating of particles by slightly soluble minerals such as ferric oxides. This coating is assumed to be less complete and thinner on highly soluble mineral particles (such as $Na_2SO_4 \cdot 10H_2O$ and $MgSO_4 \cdot 7H_2O$ with solubilities of 4 and 6.4 Normal, respectively) which usually precipitate later than do gypsum or calcite from a solution undergoing evaporation.

Surficial alluvium and Mancos Shale were sampled in four basins located in areas known to contain appreciable diffuse sources of salts. The basins are underlain in whole or partly by the saline marine Mancos Shale. The variability in soluble mineral content of the sampled materials is very large with a range in standard deviation of 0.03 to 14.88. Lower variability is associated with Mancos Shale slope samples and with crusts of terraces. The large inherent variability in soluble mineral content masks clear trends of change in this parameter.

Mancos Shale from hillslopes, the source of most of the soluble minerals in the area, contains an appreciably higher content of soluble minerals (2 percent) than alluvial samples. The highest salt concentrations (10 percent) are found in efflorescent crusts on the bedrock (Mancos Shale) bed of North Miller Creek. Soluble minerals also tend

to accumulate in the upper 5 cm of the Mesa Creek bed, being transported upward by capillary action from the layer immediately underlying it. Salt buildup in crusts does not take place in highly permeable alluvial sediment such as on the bed of West Salt Creek. In fact, soluble minerals are leached from the crusts of terraces of North Miller and West Salt Creeks. Soluble mineral content increases with depth in shallow alluvium overlying Mancos Shale. The mean salt content of these alluvial bed materials and those in the vicinity of saline shale hillslopes (e.g., section G11) is very high (3-5 percent). No apparent trend in soluble mineral content with depth takes place in the generally sterile alluvium of terraces or in the bed of West Salt Creek.

The finding that thick alluvial deposits have low salt contents prompted sampling of alluvium retained by stockponds. Samples from stockponds (all G1C and G4 data summarized in Table A2 of the Appendix) were analyzed for soluble mineral content. Site G1 is located in the middle Leach Creek Basin (see Figure 2.3) where a stockpond receives runoff from Mancos Shale terrain that is appreciably covered by sandy soil and coarse alluvium capping pediment benches. The data from Table A2 show that the stockpond sediment (B1C samples) is <u>not</u> more saline than the bed materials in the upstream channel reach (G1B samples). The sediment which accumulated in the Crow Stockpond (site G4) does contain high amounts of soluble minerals. However, this salinity is attributed to the highly dissected Mancos Shale basin above this sediment-retaining structure. Therefore, it may be concluded that aggradation or sedimentation does not necessarily imply a high soluble mineral content in the deposited sediments. In fact, the measured high salinities of seeps originating downstream from stockponds afford an

explanation for the relatively low salt content of the retained sediments. Thus, not only do deep alluvial fills lack high salt content, but even artificially retained sediments loose much of their soluble minerals initially during transport and thence by leaching.

Mancos Shale is widely recognized as the largest major source of salinity in the Upper Colorado River Basin. However, the presence of a large number of saline seeps, the high salinity of section G11 in West Salt Creek (Table 4.2) as well as the overall high soluble mineral content of selected samples from the Mesa Verde marine Shales (samples G20 of Tables A1 and A2 of the Appendix) leave little doubt that the Mesa Verde Formation is also an important contributor of salinity to the Colorado River. A study of this source is recommended.

Hem (1970) and Lane (1975) have summarized much of the literature on the relations between water quantity and water quality. In general, TDS concentration decreases with increase in discharge due to dilution. However, TDS concentration initially increases on the rising limb of hydrographs (Miller and Drever, 1977) and especially in runoff from basins contributing substantial salinity from diffuse sources (Mundorff, 1972). Ponce (1975) has shown that the quality of overland flow follows a similar pattern. It is therefore suggested that saline crust accumulations constitute a major contributing source of salts to the storm runoff. Analysis of samples from a single low magnitude runoff-producing storm in West Salt Creek (Table 4.2) substantiates this hypothesis.

5.2 Implications

The rate of dissolution of the soluble constituents of Mancos Shale and alluvium varies considerably. The time required for a sediment:

water mixture to approach partial chemical equilibrium increases as sediment concentration increases and as the soluble mineral content of the mixed sediment decreases. This time interval ranges from a few minutes to several days. These results imply that the aqueous composition of stormwater changes downstream and may become constant over varying lengths of channel. Runoff from tributaries with a high suspended sediment concentration may very likely be chemically unequilibrated at the confluence with the main stem of the drainage basin. Additional soluble minerals will dissolve upon mixing with the more dilute water of the main stem. This dilution effect certainly applies to tributary runoff supersaturated or saturated with respect to a major potentially-soluble mineral that is present in the transported sediment; it also applies to runoff undersaturated with respect to such minerals because of the postulated presence of particle coatings.

The yield of dissolved solids from the semiarid drainage basins of the Upper Colorado River Basin should be greater than that calculated from EC measurements at gaging stations or from the analysis of water samples from tributary runoff. The chemical analyses fail to consider the dilution effect (which might increase the dissolved yield by as much as 500 percent) while the EC measurements also fail to consider whether the runoff is kinetically equilibrated with the transported sediment. It may be added that higher solute yields mean that the rate of chemical denudation is higher. In fact, the ratio of chemical denudation to denudation by erosion of particulate matter may therefore increase considerably.

Efflorescent crusts, Mancos Shale slope materials and shallow alluvium overlying Mancos Shale contain the highest quantities of

soluble minerals. Storm flow from bedrock channels in Mancos Shale terrain and in shallow alluvium should therefore contain very high TDS concentrations. Mancos Shale should also be the source of sodium-rich runoff. These high salt-yielding areas also contribute the highest sediment yields. The mean sediment yield from ungrazed Badger Wash basins (Lusby, Reid and Knipe, 1971) is 4700-6100 metric tons/km^2/yr (2000-2600 tons/mi^2/yr) with a maximum of 38,500 metric tons/km^2/yr (16,400 tons/mi^2/yr) using an average specific weight of 85 pounds/ft^3. These figures are very high in comparison with the mean worldwide maximum of 3520 metric tons/km^2/yr (1500 tons/mi^2/yr) in semiarid regions (Langbein and Schumm, 1958).

One of the objectives of this study is to relate potential yield of salts of surficial deposits (i.e., their soluble mineral content) to sediment yield and to channel morphology. Mancos Shale and associated alluvial materials are gullied throughout the entire Upper Colorado River Basin. The gullies may have been formed at the end of the 19th century by climatic changes and/or by overgrazing (Schumm and Hadley, 1957). It is concluded that areas underlain by Mancos Shale and associated shallow alluvial deposits are presently major diffuse sources of salts and that they contribute significant amounts of both sediment and solutes at any time but especially when gullied. Therefore, another recommendation is the need to delineate or map the Mancos Shale bedrock exposures and associated shallow alluvial areas considered herein to be major producers of dissolved solids. Such a delineation would require careful mapping and additional sampling of the saline materials to determine their salt content, but it would serve to identify the critical salt-producing areas within the much larger Mancos Shale outcrop area.

5.3 Recommendations

The role of moisture conditions on the salt content of alluvium and weathered bedrock was not determined in this study. The soluble mineral content of crusts of surficial materials and especially of bed and lower bank materials is expected to decrease during a precipitation event and subsequently to increase due to upward capillary movement and evaporation of soil water. It is suggested that this topic be studied in detail. The role of aeolian transport of dry saline surficial deposits may be more difficult to determine but it should not be altogether neglected.

EC measurements of stream water are inadequate for estimating the solute contribution from diffuse sources of salinity such as the Price River or West Salt Creek drainage basins. An analysis of the chemical quality of water samples is necessary in order to determine the relationship of EC to TDS concentration. Half of each water sample should be filtered immediately in order to determine whether the solution had attained equilibrium. Several of the unfiltered solutions should be diluted (to the equivalent TDS value of the Colorado River at the time of sampling) and the additional dissolution taking place should be studied. Upon addition of distilled water the TDS of the solution may increase as much as 500 percent, as shown by the $11(TDS_{1:99}/TDS_{1:9})$ dilution ratios of Tables A1 and A2 of the Appendix.

Mixtures of surficial deposits and water undersaturated with respect to gypsum and calcite should be further studied to determine the mechansim which limits complete dissolution of soluble minerals. X-ray diffraction studies underway at the University of California at Davis may throw light on the mineralogic composition and quantities of particle coatings.

Erosion control in the semiarid Southwest is very costly. Instead of constructing numerous sedimentation reservoirs (which, as Wein and West (1973) showed, accumulate sediment that is too saline for revegetation and from which saline water seeps downstream) in small (1 km^2) basins it is proposed that the economics of building larger sediment retaining earth structures for channels draining at least 100 km^2 but preferably 500 km^2 (about 200 mi^2) be studied. These should be capable of retaining a flow event of about a five-year recurrence. Larger events should be allowed by proper design to leave the structure intact. Several days after a flow event, when most of the sediment has already settled in the ponded area, the water should be pumped into a nearby closed basin (such as a neighboring plugged gully) lined with an impermeable bottom. After complete evaporation of the saline ponded water, the precipitated soluble minerals could be collected and removed.

Reduction of high sediment and solute yields require conservation techniques which may be achieved by inducing local aggradation of channel reaches where the channel beds incise into Mancos Shale or where the alluvial fill is very shallow. A second recommended conservation technique is to keep the channel away from Mancos Shale outcrops by straightening reaches or defelcting them away from the valley sides such that the main channel will remain in the center of the valley floor.

One important recommendation which stems from this study is the need to map and thereby to classify those areas in the Upper Colorado River Basin known to be serious contributors of dissolved solids. Such a classification would be based on an index of salinity potential which in turn would depend on the soluble mineral content of surficial materials in these diffuse source areas. Upon completion of the salinity map it may be used by government and state officials to indicate specific hazard areas.

The compilation of a map showing the salinity hazard within the Upper Colorado River Basin must also be based on the erodibility of the terrain, which indicates the yield of sediment and associated soluble minerals. Also, the geomorphic and hydrologic characteristics of the area and the hydraulic regimen of the channelways must be specified because they describe the transport capacity of the channels.

LITERATURE CITED

Berner, R. A., 1971, Principles of Chemical Sedimentology: McGraw Hill Co., N.Y., 240p.

Billings, G. K. and Williams, H. H., 1967, Distribution of clorine in terrestrial rocks (a discussion): Geochim. et Cosmochim. Acta, 31, 2247.

Branson, F. A., and Owen, J. B., 1970, Plant cover, runoff and sediment yield relationships on Mancos Shale in Western Colorado: Water Resources Res., 6(3): 783-790.

Butler, J. N., 1964, Ionic Equilibrium--A Mathematical Approach: Addison Wesley Publ. Co., Reading, Mass., 547p.

Carrol, Dorothy, 1959, Ion exchange on clays and other minerals: Geol. Soc. Am. Bull., 70: 749-780.

Carrol, Dorothy, 1962, Rainwater as a chemical agent of geologic processes--a review: U. S. Geol. Survey Water Supply Paper 1535-G, 18p.

Davis, G. H., 1961, Geologic control of mineral composition of stream waters of the eastern slope of the southeastern Coast Ranges, California: U. S. Geol. Survey Water Supply Paper 1535-B, 30p.

Fanning, C. D. and Lyels, Leon, 1964, Salt concentration of rainfall and shallow groundwater across the Lower Rio Grande Valley: Jour. Geophys. Res., 69(4): 599-604.

Fenneman, N. M., 1931, Physiography of the Western United States: McGraw Hill Co., N.Y., 534p.

Feth, J. H., Robenson, C. E. and Polzer, W. L., 1964, Sources of mineral constituents in water from granitic rocks. Sierra Nevada, California and Nevada: U. S. Geol. Survey Water Supply Paper 1535-I, 70p.

Fisher, D. J., Erdmann, C. E. and Reeside, J. B. Jr., 1961, Cretaceous and Tertiary formations of the Book Cliffs. Carbon, Emery and Grand Counties, Utah and Garfield and Mesa Counties, Colorado: U. S. Geol. Survey Profess. Paper 332, 80p.

Garrels, R. M. and Christ, C. L., 1965, Solutions, Minerals and Equilibria: Harper and Row, N.Y., 450p.

Garrels, R. M. and Thompson, M. E., 1962, A chemical model for seawater at 25°C and one atmosphere total pressure: Am. Jour. of Sci., 360: 57-66.

Hardie, L. A., 1968, The origin of the Recent non-marine evaporite deposit of Saline Valley, Inyo County, California: Geochim. et Cosmochim. Acta, 32: 1279-1301.

Harned, H. S. and Owen, B. B., 1958, The Physical Chemistry of Electrolyte Solutions: Reinold Publ. Co., N.Y., 3rd edition, 803p.

Helgeson, H. C., 1971, Kinetics of mass transfer among silicates and aqueous solutions: Geochim. et Cosmochim. Acta, 35: 421-469.

Hem, J. D., 1970, Study and interpretation of the chemical characteristics of natural water: U. S. Geol. Survey Water Supply Paper 1473, 363p.

Hembree, C. H. and Rainwater, F. H., 1961, Chemical degradation on opposite flanks of the Wind River Range, Wyoming: U. S. Geol. Survey Water Supply Paper 1535-E, 9p.

Iorns, W. V., Hembree, C. H. and Oakland, G. L., 1965, Water Resources of the Upper Colorado River Basin--Technical Report: U. S. Geol. Survey Profess. Paper 441, 370p.

Karcz, Iaakov, 1968, Fluviatile obstacle marks from the wadis of the Negev (Southern Israel): Jour. of Sed. Petr., 38(4): 1000-1012.

Knobel, E. V. *et al.*, 1955, Soil survey of the Grand Junction area, Colorado: U. S. Dept. of Agr. Soil Survey Series 1940, 19, 118p.

Lane, W. L., 1975, Extraction of information on inorganic water quality: Colo. State Univ. Hydrol. Papers, 73, 74p.

Langbein, W. B. and Schumm, S. A., 1958, Yield of sediment in relation to mean annual precipitation: Trans. Am. Geophy. Union, 39: 1076-1084.

Laronne, J. B., 1977, Dissolution potential of surficial Mancos Shale and alluvium. Unpub. Ph.D. Dissertation, Dept. Earth Resources, Colo. State Univ., Ft. Collins, Colo., 128p.

Leythauser, Detlev, 1973, Effects of weathering on organic matter in shales: Geochim. et Cosmochim. Acta, 37: 113-120.

Lotspeich, F. B. *et al.*, 1969, Quality of waters from playas on the Southern High Plains: Water Resources Res., 5(1): 48-58.

Lusby, G. C., Reid, V. H. and Knipe, O. D., 1971, Effects of grazing on the hydrology and geology of the Badger Wash Basin in Western Colorado, 1953-1966: U. S. Geol. Survey Water Supply Paper 1532-D, 90p.

Maletic, J. T., 1973, Colorado River Water Quality Improvement Program: pres. Seminar on Agriculturally Related Pollution, Colo. State Univ., Fort Collins (unpub.).

Miller, J. P., 1961, Solutes in small streams draining single rock types, Sangre de Cristo Range, New Mexico: U. S. Geol. Survey Water Supply Paper, 1535-F, 23p.

Miller, W. R. and Drever, J. I., 1977, Water chemistry of a stream following a storm, Absaroka Mountains, Wyoming: Geol. Soc. Am. Bull., 88: 286-290.

Morgan, J. J., 1967, Applications and limitations of chemical thermodynamics in natural water systems: in Stumm, Werner, Chairman (ed.) Equilibrium Concepts in Natural Water Systems: Am. Chem. Soc., Adv. in Chem. Series, 67: 1-29.

Mundorff, J. D., 1972, Reconnaissance of chemical quality of surface water and fluvial sediment in the Price River Basin, Utah: State of Utah Dept. of Nat. Res. Tech. Publ., 39, 55p.

Ponce, S. L. II, 1975, Examination of a non-point source loading function for the Mancos Shale wildlands of the Price River Basin, Utah: Unpub. Ph.D. dissertation, Dept. Civ. and Env. Eng., Utah State Univ., Logan, Utah, 177p.

Price, Don and Waddell, K. M., 1973, Selected hydrologic data in the Upper Colorado River Basin: U. S. Geol. Survey Hydrol. Atlas Investig., HA-477, 2p.

Reineck, H. E. and Singh, I. B., 1975, Depositional Sedimentary Environments: Springer-Verlag, N. Y., 439p.

Reitemeier, R. F., 1946, Effect of moisture content on the dissolved and exchangeable ions of soils of arid regions: Soil Sci., 61: 195-214.

Schneider, E. D., 1975, Surficial geology of the Grand Junction-Fruita area, Mesa County, Colorado: Unpubl M.S. thesis, Dept. of Earth Resources, Colo. State Univ., Fort Collins, Colo., 141p.

Schumm, S. A., 1960, The effect of sediment type on the shape and stratification of some modern fluvial deposits: Am. Jour. of Sci., 258(3): 177-184.

Schumm, S. A., 1964, Seasonal variations of erosion rates and processes on hillslopes in western Colorado: Zeitschrift für Geomorphologie, 5: 215-238.

Schumm, S. A. and Hadley, R. F., 1957, Arroyos and the semiarid cycle of erosion: Am. Jour. of Sci., 255: 161-174.

Sillen, L. G. and Martell, A. E., 1964, Stability constants, supplement no. 1: Chem. Soc. Special Pub. no 25, Burlington House, London, 865p.

Skogerboe, G. V., 1972, Salinity control measures in the Grand Valley: in Managing Irrigated Agr. to Improve Water Quality, Proc. Nat. Conf. on Managing Irrigated Agr. To Improve Water Quality, Colo. State Univ., Fort Collins, Colorado, 137-146.

Snedecor, G. W. and Cochran, W. G., 1967, Statistical Methods, 6th ed.: Ames, Iowa Univ. Press, 593p.

Stokes, W. L. and Cohenour, R. E., 1956, Geologic atlas of Utah: Utah Geol. and Miner. Survey Bull., 52, 92p.

Stumm, Werner and Morgan, J. J., 1970, Aquatic Chemistry--An Introduction Emphasizing Chemical Equilibria in Natural Waters: Wiley Interscience, N.Y., 483p.

Swenson, J. L. Jr. *et al.*, 1970, Soil survey of Carbon-Emery area, Utah: U. S. Dept. Agr. Soil Cons. Service, Washington D.C., 78p.

U. S. Dept. Agr., 1954, Diagnosis and improvement of saline and alkali soils: U. S. Agr. Handbook no. 60, 160p.

U. S. Dept. Agr., 1964, Internal, unpublished data from logs of test holes in Indian Wash reservoir, site IW-1; Form SCS-533 dated Feb.-March, prepared by Elkin, A. D., Soil Cons. Service, Denver, 45p.

U. S. Dept. Commerce, 1956, Normal annual precipitation for the state of Colorado; 1:500,000 map: Environmental Science Serv. Adm., Weather Bureau.

U. S. Environ. Protect. Agency, 1972, Proc. of the Conf. in the matter of pollution of the interstate waters of the Colorado River and its tributaries--Colo., New Mex., Ariz., Calif., Nev., Wyo. and Utah, 7th Session, Las Vegas, Nev., Feb. 15-17, v.1.

U. S. Geol. Survey, 1969-1975, Water resources data for Colorado: Prepared in coop. with the State of Colo. and with other agencies (Richards, L. A., ed.).

Weast, R. C. (ed.), 1975, Handbook of Physics and Chemistry: CRC Press Inc., 55th edition.

Wein, R. W. and West, N. E., 1973, Soil changes caused by erosion control treatments on a salt desert area: Soil Sci. Soc. Am. Proc., 37: 98-103.

Wollast, R., 1967, Kinetics of the alteration of K-feldspar in buffered solutions at low temperature: Geochim et Cosmochim. Acta, 31: 635-648.

APPENDIX

Table A1. Summary of chemical analyses of solutions derived from aqueous mixtures (1:999, 1:99, 1:9, 1:4 and 1:1) of selected sediment samples.

Concentration	Sample Number	EC (μmhos cm^{-1})	Millequivalents per Liter									$\left\lvert\left(\frac{\Sigma C_i^{z+} - \Sigma C_i^{z-}}{\Sigma C_i^{z-}}\right)\right\rvert 100$ (in %)	Calculated TDS (mg/l)	$11\left(\frac{TDS_{1:99}}{TDS_{1:9}}\right)$
			Ca	Mg	Na	K	SO_4	HCO_3	Cl	NO_3	CO_3			
1:99	U5E1A	124.0	0.4	0.1	0.5	0.0	0.5	0.4	0.0	0.0	0.0	11.1	81.2	3.41
1:9	U5E1A	390.0	0.7	0.2	2.7	0.0	2.8	0.8	0.0	0.0	0.0	0.0	261.8	
1:1	U5E1A	1600.0	0.7	0.5	16.4	0.4	16.4	1.8	0.0	0.1	0.0	1.1	1316.5	
1:99	U5E1B	145.0	0.25	0.15	0.9	0.0	0.5	0.8	0.0	0.0	0.0	0.0	100.4	3.35
1:9	U5E1B	432.0	0.1	0.1	4.2	0.0	1.6	2.5	0.0	0.0	0.0	7.3	329.2	
1:1	U5E1B	1600.0	0.2	0.4	16.4	0.4	14.1	3.5	0.0	0.1	0.0	1.1	1298.5	
1:99	U5E1B	134.0	0.3	0.1	0.8	0.0	0.5	0.7	0.0	0.0	0.0	0.0	92.4	2.47
1:9	U5E1B	635.0	0.5	0.2	5.2	0.0	3.8	1.6	0.0	0.0	0.0	9.3	412.2	
1:99	U5E2A	127.0	0.5	0.1	0.5	0.0	0.6	0.5	0.0	0.0	0.0	0.0	82.1	2.85
1:9	U5E2A	540.0	1.5	0.5	2.7	0.0	3.4	0.9	0.0	0.0	0.0	9.3	316.4	
1:1	U5E2A	2400.0	8.4	4.7	15.9	0.7	27.7	0.9	0.0	0.0	0.0	3.9	2003.8	
1:99	U5E2B	168.0	0.7	0.2	0.6	0.0	0.8	0.5	0.0	0.0	0.0	15.4	99.2	2.51
1:9	U5E2B	650.0	1.4	0.6	4.6	0.0	6.1	0.0	0.0	0.0	0.0	8.2	434.1	
1:1	U5E2B	3800.0	12.8	7.6	33.3	0.7	51.6	0.7	0.0	0.4	0.0	3.2	3687.7	
1:99	U5E2C	185.0	0.8	0.3	0.6	0.0	1.0	0.4	0.0	0.0	0.0	21.4	507.1	2.30
1:9	U5E2C	725.0	2.1	0.9	4.6	0.0	6.9	0.4	0.0	0.0	0.0	2.7	3837.7	
1:1	U5E2C	4200.0	17.6	8.6	28.9	0.8	53.9	0.8	0.1	0.8	0.0	0.9	105.9	
1:99	U5E2D	321.0	0.9	0.3	1.6	0.0	2.4	0.2	0.0	0.0	0.0	7.7	185.9	1.65
1:9	U5E2D	1770.0	3.2	1.5	14.1	0.0	16.9	0.4	0.0	0.0	0.0	8.7	1242.6	
1:1	U5E2D	11200.0	21.1	17.9	123.0	1.4	152.3	0.8	5.0	2.5	0.0	1.7	11058.0	
1:99	U5E3A	476.0	4.9	0.1	0.2	0.0	4.6	0.2	0.0	0.0	0.0	10.4	337.2	3.18
1:9	U5E3A	1350.0	17.4	0.3	0.2	0.0	16.1	0.6	0.0	0.0	0.0	7.2	1166.8	
1:1	U5E3A	2100.0	30.8	0.7	0.2	0.4	30.5	0.6	0.0	0.1	0.0	2.9	2153.7	
1:99	U5E3B	426.0	3.9	0.3	0.2	0.0	3.9	0.2	0.0	0.0	0.0	7.3	285.9	5.34
1:9	U5E3B	800.0	8.0	0.7	0.4	0.0	8.2	0.4	0.0	0.0	0.0	5.8	596.3	
1:1	U5E3B	2200.0	30.2	3.3	0.9	0.7	32.4	0.6	0.0	0.1	0.0	6.0	2292.4	

Table A1. Continued.

Concentration	Sample Number	EC (μmhos cm^{-1})	Millequivalents per Liter									$\left\|\left(\frac{\Sigma C_i^{z+} - \Sigma C_i^{z-}}{\Sigma C_i^{z-}}\right)\right\| 100$ (in %)	Calculated TDS (mg/l)	$11\left(\frac{TDS_{1:99}}{TDS_{1:9}}\right)$
			Ca	Mg	Na	K	SO_4	HCO_3	Cl	NO_3	CO_3			
1:99	U5E3C	423.0	4.3	0.1	0.1	0.0	3.9	0.2	0.0	0.0	0.0	4.9	289.2	3.06
1:9	U5E3C	1200.0	14.2	0.7	0.4	0.0	15.1	0.2	0.0	0.0	0.0	0.0	1039.7	
1:1	U5E3C	3800.0	28.1	7.6	19.1	0.8	54.7	0.5	1.6	0.1	0.0	2.3	3846.6	
1:99	U5E4A	317.0	1.0	0.4	1.6	0.0	2.3	0.5	0.0	0.0	0.0	7.1	202.7	1.59
1:9	U5E4A	2150.0	4.2	3.5	13.8	0.0	20.0	0.0	0.0	0.0	0.0	7.5	1404.6	
1:1	U5E4A	15000.0	21.5	41.8	168.0	1.4	222.6	0.7	12.7	0.6	0.0	1.7	16077.8	
1:99	U5E4B	187.0	0.9	0.3	0.5	0.0	0.9	0.6	0.0	0.0	0.0	13.3	113.0	0.94
1:9	U5E4B	1800.0	3.9	1.8	14.9	0.0	18.0	0.3	0.0	0.0	0.0	12.3	1325.4	
1:1	U5E4B	3300.0	13.7	8.4	22.1	0.6	44.5	0.5	0.5	0.0	0.0	1.5	3093.8	
1:99	U5E4C	85.6	0.3	0.1	0.3	0.0	0.6	0.0	0.0	0.0	0.0	16.7	42.9	1.49
1:9	U5E4C	450.0	1.0	0.5	3.2	0.0	3.5	0.8	0.0	0.0	0.0	9.3	316.6	
1:1	U5E4C	1700.0	1.2	1.0	15.4	0.3	16.0	1.1	0.1	0.0	0.0	2.9	1241.1	
1:99	U6A1	6100.0	5.4	19.5	57.4	0.0	76.4	0.5	1.8	0.0	0.0	4.3	5428.8	1.48
1:9	U6A1	35000.0	26.9	158.1	421.2	0.0	578.1	1.9	10.0	0.0	0.0	2.8	40381.5	
1:1	U6A1	95000.0	23.5	2100.0	2700.0	23.8	4600.0	12.1	190.0	0.6	1.0	0.9	317519.6	
1:99	M2C1	77.2	0.4	0.1	0.1	0.0	0.5	0.0	0.0	0.0	0.0	20.0	35.5	1.68
1:9	M2C1	422.0	2.8	0.7	0.2	0.0	3.4	0.0	0.0	0.0	0.0	11.8	232.5	
1:1	M2C1	1300.0	11.0	3.6	0.2	0.4	14.8	0.8	0.0	0.1	0.0	3.2	1050.3	
1:99	M2C2	106.0	0.5	0.2	0.2	0.0	0.7	0.2	0.0	0.0	0.0	0.0	62.9	6.76
1:9	M2C2	284.0	0.3	0.2	0.8	0.0	0.3	1.0	0.0	0.0	0.0	0.0	102.3	
1:1	M2C2	1500.0	13.3	3.3	1.1	0.3	16.9	0.7	0.0	0.3	0.0	0.6	1216.7	
1:99	M2C3	35.8	0.2	0.1	0.1	0.0	0.3	0.0	0.0	0.0	0.0	33.3	21.9	3.33
1:9	M2C3	139.0	0.6	0.2	0.2	0.0	0.6	0.4	0.0	0.0	0.0	0.0	72.3	
1:1	M2C3	400.0	2.8	0.9	0.1	0.2	3.0	0.6	0.0	0.1	0.0	8.1	264.1	
1:99	M2D1	72.0	0.55	0.1	0.15	0.0	0.3	0.45	0.0	0.0	0.0	6.7	57.6	6.30
1:9	M2D1	165.0	0.9	0.1	0.4	0.0	0.7	0.7	0.0	0.0	0.0	0.0	104.8	
1:1	M2D1	400.0	4.2	0.3	0.2	0.3	3.1	1.9	0.0	0.0	0.0	0.0	368.9	
1:99	M2D4-5	173.0	1.2	0.1	0.1	0.0	1.0	0.45	0.0	0.0	0.0	3.5	87.8	1.42
1:9	M2D4-5	841.0	8.9	1.0	0.2	0.0	9.8	0.7	0.0	0.0	0.0	1.0	678.0	
1:1	M2D4-5	2400.0	26.9	6.1	0.5	0.2	31.2	1.9	0.0	0.0	0.0	1.8	2173.8	

Table A1. Continued.

Concentration	Sample Number	EC (μmhos cm^{-1})	Millequivalents per Liter									$\left\lvert\left(\frac{\Sigma C_i^{z+} - \Sigma C_i^{z-}}{\Sigma C_i^{z-}}\right)\right\rvert 100$ (in %)	Calculated TDS (mg/l)	$11\left(\frac{TDS_{1:99}}{TDS_{1:9}}\right)$
			Ca	Mg	Na	K	SO_4	HCO_3	Cl	NO_3	CO_3			
1:99	M2D8-9	388.0	2.3	0.7	0.4	0.0	3.0	0.3	0.0	0.0	0.0	3.0	226.2	2.73
1:9	M2D8-9	1140.0	8.2	3.6	2.3	0.0	13.0	0.4	0.0	0.0	0.0	5.2	909.8	
1:1	M2D8-9	4800.0	20.6	29.0	18.1	0.4	61.4	0.7	0.8	0.1	0.0	8.1	4229.3	
1:99	M3A1	168.0	1.0	0.2	0.2	0.0	1.0	0.3	0.0	0.0	0.0	7.7	93.4	1.54
1:9	M3A1	920.0	7.5	2.1	1.1	0.0	9.2	0.4	0.0	0.0	0.0	12.5	667.4	
1:1	M3A1	2200.0	15.0	7.7	5.8	0.3	30.2	0.7	0.0	0.1	0.0	7.1	2038.7	
1:99	M3A12-13	235.0	1.6	0.2	0.1	0.0	1.6	0.3	0.0	0.0	0.0	0.0	132.0	3.03
1:9	M3A12-13	642.0	5.1	1.4	0.9	0.0	6.7	0.3	0.0	0.0	0.0	5.7	480.0	
1:1	M3A12-13	2400.0	15.2	8.6	7.1	0.3	30.2	0.7	0.0	0.0	0.0	1.0	2077.4	
1:99	M3A23-24	900.0	9.9	0.5	0.3	0.0	9.5	0.3	0.0	0.0	0.0	9.2	686.0	4.15
1:9	M3A23-24	1980.0	24.2	2.7	1.8	0.0	25.8	0.3	0.0	0.0	0.0	10.0	1816.7	
1:1	M3A23-24	3700.0	25.1	16.1	11.9	0.4	47.4	0.7	0.1	0.1	0.0	10.8	3295.2	
1:99	M3A33-34	832.0	9.0	0.6	0.2	0.0	8.5	0.3	0.0	0.0	0.0	11.4	618.8	3.98
1:9	M3A33-34	1950.0	22.4	3.0	1.7	0.0	24.3	0.3	0.0	0.0	0.0	10.2	1710.0	
1:1	M3A33-34	3500.0	25.2	18.0	8.6	0.5	48.4	0.7	0.1	0.1	0.0	6.1	3318.8	
1:99	M3B1	67.1	0.4	0.1	0.1	0.0	0.2	0.4	0.0	0.0	0.0	0.0	45.6	5.13
1:9	M3B1	199.0	1.15	0.35	0.2	0.0	0.7	1.05	0.0	0.0	0.0	2.9	97.7	
1:1	M3B1	500.0	3.8	0.5	0.2	0.6	2.8	2.0	0.0	0.0	0.0	6.3	343.4	
1:99	M3B9	329.0	2.3	0.4	0.2	0.0	2.6	0.0	0.0	0.0	0.0	11.5	180.4	2.27
1:9	M3B9	1090.0	10.3	1.9	1.3	0.0	12.5	0.2	0.0	0.0	0.0	6.3	872.7	
1:1	M3B9	4100.0	28.3	16.9	11.7	0.2	46.0	1.4	6.2	1.9	0.0	4.8	3681.8	
1:99	M3B17-18	271.0	1.9	0.2	0.2	0.0	2.0	0.2	0.0	0.0	0.0	4.6	153.4	2.70
1:9	M3B17-18	881.0	8.0	1.2	0.7	0.0	8.8	0.2	0.0	0.0	0.0	10.0	625.9	
1:1	M3B17-18	3200.0	29.2	9.9	5.1	0.5	37.6	1.1	4.0	2.0	0.0	0.0	2981.2	
1:99	M3H1-2	448.0	3.5	0.4	0.3	0.0	4.0	0.0	0.0	0.0	0.0	5.0	274.0	1.56
1:9	M3H1-2	2100.0	23.6	3.5	2.6	0.0	28.2	0.0	0.0	0.0	0.0	5.3	1929.7	
1:1	M3H1-2	3200.0	24.5	12.7	16.6	0.0	49.0	0.0	0.0	0.0	0.0	9.8	3380.5	
1:99	M3K16-18	795.0	7.9	0.5	0.2	0.0	8.5	0.0	0.0	0.0	0.0	1.3	577.3	3.61
1:9	M3K16-18	2100.0	23.4	2.2	1.4	0.0	25.6	0.0	0.0	0.0	0.0	5.5	1757.5	
1:1	M3K16-18	2610.0	23.9	13.8	9.4	0.0	46.2	0.0	0.0	0.0	0.0	2.0	3081.9	

Table A1. Continued.

Concentration	Sample Number	EC (μmhos cm^{-1})	Millequivalents per Liter									$\left\|\left(\frac{\Sigma C_i^{z+} - \Sigma C_i^{z-}}{\Sigma C_i^{z-}}\right)\right\| 100$ (in %)	Calculated TDS (mg/l)	$11\left(\frac{TDS_{1:99}}{TDS_{1:9}}\right)$
			Ca	Mg	Na	K	SO_4	HCO_3	Cl	NO_3	CO_3			
1:99	M3K22-24	922.0	10.2	0.3	0.2	0.0	10.3	0.0	0.0	0.0	0.0	4.9	707.4	4.49
1:9	M3K22-24	2050.0	22.2	2.7	1.7	0.0	25.3	0.0	0.0	0.0	0.0	5.1	1732.0	
1:1	M3K22-24	2670.0	24.9	6.9	5.2	0.0	36.0	0.0	0.0	0.0	0.0	2.8	2431.5	
1:99	M3L1	372.0	3.0	0.2	0.1	0.0	2.6	0.0	0.0	0.0	0.0	26.9	226.3	3.22
1:9	M3L1	958.0	9.9	1.2	0.7	0.0	10.2	0.9	0.0	0.0	0.0	6.3	773.9	
1:1	M3L1	2900.0	29.3	7.2	3.7	0.7	37.5	1.7	1.4	0.2	0.0	0.2	2754.1	
1:1	M3L4-5	3400.0	28.8	15.9	4.0	0.4	41.7	1.3	4.4	0.6	0.0	2.3	3153.5	
1:99	M3L8-9	203.0	1.3	0.2	0.2	0.0	1.2	0.2	0.0	0.0	0.0	21.4	102.9	
1:1	M3L8-9	3200.0	27.1	11.2	5.9	0.6	37.5	0.7	6.0	0.2	0.0	0.9	2907.3	
1:99	M4B1	760.0	5.9	0.8	1.4	0.0	7.8	0.0	0.0	0.0	0.0	3.9	534.8	2.94
1:9	M4B1	2460.0	15.2	3.9	11.2	0.0	29.0	0.0	0.0	0.0	0.0	4.5	2002.4	
1:1	M4B1	10500.0	19.5	29.7	92.6	0.0	123.4	1.3	7.9	0.0	0.0	6.9	8807.7	
1:99	G10XC1	114.0	0.9	0.1	0.1	0.0	0.1	0.9	0.0	0.0	0.0	10.0	81.3	
1:99	G7B1	112.0	0.9	0.2	0.1	0.0	0.3	0.8	0.0	0.0	0.0	9.1	86.0	
1:4	G7B1	465.0	3.4	0.9	0.3	0.0	3.1	1.3	0.0	0.0	0.0	4.5	314.2	
1:99	G7A1	148.0	1.2	0.0	0.0	0.0	0.7	0.8	0.0	0.0	0.0	0.0	110.1	3.75
1:9	G7A1	500.0	4.1	0.6	0.1	0.0	3.8	0.8	0.0	0.0	0.0	4.4	323.1	
1:4	G7A1	860.0	8.6	1.1	0.2	0.0	9.0	0.9	0.0	0.0	0.0	0.0	677.5	
1:1	G7A1	2000.0	22.5	3.5	0.3	0.3	24.9	0.4	0.0	0.3	0.0	5.9	1751.0	
1:99	G8A1	2350.0	3.1	1.3	16.2	0.0	25.2	0.9	0.0	0.0	0.0	14.5	1715.6	1.11
1:9	G8A1	16000.0	21.2	86.3	163.6	0.0	237.0	35.6	5.1	0.0	0.6	2.6	17012.9	
1:4	G8A1	36000.0	23.3	191.2	361.2	0.0	540.8	5.1	12.0	0.0	1.9	2.8	37921.6	
1:999	G8G1	122.5	1.0	0.1	0.1	0.0	0.9	0.2	0.0	0.0	0.0	0.0	79.0	1.68
1:99	G8G1	801.0	6.6	0.3	0.7	0.1	7.3	0.2	0.0	0.0	0.0	2.7	518.7	
1:9	G8G1	3040.0	28.7	3.6	6.4	0.1	34.9	0.4	0.0	0.0	0.0	11.3	2476.6	
1:1	G7A2-3	2400.0	25.2	6.0	1.8	0.3	31.8	0.6	0.0	0.1	0.0	3.7	2201.3	
1:1	G7A4-5	1600.0	12.2	4.6	3.5	0.2	19.7	0.5	0.0	0.0	0.0	1.5	1365.4	
1:1	G7A6-7	1600.0	10.6	3.3	4.6	0.2	17.7	0.4	0.0	0.1	0.0	2.8	1246.9	
1:1	G7C1	900.0	3.1	2.0	3.6	0.2	7.6	0.5	0.0	0.4	0.0	4.7	597.4	
1:1	G7C2	600.0	1.5	1.2	3.5	0.2	4.9	0.6	0.0	0.1	0.0	14.3	411.1	

Table A1. Continued.

Concentration	Sample Number	EC (μmhos cm^{-1})	Millequivalents per Liter									$\left\|\left(\frac{\Sigma C_i^{z+} - \Sigma C_i^{z-}}{\Sigma C_i^{z-}}\right)\right\| 100$ (in %)	Calculated TDS (mg/l)	$11\left(\frac{TDS_{1:99}}{TDS_{1:9}}\right)$
			Ca	Mg	Na	K	SO_4	HCO_3	Cl	NO_3	CO_3			
1:1	G7C3	700.0	2.0	1.2	3.9	0.2	6.1	0.7	0.0	0.1	0.0	5.8	494.1	
1:1	G7C4	600.0	1.5	0.9	3.5	0.2	5.5	0.6	0.0	0.1	0.0	1.6	436.3	
1:1	G7E1	300.0	2.2	0.5	0.2	0.4	0.6	0.8	0.0	1.9	0.0	0.0	265.8	
1:1	G7E2	200.0	1.0	0.5	0.3	0.4	0.9	1.0	0.0	0.2	0.0	4.8	165.3	
1:1	G7E3-4	200.0	0.8	0.6	0.2	0.6	0.6	1.1	0.0	0.1	0.0	18.2	153.5	
1:1	G7E5-6	1500.0	15.1	1.9	1.0	0.4	16.9	0.5	0.0	0.1	0.0	5.1	1212.8	
1:99	G8G1-0.061	1162.0	12.0	0.6	0.9	0.0	13.0	0.2	0.0	0.0	0.0	2.3	905.1	
1:99	G8G10.061-	940.0	9.2	0.4	0.6	0.0	10.1	0.1	0.0	0.0	0.0	0.0	694.2	
1:99	G8G10.125	710.0	6.2	0.2	0.5	0.0	6.6	0.2	0.0	0.0	0.0	1.5	467.4	
1:99	G8G11-	768.0	7.3	0.4	0.7	0.0	8.0	0.2	0.8	0.0	0.0	6.7	592.1	
1:99	G8G10.25-	825.0	8.2	0.4	0.6	0.0	8.8	0.2	0.0	0.0	0.0	2.2	617.9	
1:99	G8G10.5-	685.0	6.2	0.5	0.8	0.0	6.9	0.2	0.0	0.0	0.0	5.6	492.3	
1:99	G8G12-	789.0	7.4	0.4	0.7	0.0	8.0	0.2	0.0	0.0	0.0	3.7	565.7	
1:99	G8G14-	830.0	9.1	0.3	0.5	0.0	9.1	0.3	0.0	0.0	0.0	5.3	652.9	
1:99	G8G18-	985.0	9.1	0.4	0.6	0.0	9.4	0.2	0.0	0.0	0.0	5.2	664.7	
1:99	(G8G18-)	112.5	0.6	0.3	0.4	0.0	0.9	0.5	0.0	0.0	0.0	7.1	90.6	
1:99	U5D1A-0.061	182.0	1.1	0.2	0.7	0.1	1.3	0.4	0.0	0.0	0.0	23.5	131.3	
1:99	U5D1A0.061-	186.5	0.9	0.2	0.7	0.1	1.3	0.3	0.0	0.0	0.0	18.8	121.2	
1:99	U5D1A0.125-	234.5	1.0	0.2	0.9	0.1	1.4	0.4	0.0	0.0	0.0	22.2	138.5	
1:99	U5D1A0.25-	223.5	1.0	0.2	0.8	0.1	1.3	0.5	0.0	0.0	0.0	16.7	137.5	
1:99	U5D1A0.5-	224.0	1.0	0.2	0.9	0.1	1.3	0.2	0.0	0.0	0.0	46.7	143.6	
1:99	U5D1A1-	234.0	1.3	0.2	0.9	0.1	0.6	0.6	0.0	0.0	0.0	108.3	118.5	
1:99	U5D1A2-	120.0	0.4	0.2	0.9	0.1	0.7	0.8	0.0	0.0	0.0	6.7	167.5	
1:99	U5D1A4-	128.5	0.4	0.2	0.8	0.1	0.6	0.6	0.0	0.0	0.0	25.0	98.2	
1:99	U5D1A8-	110.0	0.4	0.2	0.7	0.2	0.7	0.6	0.0	0.0	0.0	15.4	104.6	
1:1	G20A	2250.0	30.6	0.4	0.2	0.5	28.9	1.1	0.0	0.0	0.0	5.7	2097.4	
1:1	G20D	2220.0	32.6	0.9	0.2	0.6	29.9	1.1	0.0	0.0	0.0	10.7	2195.5	

Table A2. Summary of EC, calculated TDS concentrations and dilution factors of aqueous mixtures of samples collected in the studied basins.

Sample Number[a]	Depth (cm)	Type[b]	EC (μmhos cm^{-1} at 25°C)			TDS (mg l^{-1})		11 $\frac{TDS_{1:99}}{TDS_{1:9}}$
			1:1	1:9	1:99	1:9	1:99	
U5A1	0.0- 1.0	CMS	2300	762.0	132.0	571.6	80.1	1.54
U5A2	0.0- 14.0	MS	2200	1038.0	318.0	808.4	214.6	2.92
U5A3	14.0- 25.0	MS	3900	1235.0	296.0	982.3	198.0	2.22
U5B1	0.0- 1.5	CT	1700	655.0	140.0	482.4	85.5	1.95
U5B2	1.5- 16.0	T	1900	898.0	66.0	687.2	36.8	0.59
U5B3	16.0- 24.0	T	1800	357.0	79.7	244.3	45.5	2.05
U5B4	24.0- 32.5	T	2200	442.0	93.8	310.4	54.6	1.93
U5B5	32.5- 38.0	T	1700	446.0	68.1	313.5	38.1	1.34
U5C1A (1 of 2)	0.0- 1.5	CAM	3400	724.0	132.0	539.8	80.1	1.63
U5C1A (2 of 2)	0.0- 1.5	CAM	2400	600.0	92.7	437.3	53.9	1.36
U5C1B-C	1.5- 32.0	AM	4000	569.0	142.0	412.0	86.9	2.32
U5C1D-E	32.0- 50.0	AM	4400	761.0	147.0	570.8	90.3	1.74
U5C1F-G	50.0- 70.0	AM	4400	650.0	121.0	478.3	72.6	1.67
U5C2A	0.0- 1.0	CAM	2900	542.0	135.0	390.1	82.1	2.32
U5C2B	1.0- 12.0	AM	2200	563.0	147.0	407.1	90.3	2.44
U5C2C	12.0- 21.0	AM	3100	466.0	88.5	329.4	51.1	1.71
U5C2D	21.0- 33.0	AM	2400	792.0	149.0	596.9	91.7	1.69
U5C2E	33.0- 43.0	AM	3400	722.0	142.0	538.1	86.9	1.78
U5C3A	0.0- 1.5	CLT	1400	439.0	97.2	308.0	56.8	2.03
U5C3B	1.0- 15.0	LT	1600	459.0	87.2	323.8	50.3	1.71
U5C3C-D	15.0- 34.0	LT	1700	641.0	214.0	470.9	137.6	3.21
U5C3E-F	34.0- 53.0	LT	1700	666.0	127.0	491.5	76.7	1.72
U5C4A	0.0- 1.0	EB	6500	1420.0	242.0	1148.7	158.0	1.51
U5C4B	1.0- 8.0	B	1900	618.0	104.0	452.0	61.3	1.49
U5C4C	8.0- 16.0	B	3700	741.0	129.0	554.0	78.0	1.55
U5C5A	0.0- 2.0	EB	10000	1810.0	453.0	1507.9	319.1	2.33
U5C5B	2.0- 16.0	B	3700	694.0	193.0	514.8	122.6	2.62
U5C6A (1 of 2)	0.0- 0.3	EB	32600	9200.0	1345.0	9334.0	1080.9	1.27
U5C6A (2 of 2)	0.0- 1.5	CB	6100	1420.0	268.0	1148.7	177.1	1.70
U5C6B	1.5- 10.0	B	2300	608.0	112.0	443.8	66.6	1.65
U5C7A	0.0- 1.5	CA	1920	877.0	325.0	669.2	219.9	3.61

Table A2. Continued.

Sample Number[a]	Depth (cm)	Type[b]	EC (μmhos cm^{-1} at 25°C) 1:1	EC 1:9	EC 1:99	TDS (mg l^{-1}) 1:9	TDS 1:99	11 $\frac{TDS_{1:99}}{TDS_{1:9}}$
U5C7B	1.5- 10.0	A	2300	1325.0	305.0	1062.9	204.8	2.12
U5C7C	10.0- 15.0	A	2900	989.0	512.0	765.7	366.0	5.26
U5C7D	15.0- 22.0	A	3200	846.0	134.0	642.7	81.4	1.39
U5C7E	22.0- 30.0	A	4200	635.0	85.3	466.0	49.1	1.16
U5D1A	0.0- 5.0	CAM	4300	736.0	192.0	549.8	121.9	2.44
U5D1B	5.0- 16.0	AM	5200	1100.0	147.0	862.7	90.3	1.14
U5D1C	16.0- 27.0	AM	4400	642.0	129.0	471.7	78.0	1.82
U5D2A	0.0- 3.0	CUMW	3500	552.0	131.0	398.2	79.4	2.19
U5D2B	3.0- 10.0	UMW	2600	660.0	146.0	486.6	89.6	2.03
U5D3A	0.0- 1.0	EB	29000	3680.0	668.0	3341.2	493.2	1.62
U5D3B	1.0- 14.0	B	4000	499.0	133.0	355.6	80.7	2.50
U5D3C	14.0- 20.0	B	3300	486.0	127.0	345.2	76.7	2.44
U5D3D	20.0- 27.0	B	2400	491.0	85.7	349.2	49.3	1.55
U5D4A	0.0- 2.0	CAM	4700	664.0	123.0	489.9	74.0	1.66
U5D4B	2.0- 9.0	AM	3500	592.0	185.0	430.7	116.9	2.99
U5D4C	0.0- 2.0	CAM	7700	935.0	146.0	719.0	89.6	1.37
U5E1A S	0.0- 3.0	CUMW	1600	348.0	104.4	237.4	61.6	2.85
U5E1B S	3.0- 13.0	UMW	1600	555.0	250.0	400.7	163.8	4.50
U5E2A S	0.0- 2.0	CAM	2400	497.0	103.6	354.0	61.0	1.88
U5E2B S	2.0- 27.0	AM	3800	664.0	145.0	489.9	89.0	2.00
U5E2C S	27.0- 41.0	AM	4200	750.0	162.0	561.6	100.7	1.97
U5E2D S	0.0- 2.0	CLAM	11200	1840.0	325.0	1536.0	219.9	1.57
U5E3A S	0.0- 2.5	CT	2152	1380.0	482.0	1112.5	342.1	3.38
U5E3B S	2.5- 13.0	T	2005	955.0	428.0	736.3	299.4	4.47
U5E3C S	13.0- 21.0	T	3037	1205.0	438.0	955.6	307.2	3.54
U5E4A S	0.0- 0.5	EB	15000	2180.0	314.0	1857.6	211.6	1.25
U5E4B S	0.5- 13.0	B	3300	1940.0	160.0	1629.9	99.3	0.67
U5E4C S	13.0- 22.0	B	1700	407.0	75.1	283.0	42.5	1.65
U5H1	0.0- 3.0	CUMW	1900	693.0	130.5	513.9	79.0	1.69
U5H2A	0.0- 2.0	CA	2400	539.0	145.0	387.7	89.0	2.52
U5H2B	2.0- 10.0	A	4700	542.0	197.0	390.1	125.4	3.54
U5H3A	0.0- 16.0	A	1600	279.0	71.7	185.3	40.4	2.40

Table A2. Continued.

Sample Number[a]	Depth (cm)	Type[b]	EC ($\mu mhos\ cm^{-1}$ at 25°C) 1:1	EC 1:9	EC 1:99	TDS ($mg\ l^{-1}$) 1:9	TDS 1:99	11 $\frac{TDS_{1:99}}{TDS_{1:9}}$
U5H3B	0.0- 2.0	CA	500	123.0	44.3	74.0	23.5	3.50
U5H3C	16.0- 23.0	A	1900	362.0	84.8	248.1	48.8	2.16
U5H4A	0.0- 15.0	T	1100	335.0	54.0	227.5	29.4	1.42
U5H4B	0.0- 2.0	CT	200	68.8	35.5	38.6	18.4	5.23
U5H5A	0.0- 2.0	CT	200	70.6	30.3	39.7	15.4	4.26
U5H5B	2.0- 19.0	T	900	135.0	45.2	82.1	24.1	3.23
U5H5C	19.0- 26.0	T	200	58.9	33.2	32.4	17.0	5.78
U5H6A	0.0- 2.0	CUMW	3700	765.0	133.0	574.2	80.7	1.55
U5H6B	2.0- 7.0	UMW	3500	533.0	92.1	382.9	53.5	1.54
U5H6C	7.0- 16.0	UMW	3500	795.0	87.1	599.5	50.2	0.92
U5H7A	0.0- 3.0	CUMW	3200	525.0	116.0	376.5	69.3	2.02
U5H7B	3.0- 9.0	UMW	7800	975.0	159.0	753.6	98.6	1.44
U5I1A	0.0- 3.0	CUMW	1600	418.0	109.0	291.6	64.6	2.44
U5I1B	0.0- 3.0	CLMW	4400	689.0	149.0	510.6	91.7	1.98
U5I2A	0.0- 0.5	EB	17400	4100.0	711.0	3771.6	528.9	1.54
U5I2B	0.5- 15.0	B	2400	603.0	129.0	439.7	78.0	1.95
U5I2C	15.0- 24.0	B	1900	369.0	83.3	253.5	47.8	2.07
U5I3A	0.0- 0.5	EB	40000	8450.0	1270.0	8485.2	1013.6	1.31
U5I3B	0.5- 13.0	B	5200	935.0	255.0	719.0	167.5	2.56
U5I4A	0.0- 1.5	CUMW	1500	284.0	59.9	189.0	33.0	2.21
U5I4B	1.5- 14.0	UMW	1400	251.0	60.4	164.6	33.3	2.23
U5I4C	14.0- 23.0	UMW	1200	255.0	59.7	167.5	32.9	2.16
U5I-J	0.0- 10.0	AM	4300	1660.0	450.0	1368.5	316.7	2.55
U5L1A	0.0- 0.5	EB	13100	2810.0	422.0	2469.2	294.7	1.31
U5L1B	0.5- 7.5	B	2600	763.0	133.0	572.5	80.7	1.55
U5M1A	0.0- 0.5	EB	5300	8400.0	1589.0	8428.9	1303.1	1.70
U5M1B	0.5- 11.0	B	3600	545.0	133.0	392.6	80.7	2.26
U5M2A	0.0- 0.5	EB	38700	6700.0	1230.0	6541.3	977.8	1.64
U5M2B	0.5- 16.0	B	3600	724.0	156.0	539.8	96.6	1.97
U5M3A	0.0- 3.0	CUMW	3300	524.0	184.0	375.7	116.2	3.40
U5M3B	0.0- 3.0	CUMW	2590	765.0	195.0	574.2	124.0	2.38
U5P1A	0.0- 1.0	EB	46200	6950.0	711.0	6815.6	528.9	0.85
U5P1B	1.0- 11.0	B	3900	715.0	158.0	532.3	97.9	2.02

Table A2. Continued.

Sample Number[a]	Depth (cm)	Type[b]	EC (μmhos cm^{-1} at 25°C) 1:1	EC 1:9	EC 1:99	TDS ($mg\ l^{-1}$) 1:9	TDS 1:99	11 $\frac{TDS_{1:99}}{TDS_{1:9}}$
U5P2A	0.0- 3.0	CUMW	4600	802.0	103.0	605.4	60.6	1.10
U5P2B	0.0- 3.0	CUMW	1300	885.0	206.0	676.1	131.9	2.15
U5P2C	0.0- 3.0	CUMW	900	379.0	145.0	261.2	89.0	3.75
U5P2D	0.0- 2.0	CLMW	8400	2200.0	388.0	1876.7	268.2	1.57
U5P3A	1.0- 13.0	UB	4200	1121.0	212.0	881.2	136.2	1.70
U5P4A	1.0- 16.0	UB	2590	1310.0	286.0	1049.4	190.5	2.00
U5P4B	16.0- 27.0	B	3900	852.0	147.0	647.9	90.3	1.53
AT U5PA	0.0- 1.5	CLT	800	365.0	63.6	250.4	35.3	1.55
AT U5PB	1.5- 13.5	LT	2210	1020.0	56.0	792.7	30.6	0.42
AT U5PC	13.5- 24.5	LT	1200	345.0	72.5	235.1	40.9	1.91
AT U5PD	24.5- 32.0	LT	2500	569.0	150.0	412.0	92.4	2.47
AT U5PE	32.0- 40.0	LT	3900	574.0	174.0	416.1	109.1	2.81
U5R1A	0.0- 1.5	CT	600	131.0	39.5	79.4	20.7	2.87
U5R1B	1.5- 20.0	T	800	584.0	94.6	424.2	55.1	1.43
U5R1C	20.0- 28.0	T	1600	624.0	103.0	456.9	60.6	1.46
U5R2A	0.0- 2.0	EA	15800	3020.0	495.0	2677.0	352.4	1.45
U5R2B	2.0- 18.0	A	1800	676.0	141.0	499.8	86.2	1.90
U5R2C	18.0- 22.0	A	2570	577.0	120.3	418.5	72.2	1.90
U5R2D	22.0- 32.0	T	1300	529.0	95.3	379.7	55.6	1.61
U5R3A	0.0- 0.5	EB	56500	9500.0	1400.0	9676.0	1130.6	1.29
U5R3B	0.5- 16.0	B	4700	859.0	169.0	643.8	105.6	1.78
U5R4A	0.0- 1.0	EA	24600	4395.0	479.0	4077.1	339.7	0.92
U5R4B	1.0- 5.0	A	12100	2540.0	550.0	2204.8	396.6	1.98
U5R4C	5.0- 12.0	A	6500	1950.0	250.0	1639.3	163.8	1.10
U5UA	0.0- 1.0	CT	200	84.2	30.9	48.4	15.7	3.57
U5UB	1.0- 13.0	T	200	57.2	37.3	31.4	19.4	6.80
U5UC	13.0- 25.0	T	100	57.7	33.0	31.7	16.9	5.87
U5UD	25.0- 33.0	T	200	67.8	29.5	37.9	14.9	4.33
U5Z1A	0.0- 2.0	CT	800	217.0	45.9	139.8	24.5	1.93
U5Z1B	2.0- 15.0	T	700	314.0	143.0	211.6	87.6	4.55
U6A1 S	0.0- 0.5	EB	95000	30000.0	6000.0	35125.2	5780.1	1.81
U6A2	0.5- 3.0	EB	12200	2160.0	369.0	1838.5	253.5	1.52

Table A2. Continued.

Sample Number[a]	Depth (cm)	Type[b]	EC (μmhos cm^{-1} at 25°C) 1:1	EC 1:9	EC 1:99	TDS (mg l^{-1}) 1:9	TDS 1:99	11 $\frac{TDS_{1:99}}{TDS_{1:9}}$
U6A3	3.0- 20.0	B	3600	951.0	217.0	732.8	139.8	2.10
U6A4	20.0- 32.0	B	3100	1560.0	408.0	1276.4	283.8	2.45
U6A5	32.0- 43.0	B	2900	864.0	260.0	658.1	171.2	2.86
U6B	0.0- 3.0	CW	2900	1090.0	288.0	854.0	192.0	2.47
U6C1	0.0- 3.0	ELW	25100	3900.0	571.0	3565.9	413.6	1.28
U6C2	3.0- 16.0	LW	8600	1630.0	312.0	1340.8	210.0	1.72
U6C3	16.0- 24.0	LW	6700	1490.0	287.0	1212.4	191.3	1.74
U6D1	0.0- 2.0	CUW	1200	414.0	103.0	288.4	60.6	2.31
U6D2	2.0- 15.0	UW	1500	552.0	152.0	398.2	93.8	2.54
U6D3	15.0- 27.0	UW	1000	289.0	67.5	192.8	37.7	2.15
U6E1	0.0- 2.0	CT	200	74.3	32.2	42.0	16.5	4.31
U6E2	2.0- 15.0	T	100	59.2	35.8	32.6	18.5	6.26
U6E3	15.0- 27.0	T	100	66.4	33.9	37.1	17.4	5.17
U6F1	0.0- 1.0	CMS	2400	682.0	121.0	504.8	72.6	1.58
U6F2	1.0- 11.0	MS	5600	1060.0	378.0	827.6	260.5	3.46
U6F3	11.0- 21.0	MS	10000	1200.0	241.0	951.1	157.2	1.82
U6F4	21.0- 27.0	MS	11100	1590.0	297.0	1304.0	198.8	1.60
U6F5	27.0- 32.0	MS	10000	1170.0	298.0	924.5	199.5	2.37
U6G1	0.0- 12.0	CUW	6700	1390.0	371.0	1121.5	255.1	2.50
U6G2	12.0- 23.0	UW	8400	1420.0	308.0	1148.7	207.0	1.98
U6G3-4	23.0- 40.0	UW	10000	1760.0	105.0	1461.3	61.9	0.47
U6G5-6	40.0- 62.0	UW	8600	1920.0	332.0	1611.0	225.2	1.54
U6G7-8	62.0- 82.0	UW	8400	1920.0	369.0	1611.0	253.5	1.73
G1B1	0.0- 2.0	CB	1915		181.0		114.1	
G1B2	2.0- 13.0	B	1940		234.0		152.1	
G1B3	13.0- 22.0	B	1380		209.0		134.0	
G1B4	22.0- 31.0	B	1040		141.0		86.2	
G1B5	31.0- 41.0	B	1725		75.4		42.7	
G1B6	41.0- 47.0	B	1145		155.0		95.9	
G1B7	47.0- 54.0	B	2100		122.0		73.3	
G1C1	0.0- 2.0	CR	603		53.0		28.8	
G1C2-3	2.0- 22.0	R	1030		89.0		51.5	

Table A2. Continued.

Sample Number[a]	Depth (cm)	Type[b]	EC (μmhos cm^{-1} at 25°C) 1:1	EC 1:9	EC 1:99	TDS ($mg\ l^{-1}$) 1:9	TDS 1:99	$\frac{TDS_{1:99}}{TDS_{1:9}}$
G1C4-5	22.0- 44.0	R	2150		104.0		61.3	
G1C6-7	44.0- 67.0	R	2440		98.0		57.3	
G1C(2)1	0.0- 1.0	CR	350		47.0		25.2	
G1C(2)2	1.0- 11.0	R	555		49.0		26.4	
G1C(2)3	11.0- 21.0	R	1950		94.0		54.7	
G1C(2)4	21.0- 32.0	R	2080		158.0		98.0	
G1C(2)5	32.0- 41.0	R	1970		180.0		113.4	
G1C(2)6	41.0- 51.0	R	1950		112.0		66.6	
G1C(2)7	51.0- 58.0	R	1650		95.0		55.4	
G1C(2)8	58.0- 65.0	R	1350		80.0		45.7	
G1C(3)1	0.0- 9.5	UR	600		54.0		29.4	
G1C(3)2	9.5- 17.0	R	580		56.0		30.6	
G1C(3)3	17.0- 26.0	R	860		64.0		35.6	
G1C(3)4	26.0- 34.0	R	875		59.5		32.8	
G1C(3)5	34.0- 42.0	R	1655		156.0		96.6	
G1C(3)6	42.0- 51.5	R	1850		195.0		124.0	
G1D1	0.0- 1.0	CLAM	6400		305.0		204.8	
G1D2	1.0- 9.0	LAM	6250		293.0		195.8	
G1D3	9.0- 14.0	LAM	2640		186.0		117.6	
G1D4	14.0- 23.5	LAM	1920		174.0		109.1	
G1D5	23.5- 31.5	LAM	1910		555.0		400.7	
G1E1	0.0- 0.8	CMS	249		48.0		25.8	
G1E2	0.8- 14.5	MS	1880		220.0		142.0	
G1E3	14.5- 24.0	MS	3220		760.0		570.0	
G1E4	24.0- 35.0	MS	6500		570.0		412.8	
G1E5	missing							
G1E6	44.0- 51.0	MS	9300		485.0		344.5	
G1E7	51.0- 61.5	MS	8800		420.0		293.1	
G2A1	0.0- 13.0	B	2140		670.0		494.8	
G2A2	13.0- 22.0	B	2250		490.0		348.4	
G2A3	22.0- 38.0	B	2130		450.0		316.7	
G2A4	38.0- 45.0	B	2180		510.0		364.4	

Table A2. Continued.

Sample Number[a]	Depth (cm)	Type[b]	EC (μmhos cm^{-1} at 25°C) 1:1	EC 1:9	EC 1:99	TDS (mg l^{-1}) 1:9	TDS 1:99	11 $\frac{TDS_{1:99}}{TDS_{1:9}}$
G2D1	0.0- 1.0	CT	2070		207.0		132.6	
G2D2-3	1.0- 26.0	T	2150		465.0		328.6	
G2D4-5	26.0- 47.5	T	2540		126.0		76.0	
G4A1	0.0- 1.0	CR	3200		420.0		293.1	
G4A2	1.0- 12.0	R	3200		280.0		186.0	
G4A3	12.0- 22.0	R	2550		217.0		139.8	
G4A4	22.0- 30.5	R	2640		310.0		208.5	
G4A5	30.5- 42.0	R	2600		290.0		193.5	
G4A6	42.0- 48.5	R	2900		330.0		223.7	
G4B1	0.0- 1.0	CR	5300		628.0		460.2	
G4B2	1.0- 11.5	R	3000		297.0		198.8	
G4B3	11.5- 21.0	R	2480		235.0		152.9	
G4B4	21.0- 31.0	R	2040		220.0		142.0	
G4B5	31.0- 40.0	R	2130		198.0		126.2	
G4B6	40.0- 49.0	R	2310		242.0		158.0	
G4B7	49.0- 61.0	R	1550		288.0		192.0	
G4B8	61.0- 71.0	R	2460		148.0		91.0	
G4B9	71.0- 80.0	R	2400		166.0		103.5	
G4C1	0.0- 5.0	UR	3800		338.0		229.8	
G4C2	5.0- 13.0	R	2700		177.0		111.3	
G4C3	13.0- 29.0	R	2550		175.0		109.8	
G4C4	29.0- 37.0	R	2550		208.0		133.3	
G4C5	37.0- 46.0	R	2350		214.0		137.6	
G4C6	46.0- 58.5	R	2430		241.0		157.4	
G5C1	0.0- 3.0	CMS	2860		277.0		183.8	
G5C2	3.0- 14.5	MS	8500	2170.0	360.0	1848.0	246.6	1.47
G5C3	14.5- 21.0	MS	6250		227.0		147.0	
G5E1	0.0- 3.0	CMS	9200		126.0		76.0	
G4E2	3.0- 16.0	MS	9700		360.0		246.6	
G5E3	16.0- 26.0	MS	9000		288.0		192.0	
G5E4	26.0- 35.0	MS	7600		330.0		233.8	
G2OA	0.0- 2.0	C-MesaVerde	1975	1050.0	222.0	881.9	143.4	1.79

Table A2. Continued.

Sample Number[a]	Depth (cm)	Type[b]	EC (μmhos cm^{-1} at 25°C) 1:1	EC 1:9	EC 1:99	TDS (mg l^{-1}) 1:9	TDS 1:99	11 $\frac{TDS_{1:99}}{TDS_{1:9}}$
G2OC	0.0- 2.0	C-MesaVerde	2060	550.0	98.8	396.6	57.9	1.60
G2OE	0.0- 2.0	C-MesaVerde	239	106.5	42.0	62.9	22.2	3.88
G7A1 S	0.0- 13.0	UB	2000	435.0	61.0	304.9	33.7	1.22
G7A2-3 S	13.0- 33.0	B	2400	413.0	63.6	287.7	35.3	1.35
G7A4-5 S	33.0- 51.5	B	1600	353.0	58.3	241.2	32.0	1.46
G7A6-7 S	51.5- 64.5	B	1600	373.0	72.8	256.6	41.1	1.76
G7B1 S	0.0- 9.5	UB	600	168.0	36.9	104.9	19.2	2.01
G7B2	9.5- 24.5	B	600	215.5	46.8	138.7	25.0	1.98
G7B3-4	24.5- 42.0	B	600	170.0	42.6	106.3	22.5	2.33
G7B5-6	42.0- 60.5	B	500	199.0	48.5	126.9	26.1	2.26
G7B7-8	60.5- 73.5	B	500	269.0	52.0	177.9	28.2	1.74
G7C1 S	0.0- 13.5	UB	900	166.0	40.3	103.5	21.2	2.25
G7C2 S	13.5- 24.0	B	600	171.0	43.3	107.0	22.9	2.35
G7C3 S	24.0- 33.0	B	700	127.0	38.5	76.7	20.1	2.88
G7C4 S	33.0- 41.5	B	600	174.0	49.3	109.1	26.5	2.67
G7D1	0.0- 1.7	CB	3000	1164.0	135.0	919.2	82.1	0.98
G7D2	1.7- 25.0	B	600	166.0	54.6	103.5	29.8	3.17
G7D3-4	25.0- 44.5	B	500	135.0	37.5	82.1	19.5	2.61
G7D5-6	44.5- 62.5	B	300	111.0	38.1	65.9	19.9	3.32
G7D7-8	62.5- 72.0	B	300	92.7	38.5	53.9	20.1	4.10
G7E1 S	0.0- 12.0	UT	300	64.8	29.7	36.1	15.0	4.57
G7E2 S	12.0- 19.0	T	200	47.7	29.1	25.6	14.7	6.32
G7E3-4 S	19.0- 39.5	T	200	58.8	29.9	32.3	15.1	5.14
G7E5-6 S	39.5- 55.5	T	1500	374.0	74.0	257.4	41.8	1.79
G8A1 S	0.0- 2.0	CB	4600	1239.0	281.0	985.9	186.8	2.08
G8A2	2.0- 13.0	B	3700	859.0	93.1	653.8	54.1	0.91
G8A3-4	13.0- 31.0	B	3300	960.0	199.0	740.6	126.9	1.88
G8A5-6	31.0- 48.5	B	4800	990.0	138.0	766.6	84.2	1.21
G8A7UP	48.5- 58.0	B	3900	1100.0	126.0	862.7	76.0	0.97
G8A7LOW	48.5- 58.0	B	8400	2250.0	520.0	1924.6	372.4	2.13
G8A8	58.0- 69.0	B	8400	2160.0	417.0	1838.5	290.8	1.74
G8A9-10	69.0- 93.0	B	9100	1930.0	392.0	1620.5	271.3	1.84
G8A11-12	93.0-118.5	B	7700	1470.0	450.0	1194.2	316.7	2.92

Table A2. Continued.

Sample Number[a]	Depth (cm)	Type[b]	EC (μmhos cm^{-1} at 25°C) 1:1	EC 1:9	EC 1:99	TDS (mg l^{-1}) 1:9	TDS 1:99	11 $\frac{TDS_{1:99}}{TDS_{1:9}}$
G8B1	0.0- 0.3	EB	71600	12500.0	2130.0	13162.1	1809.9	1.51
G8B2	0.3- 14.5	B	7400	1320.0	223.0	1058.4	144.1	1.50
G8B3	14.5- 25.5	B	5400	971.0	113.0	750.1	67.3	0.99
G8B4UP	25.5- 35.5	B	5900	970.0	120.0	749.3	72.0	1.06
G8B4LOW	35.5- 41.5	B	5400	1425.0	239.0	1153.3	155.8	1.49
G8B5	41.5- 54.0	B	6100	1190.0	270.0	942.3	178.6	2.08
G8B6	54.0- 70.0	B	5700	950.0	194.0	732.0	123.3	1.85
G8B7-8	70.0- 98.0	B	5000	1590.0	243.0	1304.0	158.7	1.34
G8C1	0.0- 5.0	UB	800	335.0	60.3	227.5	33.3	1.61
G8C2	5.0- 14.0	B	3300	1395.0	223.0	1126.1	144.1	1.41
G8C3	14.0- 21.0	B	5200	1551.0	340.0	1268.2	231.3	2.01
G8C4	21.0- 39.0	B	4000	1749.0	359.0	1451.1	245.8	1.86
G8E1	0.0- 17.0	UA	2800	1150.0	224.0	906.8	144.9	1.76
G8E2	17.0- 26.0	A	3900	1500.0	318.0	1221.5	214.6	1.93
G8E3-4	26.0- 45.5	A	5300	1851.0	497.0	1546.3	354.0	2.52
G8E5-6	45.5- 62.0	A	4200	2410.0	751.0	2078.7	562.4	2.98
G8F1	0.0- 2.0	UW	5400	2140.0	172.0	1819.4	107.7	0.65
G8F2	2.0- 13.0	W	6300	1835.0	200.0	1531.3	127.6	0.92
G8F3	13.0- 27.0	W	2100	1050.0	173.0	818.9	108.4	1.46
G8F4	27.0- 35.0	W	2600	935.0	177.0	719.0	111.2	1.70
G8F5	35.0- 53.0	W	3100	950.0	139.0	732.0	84.8	1.27
G8G1 S	0.0- 12.5	UW	5400	1930.0	551.0	1620.5	397.4	2.70
G8G2	12.5- 18.5	W	3500	1990.0	599.0	1677.0	436.4	2.86
G8G3	18.5- 22.0	W	3300	2375.0	857.0	2044.9	652.1	3.51
G8G4	22.0- 28.0	W	3600	2210.0	609.0	1886.3	444.6	2.59
G8H1	0.1- 12.5	UW	200	56.3	28.8	30.8	14.5	5.18
G8H2	12.5- 20.5	W	100	47.6	24.3	25.5	12.0	5.18
G8H3	20.5- 36.0	W	200	50.8	20.6	27.4	10.0	4.01
G8H4	36.0- 46.5	W	400	59.7	21.2	32.9	10.3	3.44
G8I1	0.0- 1.0	CT	200	102.0	22.8	60.0	11.2	2.05
G8I2-3	1.0- 24.5	T	100	46.8	26.4	25.0	13.2	5.81
G8I4-5	24.5- 45.5	T	200	80.5	30.3	46.0	15.4	3.68

Table A2. *Continued.*

Sample Number[a]	Depth (cm)	Type[b]	EC (μmhos cm^{-1} at 25°C) 1:1	EC 1:9	EC 1:99	TDS (mg l^{-1}) 1:9	TDS 1:99	11 $\frac{TDS_{1:99}}{TDS_{1:9}}$
G8I6-7	45.5- 72.5	T	1400	419.0	64.3	292.3	35.7	1.34
G8I8-9	72.5- 90.5	T	1200	323.0	54.3	218.4	29.6	1.49
G8I10-11	90.5-108.5	T	2000	550.0	85.3	396.6	49.1	1.36
G9A1	0.0- 1.5	CB	2000	458.0	81.1	323.0	46.4	1.58
G9A2	1.5- 7.5	B	640	111.0	36.2	65.9	18.8	3.14
G9A3	7.5- 21.0	B	400	113.0	36.2	67.3	18.8	3.07
G9A4	21.0- 29.0	B	200	80.3	36.0	45.9	18.7	4.48
G9A5	29.0- 39.5	B	200	65.7	35.4	36.6	18.3	5.50
G9A6UP	39.5- 48.0	B	200	70.5	34.8	39.6	18.0	5.00
G9A6LOW	39.5- 48.0	B	200	65.6	35.3	36.6	18.2	5.47
G9A7	48.0- 59.5	B	200	54.3	28.5	29.6	14.4	5.35
G9A8-9	59.5- 82.5	B	200	55.1	33.8	30.1	17.4	6.36
G9A10-11	82.5-102.0	B	300	87.3	40.1	50.4	21.1	4.61
G9A12-13	102.0-128.0	B	300	79.3	39.3	45.2	20.6	5.01
G9A14-15	128.0-144.5	B	200	71.9	42.0	40.5	22.2	6.03
G9A16-17	144.5-165.0	B	200	90.2	42.0	52.2	22.2	4.68
G9A18-19	165.0-184.0	B	500	75.3	39.3	42.7	20.6	5.31
G9A20-21	184.0-206.0	B	300	93.5	41.4	54.4	21.8	4.41
G9B1	0.0- 1.2	CB	1200	243.0	47.7	158.7	25.6	1.77
G9B2	0.0- 3.0	CB	1300	221.0	51.2	142.7	27.7	2.14
G9B3	0.0- 3.5	DB	1200	251.0	43.8	164.6	23.2	1.55
G9B4	0.0- 1.5	CB	1500	259.0	51.7	170.5	28.0	1.81
G9B5	0.0- 1.5	CB	1400	302.0	75.8	202.5	43.0	2.34
G9B6	0.0- 1.5	CB	1300	386.0	75.7	266.7	42.9	1.77
G9C1	1.0- 16.0	UA	200	57.6	29.7	31.6	15.0	5.22
G9C2	16.0- 26.0	A	100	73.6	29.5	41.6	14.9	3.94
G9C3	26.0- 35.0	A	100	77.5	35.2	44.1	18.2	4.54
G9C4	35.0- 43.0	A	200	82.1	33.1	47.0	17.0	3.98
G9D1	0.0- 2.5	CW	521	119.0	34.1	71.3	17.6	2.72
G9D2	2.5- 13.5	W	218	60.3	28.7	33.3	14.5	4.79
G9D3	13.5- 21.5	W	140	53.1	29.2	28.8	14.8	5.65
G9D4	21.5- 27.0	W	149	65.2	29.7	36.3	15.0	4.55

Table A2. Continued.

Sample Number[a]	Depth (cm)	Type[b]	EC (μmhos cm^{-1} at 25°C) 1:1	EC 1:9	EC 1:99	TDS (mg l^{-1}) 1:9	TDS 1:99	11 $\frac{TDS_{1:99}}{TDS_{1:9}}$
G9E1	0.0- 13.5	UT	185	72.2	26.3	40.7	13.1	3.54
G9E2-3	13.5- 36.0	T	152	55.3	26.6	30.2	13.3	4.84
G9E4-5	36.0- 57.5	T	139	57.5	27.9	31.5	14.0	4.89
G9F1	0.0- 1.0	CW	900	212.0	43.3	136.2	22.9	1.85
G9F2-3	1.0- 16.5	W	2200	430.0	69.7	301.0	39.1	1.43
G9F4-5	16.5- 41.5	W	2250	442.0	69.6	310.4	39.1	1.39
G9F6-7	41.5- 74.0	W	2100	424.0	66.2	296.3	36.9	1.37
G9G1	0.0- 12.5	UW	4500	744.0	83.3	556.5	47.8	0.94
G9G2-3	12.5- 35.0	W	4900	735.0	82.1	549.0	47.0	0.94
G9G4-5	35.0- 74.5	W	3500	502.0	63.0	358.0	34.9	1.07
G9H1	0.0- 1.0	CT	199	71.6	38.6	40.3	20.2	5.51
G9H2	1.0- 13.0	T	300	93.6	43.0	54.5	22.8	4.60
G9H3-4	13.0- 34.0	T	1200	420.0	79.1	293.1	45.1	1.69
G9H5-6	34.0- 51.5	T	1800	616.0	106.0	450.3	62.6	1.53
G9H7-8	51.5- 69.5	T	1600	514.0	82.0	367.6	47.0	1.41
G9H9-10	69.5- 90.0	T	1900	524.0	93.0	375.7	54.1	1.58
G9H11-12	90.0-112.5	T	6200	1000.0	146.0	775.3	89.6	1.27
G9H13-14	112.5-128.5	T	4500	771.0	128.0	579.2	77.4	1.47
G9H15-16	128.5-151.5	T	3300	592.0	87.1	430.7	50.2	1.28
G10A1 (1 of 2)	0.0- 1.0	CB	1700	404.0	60.0	280.6	33.1	1.30
G10A1 (2 of 2)	0.0- 1.0	CB	1300	250.0	53.1	163.8	28.8	1.93
G10A1Y	0.0- 2.0	CB	3100	405.0	67.0	281.4	37.4	1.46
G10A2	1.0- 12.5	B	700	138.0	32.2	84.2	16.5	2.16
G10A3	12.5- 24.5	B	400	87.5	36.7	50.5	19.1	4.16
G10A4-5	24.5- 34.5	B	300	93.2	41.9	54.2	22.1	4.49
G10B1	0.0- 1.0	CA	300	143.0	41.9	87.6	22.1	2.78
G10B2	1.0- 12.5	A	300	97.2	45.4	56.8	24.2	4.69
G10B3-4	12.5- 33.0	A	1400	414.0	63.0	288.4	34.9	1.33
G10B5-6	33.0- 55.5	A	3100	726.0	114.0	541.4	67.9	1.38
G10C1	0.0- 2.0	CW	500	143.0	38.4	87.6	20.1	2.52
G10C2	2.0- 10.5	W	1200	231.0	43.5	150.0	23.1	1.69
G10C3	10.5- 16.5	W	1700	304.0	57.6	204.0	31.6	1.70

Table A2. Continued.

Sample Number[a]	Depth (cm)	Type[b]	EC (μmhos cm^{-1} at 25°C) 1:1	EC 1:9	EC 1:99	TDS (mg l^{-1}) 1:9	TDS 1:99	11 $\frac{TDS_{1:99}}{TDS_{1:9}}$
G10C4	16.5- 37.0	W	1400	282.0	57.0	187.5	31.2	1.83
G10C5	37.0- 47.0	W	1300	253.0	42.5	166.1	22.5	1.49
G10D1	0.0- 10.0	UT	200	101.0	30.3	59.3	15.4	2.86
G10D2	10.0- 19.0	T	200	74.4	37.7	42.1	19.6	5.12
G10D3-4	19.0- 38.0	T	300	104.0	39.2	61.3	20.5	3.68
G10D5-6	38.0- 63.0	T	1000	249.0	52.2	163.1	28.3	1.91
G10XA1	0.0- 1.0	CB	1300	258.0	62.7	169.7	34.8	2.26
G10XA2	0.0- 1.0	CB	1500	255.0	54.6	167.5	29.8	1.96
G10XA3	1.0- 10.0	B	400	130.0	32.1	78.7	16.4	2.29
G10XA4	10.0- 20.5	B	300	96.4	47.9	56.3	25.7	5.02
G10XA5	20.5- 26.5	B	200	106.5	38.2	62.9	19.9	3.48
G10XB1	0.0- 1.0	CLW	1500	509.0	86.3	363.6	49.7	1.50
G10XB2-3	1.0- 22.5	LW	5200	1680.0	299.0	1387.0	200.3	1.59
G10XB4-5	22.5- 44.0	LW	4000	1319.0	241.0	1057.5	157.2	1.64
G10XC1 S	0.0- 12.0	UT	200	105.0	27.7	61.9	13.9	2.47
G10XC2-3	12.0- 29.5	T	200	73.1	34.5	41.3	17.8	4.74
G10XC4-5	29.5- 47.0	T	200	67.3	36.1	37.6	18.7	5.47
G11A1	0.0- 7.0	UB	3500	730.0	117.0	544.8	69.9	1.41
G11A1X	0.0- 8.0	UB	3900	691.0	111.0	512.3	65.9	1.41
G11A2-3	0.8- 25.0	B	3100	735.0	108.0	549.0	63.9	1.28
G11A4-5	25.0- 39.0	B	2800	645.0	81.8	474.2	46.8	1.09
G11A6-7	39.0- 54.5	B	1750	440.0	68.7	308.8	38.5	1.37
G11B1	0.0- 1.0	CB	7400	2210.0	361.0	1886.3	247.4	1.44
G11B2	1.0- 9.5	B	4000	649.0	79.3	477.5	45.2	1.04
G11B3-4	9.5- 32.0	B	3100	654.0	86.8	481.6	50.0	1.14
G11B5-6	32.0- 49.5	B	2600	510.0	80.5	364.4	46.0	1.39
G11B7-8	49.5- 67.5	B	2300	769.0	125.0	577.5	75.3	1.43
G11B9-10	67.5- 79.0	B	4000	551.0	78.0	397.4	44.4	1.23
G11C1	0.0- 2.0	CA	20000	2830.0	345.0	2488.9	235.1	1.04
G11C2	2.0- 16.5	A	10400	1960.0	264.0	1648.7	174.2	1.16
G11C3-4	16.5- 35.5	A	8700	1419.0	209.0	1147.8	134.0	1.28
G11C5-6	35.5- 47.0	A	5200	1379.0	156.0	1111.6	96.6	0.96

Table A2. Continued.

Sample Number[a]	Depth (cm)	Type[b]	EC (μmhos cm^{-1} at 25°C) 1:1	EC 1:9	EC 1:99	TDS ($mg\ l^{-1}$) 1:9	TDS 1:99	11 $\frac{TDS_{1:99}}{TDS_{1:9}}$
G11C7-8	47.0- 67.0	A	6500	169.0	186.0	105.6	117.6	12.25
G11D1	0.0- 2.0	CW	5600	1065.0	135.0	832.0	82.1	1.09
G11D2-3	2.0- 19.0	W	7500	1455.0	208.0	1180.5	133.3	1.24
G11D4-5	19.0- 42.0	W	5800	1139.0	124.0	897.1	74.6	0.91
G11E1	0.0- 2.0	CT	300	189.0	45.6	119.7	24.3	2.23
G11E2-3	2.0- 26.4	T	300	91.4	37.6	53.0	19.6	4.07
G11E4-5	26.5- 40.0	T	400	112.0	41.2	66.6	21.7	3.58
G11E6-7	40.0- 67.5	T	600	149.0	34.0	91.7	17.5	2.10
M1A1	0.0- 1.0	CB	2200	496.0	148.0	353.2	91.0	2.83
M1A2	0.0- 9.0	B	2100	692.0	249.0	513.1	163.1	3.50
M1A3-4	9.0- 30.0	B	3200	859.0	294.0	653.8	196.5	3.31
M1A5-6	30.0- 49.5	B	4200	899.0	298.0	688.1	199.5	3.19
M1A7-8	49.5- 71.5	B	2700	1145.0	372.0	902.4	255.8	3.12
M1B1	0.0- 2.0	EB	10200	1670.0	322.0	1377.8	217.6	1.74
M1B2	2.0- 19.0	B	3400	592.0	191.0	430.7	121.2	3.10
M1B3	19.0- 28.5	B	2800	849.0	269.0	645.3	177.9	3.03
M1C1	0.0- 2.0	CA	5200	1350.0	382.0	1085.4	263.6	2.67
M1C2	2.0- 15.0	A	11300	1900.0	560.0	1592.2	404.7	2.80
M1C3-4	15.0- 31.0	A	12700	1860.0	519.0	1554.7	371.6	2.63
M1C5-6	31.0- 44.5	A	12700	1755.0	424.0	1456.6	296.3	2.24
M1C7-8	44.5- 60.5	A	13700	1570.0	473.0	1285.6	334.9	2.87
M1C9-10	60.5- 78.0	A	13300	1680.0	420.0	1387.0	297.8	2.36
M1C11-12	78.0- 93.0	A	13700	1755.0	311.0	1456.6	209.3	1.58
M1D1	0.0- 5.0	D	7900	1245.0	419.0	991.2	292.3	3.24
M1D2	0.0- 10.0	D	6300	1450.0	250.0	1176.0	163.8	1.53
M1E1	0.0- 1.0	CW	14500	2590.0	585.0	2253.5	425.0	2.07
M1E2-3	1.0- 19.0	W	28200	3700.0	689.0	3361.5	510.6	1.61
M1E4-5	19.0- 30.5	W	9800	1749.0	408.0	1451.1	283.8	2.15
M2A1	0.0- 14.0	UB	3900	1025.0	272.0	797.1	180.1	2.49
M2A2UP	14.0- 16.0	B	3600	942.0	195.0	725.1	124.0	1.88
M2A2LOW	16.0- 21.5	MB	2790	489.0	285.0	347.6	189.8	6.01
M2B1	0.0- 1.0	CLAM	1600	292.0	40.5	195.0	21.3	1.20

Table A2. Continued.

Sample Number[a]	Depth (cm)	Type[b]	EC (μmhos cm^{-1} at 25°C) 1:1	EC 1:9	EC 1:99	TDS ($mg\ l^{-1}$) 1:9	TDS 1:99	11 $\frac{TDS_{1:99}}{TDS_{1:9}}$
M2B2	1.0- 8.0	LAM	2000	646.0	77.7	475.0	44.2	1.02
M2C1 S	0.0- 3.0	CAM	1300	373.0	54.6	256.6	29.8	1.28
M2C2 S	3.0- 6.0	AM	1500	256.0	83.8	168.3	48.1	3.14
M2C3 S	6.0- 14.0	MW	400	86.7	26.0	50.0	13.0	2.86
M2D1 S	0.0- 1.0	CAM	452	120.0	47.5	72.0	25.5	3.90
M2D2-3	1.0- 24.0	MW	2000	424.5	90.0	296.7	52.1	1.93
M2D4-5 S	24.0- 41.5	MW	2400	758.0	254.0	568.3	166.8	3.23
M2D6-7	41.5- 62.0	MW	3000	959.0	334.0	739.8	226.7	3.37
M2D8-9 S	62.0- 72.0	MW	4800	1044.0	311.0	813.6	209.3	2.83
M3A1 S	0.0- 9.0	UB	2350	704.0	115.0	523.1	68.6	1.44
M3A2-3	9.0- 29.5	B	1700	615.0	76.5	449.5	43.4	1.06
M3A4-5-6	29.5- 53.0	B	2000	780.0	209.0	586.8	134.0	2.51
M3A7-8-9	53.0- 74.5	B	2100	893.0	167.0	682.9	104.2	1.68
M3A10-11	74.5- 88.0	B	2400	719.0	412.0	535.6	286.9	5.89
M3A12-13 S	88.0-100.5	B	2445	580.0	176.0	420.9	110.5	2.89
M3A14-15	100.5-120.5	B	2700	780.0	301.0	586.8	201.8	3.78
M3A16-17-18	120.5-143.5	B	2500	998.0	357.0	773.6	244.3	3.47
M3A19-20-21	143.5-169.0	B	2450	1300.0	372.0	1040.5	255.8	2.70
M3A22UP	169.0-175.0	B	3200	1560.0	431.0	1276.4	301.7	2.60
M3A22LOW	169.0-175.0	B	3900	1700.0	774.0	1405.6	581.7	4.55
M3A23-24 S	175.0-196.5	B	3052	1367.0	286.5	1100.8	190.9	1.91
M3A25-26	196.5-210.0	B	3900	1475.0	674.0	1198.7	498.2	4.57
M3A27-28-29	210.0-240.0	B	3600	1374.0	882.0	1107.1	673.5	6.69
M3A30-31-32	240.0-275.0	B	3400	1630.0	631.0	1340.8	462.7	3.80
M3A33-34 S	275.0-296.0	B	2900	1705.0	767.0	1410.2	575.8	4.49
M3B1 S	0.0- 0.8	CT	578	147.0	55.3	90.3	30.2	3.68
M3B2	0.8- 12.0	T	1900	365.0	81.5	250.4	46.6	2.05
M3B3-4-5	12.0- 41.0	T	2400	841.0	171.0	638.5	107.0	1.84
M3B6-7-8	41.0- 68.5	T	3700	1445.0	391.0	1171.4	270.5	2.54
M3B9 S	68.5- 78.5	T	4100	1050.0	274.0	818.9	181.6	2.44
M3B10-11	78.5- 99.5	T	4200	1075.0	219.0	840.8	141.2	1.85
M3B12-13-14	99.5-137.5	T	3400	1540.0	357.0	1258.1	244.3	2.14

Table A2. Continued.

Sample Number[a]	Depth (cm)	Type[b]	EC (μmhos cm^{-1} at 25°C) 1:1	EC 1:9	EC 1:99	TDS (mg l^{-1}) 1:9	TDS 1:99	11 $\frac{TDS_{1:99}}{TDS_{1:9}}$
M3B15-16	137.5-164.5	T	3200	1195.0	302.0	946.7	202.5	2.35
M3B17-18 S	164.5-189.5	T	3200	849.0	245.0	645.3	160.2	2.73
M3C1	0.0- 10.0	UB	1800	698.0	216.0	518.1	139.1	2.95
M3C2	10.0- 18.5	B	1900	855.0	143.0	650.4	87.6	1.48
M3C3-4	18.5- 36.0	B	2200	884.0	91.2	675.2	52.9	0.86
M3C5-6	36.0- 51.0	B	2300	779.0	149.0	586.0	91.7	1.72
M3C7-8	51.0- 66.5	B	2600	923.0	109.0	708.7	64.6	1.00
M3C9-10	66.5- 76.5	B	2800	594.0	193.0	432.4	122.6	3.12
M3D1	0.0- 10.5	UB	1900	969.0	114.0	748.4	67.9	1.00
M3D2-3	10.5- 28.0	B	2100	659.0	93.5	485.7	54.4	1.23
M3D4-5	28.0- 46.5	B	2400	832.0	239.0	630.8	155.8	2.72
M3D6-7	46.5- 62.5	B	2400	830.0	302.0	629.1	202.5	3.54
M3D8-9	62.5- 77.0	B	2300	554.0	123.0	399.8	74.0	2.04
M3D10-11	77.0- 91.0	B	2800	708.0	199.0	526.4	126.9	2.65
M3E1	0.0- 10.0	UB	2100	749.0	177.0	560.7	111.2	2.18
M3E2	10.0- 19.5	B	1800	779.0	198.0	586.0	126.2	2.37
M3E3-4	19.5- 40.0	B	2000	823.0	235.0	623.2	152.9	2.70
M3E5-6	40.0- 60.5	B	1900	924.0	748.0	709.5	559.9	8.68
M3E7-8	60.5- 78.0	B	1450	238.0	49.4	155.1	26.6	1.89
M3E9-10	78.0- 92.0	B	2700	811.0	199.0	613.0	126.9	2.28
M3F1	0.0- 11.0	UB	1700	753.0	296.0	564.1	198.0	3.86
M3F2-3	11.0- 30.0	B	1700	716.0	130.0	533.1	78.7	1.62
M3F4-5	30.0- 49.0	B	1900	1085.0	278.0	849.6	184.6	2.39
M3F6-7	49.0- 66.5	B	2300	690.0	143.0	511.4	87.6	1.88
M3F8-9	66.5- 81.0	B	2700	823.0	153.0	623.2	94.5	1.67
M3G1	0.0- 12.0	UB	1800	1038.0	268.0	808.4	177.1	2.41
M3G2-3	12.0- 30.0	B	1900	775.0	121.0	582.6	72.6	1.37
M3G4-5	30.0- 47.5	B	1390	950.0	260.5	732.0	171.6	2.58
M3G6-7	47.5- 61.0	B	1950	781.0	252.0	587.6	165.3	3.09
M3G8-9	61.0- 80.0	B	1100	1157.0	211.5	913.0	135.8	1.64
M3H1-2 S	66.0- 78.5	T	3300	1599.0	388.0	1312.3	268.2	2.25
M3H3-4	78.5-102.0	T	3900	1542.0	360.0	1259.9	246.6	2.15

Table A2. Continued.

Sample Number[a]	Depth (cm)	Type[b]	EC (μmhos cm^{-1} at 25°C) 1:1	EC 1:9	EC 1:99	TDS (mg l^{-1}) 1:9	TDS 1:99	11 $\frac{TDS_{1:99}}{TDS_{1:9}}$
M3H5-6	102.0-127.0	T	3100	1175.0	271.0	929.0	179.4	2.12
M3H7-8	127.0-147.5	T	3100	1205.0	269.0	955.6	177.9	2.05
M3H9-10	147.5-173.5	T	2900	1145.0	252.0	902.4	165.3	2.01
M3H11-12	173.5-194.0	T	2700	850.0	188.0	646.2	119.0	2.03
M3I1	0.0- 13.0	UB	2300	849.0	189.0	645.3	119.7	2.04
M3I2	13.0- 19.5	B	2300	601.0	190.0	438.1	120.5	3.03
M3I3-4	19.5- 42.5	B	3300	1100.0	308.0	862.7	208.0	2.64
M3I5-6	42.5- 65.0	B	2600	1060.0	311.0	827.6	209.3	2.78
M3I7-8	65.0- 78.0	B	2100	569.0	240.0	412.0	156.5	4.18
M3J1	0.0- 12.5	UB	2100	589.0	146.0	428.3	89.6	2.30
M3J2-3	12.5- 32.5	B	1600	555.0	161.0	400.7	100.0	2.75
M3J4-5-6	32.5- 68.0	B	1800	969.0	259.0	748.4	170.5	2.51
M3J7-8-9	68.0- 98.0	B	2900	1029.0	319.0	800.6	215.3	2.96
M3J10-11-12	98.0-130.0	B	3300	1280.0	300.0	1022.5	201.0	2.16
M3J13-14-15	130.0-157.0	B	2600	1265.0	525.0	1009.1	376.5	4.10
M3K1	0.0- 9.5	UB	2300	755.0	189.0	565.7	119.7	2.33
M3K2-3	9.5- 34.0	B	2100	691.0	213.0	512.3	136.9	2.94
M3K4-5-6	34.0- 66.5	B	2600	1080.0	304.0	845.2	204.0	2.65
M3K7-8-9	66.5-101.5	B	3200	1210.0	214.0	960.0	137.6	1.58
M3K10-11-12	101.5-139.5	B	3500	1181.0	298.0	934.3	199.5	2.35
M3K13-14-15	139.5-171.0	B	2900	1580.0	468.0	1294.8	330.9	2.81
M3K16-17-18 S	171.0-203.5	B	3300	1560.0	592.0	1276.4	430.7	3.71
M3K19-20-21	203.5-230.0	B	2900	1490.0	611.0	1212.4	446.3	4.05
M3K22-23-24 S	230.0-261.0	B	3300	1810.0	893.0	1507.9	682.9	4.98
M3K25-26-27	261.0-299.0	B	3300	1950.0	755.0	1639.3	565.7	3.80
M3L1 S	0.0- 1.5	CA	2900	920.0	288.0	706.1	192.0	2.99
M3L2-3	1.5- 27.5	A	2800	891.0	293.0	681.2	195.8	3.16
M3L4-5 S	27.5- 51.5	W	3400	1361.0	341.0	1095.3	232.1	2.33
M3L6-7	51.5- 75.0	W	3300	1046.0	342.0	815.4	232.8	3.14
M3L8-9 S	75.0-101.5	W	3200	973.0	188.0	751.9	119.0	1.74
M3M1	0.0- 21.0	W	3900	1400.0	344.0	1130.6	234.3	2.28

Table A2. Continued.

Sample Number[a]	Depth (cm)	Type[b]	EC (μmhos cm^{-1} at 25°C) 1:1	EC 1:9	EC 1:99	TDS (mg l^{-1}) 1:9	TDS 1:99	11 $\frac{TDS_{1:99}}{TDS_{1:9}}$
M3M2-3	21.0- 54.0	W	4000	1610.0	304.0	1322.4	204.0	1.70
M3M4-5	54.0- 93.0	W	3500	1290.0	291.0	1031.5	194.3	2.07
M3M6-7	93.0-124.0	W	3700	1025.0	219.0	797.1	141.2	1.95
M3M8-9	124.0-155.0	W	3200	871.0	179.0	664.1	112.7	1.87
M4A1	0.0- 10.0	UB	1900	709.0	132.0	527.2	80.1	1.67
M4A2	0.0- 1.0	CB	3100	821.0	171.0	621.5	107.0	1.89
M4A3	10.0- 19.0	B	2600	808.0	173.0	610.5	108.4	1.95
M4A4	19.0- 29.0	B	2300	561.0	106.0	405.5	62.6	1.70
M4B1 S	0.0- 9.0	UW	8400	2125.0	485.0	1805.1	344.4	2.10
M4B2	9.0- 15.5	W	8700	2195.0	594.0	1871.9	432.4	2.54
M4B3	15.5- 24.5	W	9000	2290.0	584.0	1963.0	424.2	2.38
M4B4	24.5- 37.0	W	5800	1825.0	593.0	1521.9	431.5	3.12
M4B5	37.0- 47.0	W	5900	1895.0	489.0	1587.5	347.6	2.41

[a]The addition of the letter S to a sample number denotes that the sample solution was chemically analyzed (see Table A1). For samples M1D1 and M1D2, the letter D denotes that they are mudballs and their depths stand for their respective diameters.

[b]Symbols used in Table A2: C = crust; M = Mancos Shale; B = bed material; A = mass wasted material; U = upper; S = hillslope; W = gully wall; L = lower; E = efflorescent; R = (reservoir) or stockpond sediment. Unless M (Mancos Shale) is used, the sample is alluvium. Examples: CMS = crust of Mancos Shale from hillslope; CUMW = crust of upper part of Mancos Shale gully wall; ELW = saline crust (efflorescence) of lower part of alluvial gully wall.

Table A3a. Summary of EC variations within the aqueous mixtures (1:999, 1:99 and 1:9) of sample U5D1A.

Concentration	EC µmhos cm^{-1} @ 25°C					
	Contact Time (min)					
	13	110	200			
1:999	23.8	42.2	43.1			
	34.4	47.5	49.2			
	35.8	46.1	48.0			
	34.7	47.0	47.8			
	33.2	48.8	50.1			
	34.1	46.2	48.5			
$\bar{X}$	32.7	46.3	47.8			
$\hat{\sigma}$	4.42	2.24	2.45			
$100(\hat{\sigma}/\bar{X})$	13.5	4.8	5.1			
	Contact Time (min)					
	13	51	127	345		
1:99	100.0	129.0	144.5	157.0		
	111.0	132.1	172.0	215.5		
	106.4	132.1	144.0	157.5		
	116.2	135.2	150.0	164.5		
	116.6	137.6	151.0	170.5		
	118.4	136.0	150.2	169.5		
$\bar{X}$	111.4	133.7	152.0	172.4		
$\hat{\sigma}$	7.1	3.1	10.3	21.9		
$100(\hat{\sigma}/\bar{X})$	6.4	2.3	6.8	12.7		
	Contact Time (min)					
	18	40	80	230	315	585
1:9	515	670	810	1010	1015	1140
	460	580	730	880	925	1043
	521	560	665	775	877	940
	535	605	697	852	900	1068
	440	643	797	980	1000	1130
	518	595	680	770	800	900
$\bar{X}$	498	609	730	878	920	1037
$\hat{\sigma}$	38.5	40.8	61.2	100.8	80.3	98.4
$100(\hat{\sigma}/\bar{X})$	7.7	6.7	8.4	11.5	8.7	9.5

Table A3b. Summary of EC variations within the aqueous mixtures (1:999, 1:99, and 1:9) of sample G8G1.

Concentration	EC μmhos cm^{-1} @ 25°C					
	Contact Time (min)					
	22	85	345	1265		
1:999	62.0	95.5	115.9	121.0		
	48.7	78.2	113.7	122.5		
	43.3	86.6	185.0	204.0		
	45.8	66.4	81.2	91.9		
	42.3	68.0	96.0	107.4		
	39.7	61.8	81.2	87.4		
$\bar{X}$	47.0	76.1	112.1	122.4		
$\hat{\sigma}$	8.0	13.1	38.7	42.5		
$100(\hat{\sigma}/\bar{X})$	17.0	17.2	34.5	34.7		
	Contact Time (min)					
	26	192	240	1034		
1:99	304	650	710	801		
	382	652	704	821		
	242	555	608	782		
	289	605	667	805		
	243	555	643	720		
$\bar{X}$	292	603	666	786		
$\hat{\sigma}$	57.4	48.1	42.5	39.3		
$100(\hat{\sigma}/\bar{X})$	19.6	8.0	6.4	5.0		
	Contact Time (min)					
	16	34	68	292	497	696
1:9	2450	2680	2850	3000	3055	3060
	2365	2630	2880	3080	3130	3130
	2250	2590	2800	3020	3075	3005
	2310	2610	2805	3000	3040	3040
	2280	2545	2740	2895	2925	2965
$\bar{X}$	2331	2611	2815	2999	3045	3040
$\hat{\sigma}$	90.2	49.8	53.4	66.8	75.3	62.0
$100(\hat{\sigma}/\bar{X})$	3.9	1.9	1.9	2.2	2.5	2.0

Table A4. *Summary of calculations of ion pair associations and resulting equilibria with calcite and gypsum.*[a]

Sample	pH	Dissolved Species Ca^{2+}	Mg^{2+}	Na^{1+}	K^{1+}	SO_4^{2-}	HCO_3^{1-}	Cl^{1-}	NO_3^{1-}	$CaSO_4^{o}$	$MgSO_4^{o}$	$NaSO_4^{1-}$	KSO_4^{1-}	$CaHCO_3^{1+}$	$MgHCO_3^{1+}$	$MgOH^{1+}$	$\sqrt{\mu}$
U5E3C 1:1[b]	8	14.05	3.8	19.1	0.8	27.35	0.50	1.6	0.1								
U5E3C 1:1	8	8.27	2.02	18.35	0.77	19.07	0.47	1.6	0.1	5.75	1.78	0.75	0.3	0.3	e	e	0.26435
γ	0.8406	0.4433	0.4819	0.7948	0.7823	0.3991	0.7948			1.00	1.00	0.7948	0.7948	0.7948	0.7948	0.7948	
U5E3C 1:9[b]	8[c]	7.10	0.35	0.4	d	7.55	0.2	d	d								
U5E3C 1:9	8[c]	5.19	0.25	0.4	d	5.54	0.2	d	d	1.91	0.10	e	e	e	e	e	0.14886
γ	0.8861	0.5834	0.6060	0.8644	0.8590	0.5582	0.8644			1.00	1.00	0.8590	0.8590	0.8590	0.8590	0.8590	
U5E3C 1:99[b]	8[c]	2.15	0.05	0.1	e	1.95	0.2	d	e								
U5E3C 1:99	8[c]	1.84	0.04	0.1	e	1.63	0.2	d	e	0.31	0.1	e	e	e	e	e	0.08479
γ	0.9237	0.7108	0.7228	0.9146	0.9125	0.6996	0.9146			1.00	1.00	0.9125	0.9125	0.9125	0.9125	0.9125	

Summary of Calculations of Free Ion Product[f]

Sample Number	$(Ca^{2+})(SO_4^{2-})$ $(M^2\ l^{-2})$	$(Ca^{2+})(HCO_3^{1-})/(H^{1+})$ $(M\ l^{-1})$
U5E3C 1:1	$2.7 \cdot 10^{-5}$	164.0
U5E3C 1:9	$9.3 \cdot 10^{-6}$	52.3
U5E3C 1:99	$1.3 \cdot 10^{-6}$	25.9
Saturation	$2.5 \cdot 10^{-5}$	97.11

[a] Concentrations are in mM l^{-1}. The iterative procedure used herein is based on equations 2.4 and 2.5, and on the following constants (sources: Butler, 1964; Garrels and Christ, 1965; Sillen and Martell, 1964; Stumm and Morgan, 1970; Lane, 1975):

ion:	Ca^{2+}	Mg^{2+}	Na^{1+}	K^{1+}	$CaHCO_3^{1+}$	$MgHCO_3^{1+}$	$MgOH^{1+}$	SO_4^{2-}	HCO_3^{1-}	$NaSO_4^{1-}$	KSO_4^{1-}	H^{1+}
size parameter (A):	6	8	4	3	3	3	3	4	4	3	3	9

ion:	$CaSO_4^{o}$	$MgSO_4^{o}$	$NaSO_4^{-}$	KSO_4^{-}	$CaHCO_3^{1+}$	$MgHCO_3^{1+}$	$MgOH^{1+}$
pK_{ij}:	2.31	2.36	0.72	0.96	1.26	1.16	2.58

[b] Stochiometric concentrations.

[c] Based on assumption of constant pH upon dilution.

[d] Not determined.

[e] < 10 mM l^{-1}.

[f] Note that if ion association is not considered for U5E3C 1:9, this solution would have been expected to be saturated with respect to gypsum.

Table A5. Ionic concentrations, pH and EC of water samples[a] collected from a runoff event at West Salt Creek on July 9-10, 1975.

Section	pH	EC (μmhos cm^{-1})	meq l^{-1}								
			Ca^{2+}	Mg^{2+}	Na^{1+}	K^{1+}	Li^{1+}[b]	CO_3^{2-}	HCO_3^{1-}	Cl^{1-}	SO_4^{2-}
G10	7.7	1400	8.2	5.7	3.4	0.2		c	13.9	1.0	0.1
G10	7.7	1300	7.4	4.2	3.1	0.2		c	12.1	0.8	0.9
G10X	7.9	1300	3.0	4.9	6.7	0.2		c	11.4	1.1	0.9
G9	7.6	2100	15.2	5.1	7.0	0.3		c	3.6	0.5	20.3
G9	7.7	2000	8.7	5.2	9.1	0.2		c	8.4	1.8	13.0
G7	7.7	2800	14.1	8.4	11.4	0.3		c	13.1	0.9	18.8
G7	7.7	3400	29.2	6.9	10.0	0.3		c	6.6	1.2	37.5
G7	7.9	2700	26.1	7.4	3.6	0.3		c	2.4	0.6	34.4
G7	7.9	3500	25.9	10.2	9.8	0.3		c	3.4	1.0	43.2
G7	8.0	3200	27.0	9.6	5.6	0.3		c	3.9	0.6	34.9
G8	8.1	8700	22.9	31.6	65.0	0.5	0.01	c	4.7	3.1	106.2
G8	7.9	1900	13.4	5.3	4.8	0.3		c	3.0	0.6	17.7
G11	8.7	12000	18.8	48.8	93.0	0.4	0.02	0.5	7.0	3.4	158.8
G11	8.1	8700	13.0	36.2	64.5	0.5	0.01	c	5.7	2.6	101.0
G11	8.0	12000	17.9	56.2	98.1	0.8	0.02	c	6.1	3.3	158.8
G11	8.7	12000	18.4	57.7	90.9	0.4	0.02	0.5	7.4	3.1	156.2
G8 seep[d]	7.9	15803	19.5	93.0	128.0	0.64	c	c	11.28	6.88	225.0

[a] NO_3^{1-} < 0.01 meq l^{-1} for all samples.

[b] Li^{1+} concentrations < 0.01 meq l^{-1} are shown as blanks.

[c] No determination.

[d] The seep sample was analyzed at the University of California at Davis, Water Quality Laboratory.